

Third Generation Amperometric Biosensors

Een wetenschappelijke proeve op het gebied van de natuurwetenschappen,
in het bijzonder de chemie

Proefschrift

ter verkrijging van de graad van doctor aan de Katholieke Universiteit
Nijmegen, volgens besluit van het College van Decanen in het openbaar te
verdedigen op donderdag 8 oktober 1992, des namiddags te 3.30 uur precies

door

Cornelis Gerardus Josephus Koopal

Geboren op 15 december 1964 te Amersfoort

Promotor: Prof. Dr. R.J.M. Nolte

Copromotor: Dr. M.C. Feiters

CIP-gegevens Koninklijke Bibliotheek, Den Haag

Koopal, Cornelis Gerardus Josephus

Third generation amperometric biosensors / Cornelis

Gerardus Josephus Koopal. - [S.1. : s.n.]

Proefschrift Nijmegen. - Met samenvatting in het
Nederlands.

ISBN 90-9005150-3

Trefw.: biosensoren

Copyright © 1992 by C.G.J. Koopal, Utrecht, The Netherlands

Omslag Martin van der Vaart

Het in dit proefschrift beschreven onderzoek werd gefinancierd door de Stichting voor de Technische Wetenschappen (STW, project nrs. BST 88.1528 & NCH 11.2488). De verschijning van dit proefschrift werd mede mogelijk gemaakt door financiële steun van de Nederlandse Organisatie voor Toegepast Natuurwetenschappelijk Onderzoek TNO, Hoofdgroep Voeding, Applikon Dependable Instruments B.V. en Antec Leyden B.V.

All bodies whatsoever, though they have no sense, yet they have perception

Francis Bacon, 1561-1626

Aan Rahel

Dankwoord

Life is not so short but that there is always time enough for courtesy.
Ralph Waldo Emerson, 1803-1882

Het boekwerk dat U zojuist hebt opengeslagen is het resultaat van een promotie-onderzoek, uitgevoerd op drie verschillende lokaties in Nederland. Het is daarom niet zozeer een probleem van *wie te bedanken*, maar van *waar te beginnen*. Een chronologische volgorde is niet alleen de meest logische oplossing, het is mijns inziens tevens de minst gekleurde. Het is daarom dat ik voor deze volgorde heb gekozen. Zoals U zult ervaren leidt dit tot een omvangrijke, maar zeker niet uitputtende lijst met namen van mensen die ik zeer erkentelijk ben voor de geboden steun bij mijn onderzoek.

Om in Nijmegen te beginnen, wil ik mijn promotor, Prof. Dr. Roeland Nolte, bedanken voor de mij geboden mogelijkheid dit onderzoek uit te voeren en voor de enthousiaste en bezielende, maar vooral kritische wijze, waarop hij heeft bijgedragen aan de totstandkoming van dit proefschrift. Ditzelfde geldt voor mijn copromotor, Dr. Martin Feiters, die aldoor met veel belangstelling het onderzoek heeft gevolgd.

Alle (ex)medewerkers op zowel de derde verdieping als in practicumzaal VII ben ik erkentelijk voor de prettige werksfeer in het laboratorium. Patricia Gosling wil ik met name bedanken voor het uitfilteren van de storende onvolkomenheden in de engelstalige teksten. Helene Amatdjais, Peter van Galen, Pieter van de Meer, Wim van Luyn, Ad Swolfs en Ruud Zwijnen wil ik danken voor hun praktische ondersteuning. Dankzij de inzet van de heren Van Bommel, Schoutissen en Schut van elektronica is op eigenzinnige wijze met succes een brug geslagen tussen de elektronica en de chemie. Dit is mede te danken aan de inbreng van Dr. Van der Linden, die ik daarom hier ook niet onvernoemd wil laten.

Delft is de volgende lokatie waar een belangrijk deel van het onderzoek heeft plaatsgehad. Op het TNO-Zuidpolder complex was het bij de chemici goed toeven. Met name Barteld de Rooter, Theo Kok en Paul Buijsen en elders op het complex Arie Draaijer en Jos Goossen, hebben een wezenlijk aandeel ingebracht. Mijn dank hiervoor.

Tenslotte ben ik neergestreken in Zeist bij de TNO-lokatie aldaar. Op deze plek is het grootste deel van het onderzoek uitgevoerd en ik wil daarom iedereen van de

afdeling Biotechnologie bedanken voor de fijne sfeer. Mijn naaste collega's Ine Bos, Ron van den Dool, Bob Eijnsma, Bram van der Gaag, Richard Schasfoort, Angela Severs en Everhard de Vries wil ik met name vermelden. Ook buiten de afdeling heb ik veel hulp ontvangen op deze lokatie. Mijn dank gaat vooral uit naar Matty van Haren, Rolf Roukes, Nico Geluk en Freek van Veenendaal.

Wout van Bennekom en Joop Hoogvliet hebben met hun elektrochemische kennis en inbreng een flinke impuls aan het onderzoek gegeven, waarvoor mijn dank.

Ryszard Czajka, I thank you for the terrific collaboration we had and I deeply appreciate your contribution to the most imaginative part of this thesis. Ook Prof. Dr. Van Kempen en Jan Gerritsen dank ik voor hun inzet en medewerking.

Joop Pieters wil ik bedanken voor de enthousiaste wijze waarop hij mij heeft ingewijd in de geheimen van de elektronenmicroscopie.

Mijn ouders wil ik bedanken voor het enthousiasme waarmee zij mijn onderzoek hebben gevolgd.

Rahel, jou dank ik, niet alleen voor je grote bijdrage aan het vele schrijfwerk, maar voor alles ook voor je geduld en voor de stimulerende wijze waarop je deze promotieperiode met me hebt gedeeld.

Hees.

Table of contents

1 General introduction	1
1.1 Background of the present investigation	1
1.2 Scope of the thesis	3
2 Literature survey	7
2.1 Elements of a biosensor	7
2.2 Biosensors of the first, second, and third generation	8
2.3 Glucose oxidase	10
2.4 Conducting polymers	11
2.5 Electrochemical techniques	15
2.6 Scanning tunneling microscopy	20
2.7 Theoretical aspects of amperometric biosensors	21
3 Synthesis and characterization of polymer modified electrodes for possible use in amperometric biosensors	33
3.1 Introduction	33
3.2 Synthesis of monomers	34
3.3 Synthesis of polymers	37
3.4 Enzyme adsorption	42
3.5 Conclusions	43
3.6 Experimental	43
4 Amperometric glucose sensor based on glucose oxidase immobilized within polypyrrole microtubules	55
4.1 Introduction	55
4.2 Results and discussion	57
4.3 Conclusions	74
4.4 Materials and methods	74

5 Scanning tunneling microscopy study of polypyrrole and of glucose oxidase. A model for the electronic interaction between glucose oxidase and polypyrrole in microtubular form	79
5.1 Introduction	79
5.2 Results and discussion	81
5.3 Conclusions	92
5.4 Experimental section	93
6 Third generation amperometric biosensor for glucose. Polypyrrole deposited within a matrix of uniform latex particles as mediator	97
6.1 Introduction	97
6.2 Results and discussion	99
6.3 Conclusions	111
6.4 Materials and methods	112
7 Kinetic study of the performance of the biosensors	117
7.1 Introduction	117
7.2 Results	118
7.3 Discussion	125
7.4 Concluding remarks	127
7.5 Materials and methods	128
8 Highly stable first generation glucose sensor utilizing latex particles as the enzyme immobilizing matrix	131
8.1 Introduction	131
8.2 Results and discussion	132
8.3 Conclusion	141
8.4 Experimental	141
Summary	145
Samenvatting	147
Curriculum vitae	149

1 General introduction

1.1 Background of the present investigation

Life today is becoming increasingly dependent on automation. More and more, processes are being controlled by systems that function with a high degree of autonomy. To make this possible, especially in industry fast data collection and processing, often with feedback loops, is needed. The number of control parameters that must be handled becomes too high for reliable manual operation and automated control is inevitable when optimal performance is desired.¹ The enormous progress in the development of micro-electronics has made fast and reliable data computing and processing relatively easy. However, the accurate and rapid collection of data is still a bottleneck in automated process control. Chemical sensors can simplify data acquisition to a great extent. Selective measurement of various parameters at the same time is possible and can be used to control the automated process. Because of this, the development of chemical sensors has received a great deal of scientific attention in recent years. Not only the chemical industry may benefit from these sensors but also the food industry, bio-industry, and medicine. Furthermore, there is a fast and growing need for sensing devices for environmental control. A sensor must give a selective and fast response to the presence of a specific compound in a complex mixture of components. About this selectivity, biosensors are the most promising devices today.^{2,3}

Sensors can be divided into physical, chemical, and biochemical sensors. Physical sensors measure traditional parameters such as temperature, pressure, humidity, and flow rate. They are generally not considered to be real sensors. According to a preliminary nomenclature proposal (IUPAC),⁴ chemical sensors are miniaturized devices that detect a chemical compound selectively and reversibly. The detection is accompanied by a concentration dependent electrical signal. Chemical sensors that make use of biological molecules, e.g., receptor proteins, antibodies, or enzymes, are called biosensors. Of all sensors, biosensors are the most selective ones. This is due to the intrinsic, highly selective properties of the biomolecular species inside the sensor. Biosensors suffer, however, from one severe drawback, namely instability of

the biological receptor molecule. These receptor molecules are subject to denaturation. Therefore, increasing the stability of the biomolecule is one of the major issues in biosensor research. Biological activity can be preserved by storing the biosensors under the right conditions, e.g., low temperatures. This may give long "off-line" lifetimes. Of greater interest is the lifetime of the biosensor under working conditions. Currently, this lifetime is still very limited. The stability of the biomolecule can be enhanced by immobilization. A range of immobilization techniques have been described in the literature.⁵⁻¹² Some of these techniques will be used in the next chapters of this thesis.

A classical chemical sensor is the pH-electrode. This electrode was already invented at the beginning of this century, when the pH-sensitivity of certain glass membranes was discovered.¹³ At that time the importance of this sensor was not recognized. Nowadays, a pH-electrode has become an indispensable instrument. After its invention many other ion selective electrodes (ISE's) followed and now a dozen cations and anions can be measured selectively by potentiometric measurements with these electrodes.¹⁴ More recently, other chemical sensors, based on semi-conducting materials, have been developed for the selective detection of various gases,¹⁵ ions, and even biomolecules.¹⁶ A number of detection principles have been described in the literature.^{17,18} The detailed description of these principles is, however, outside the scope of this thesis.

Biosensors were first mentioned as such in the literature in 1977.¹⁹ Before that time, devices that contained a biological sensing element were simply referred to as electrodes with a description of the kind of sensing component, e.g., enzyme electrode.²⁰ Now, commercial biosensors are available for a number of substrates like glucose, lactate, urea, and penicillin. As already mentioned, medicine has a major interest in biosensor development,²¹ because stable and reliable biosensors would make possible on line and in-vivo monitoring of biologically important compounds, such as metabolites, hormones, and drugs.²² This may lead to, for instance, the integration of an *in-vivo* blood sugar monitor with an automatic insulin delivery system for diabetes mellitus patients.

In the field of biotechnology, biosensors could be used for fermentation control by following fluctuations in the nutrients and adjusting their levels, when necessary.²³ In environmental technology biosensors could be used to monitor pollutants, pesticides, and herbicides. In food technology the concentration of various nutrients, the quality and freshness, contamination by micro-organisms, and the presence of prohibited components could be detected for all kinds of foodstuffs. In space research, biosensors could facilitate the monitoring of certain metabolic processes under influence of reduced gravity. Last but not least, the military industry is interested in biosensors for chemical and biological defence.

The potential use of sensors in a great number of different disciplines has led to a great deal of research activity. In 1991, more than 3000 publications and 300 patents

appeared on biosensors. In view of these figures, however, the number of commercially available biosensor devices is still very small.

1.2 Scope of the thesis

The main goal of the work described in this thesis is to develop biosensors containing electrodes that communicate directly with redox enzymes. For these so-called biosensors of the third generation intrinsically conducting polymers are used as electrode materials.

A description of the elements of a biosensor will be presented in Chapter 2. In this chapter a literature survey on biosensors based on redox enzymes and conducting

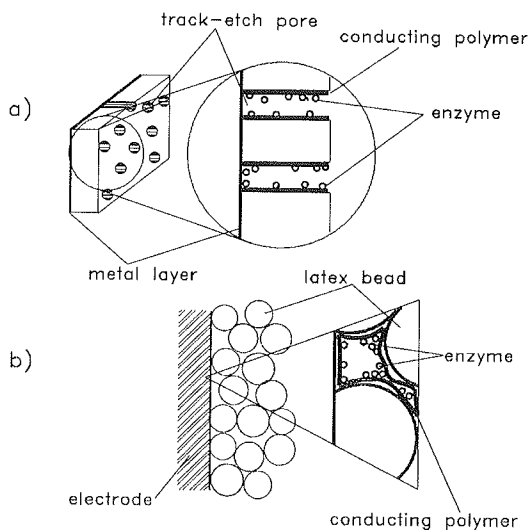


Figure 1. Schematic representation of the two microporous biosensors based on conducting polymers: (a) track-etch membrane biosensor; (b) latex membrane biosensor.

polymers will also be given, as well as a model that predicts the performance of a third-generation biosensor.

Tailor-made electrode materials which have the chemical and physical properties that are needed to make the electrode compatible with biological molecules require the synthesis of special conducting polymers.²⁴⁻³³ The polymers that we have synthesized and tested for use in a third-generation amperometric biosensor are

presented in Chapter 3. Glucose oxidase has been chosen as a model redox enzyme to test the usefulness of the materials.

The construction of a third-generation glucose sensor is described in Chapter 4. This sensor contains glucose oxidase, which is absorbed in hollow poly(pyrrole) microtubules which in turn are incorporated in track-etch membranes (see Figure 1a).

In Chapter 5 the track-etch poly(pyrrole) biosensor is characterized by means of scanning tunneling microscopy. A model explaining the direct interaction between the enzyme and the electrode is proposed in this chapter.

A different type of biosensor that functions according to the same principle as the track-etch membrane biosensor is presented in Chapter 6. In this sensor glucose oxidase is adsorbed on poly(pyrrole) which is incorporated inside the inter-spherical pores of a membrane composed of uniform latex particles (see Figure 1b).

The biochemical characterization of the two third-generation biosensors is given in Chapter 7. The performance of the sensors is evaluated by means of the model presented in Chapter 2.

Finally, in Chapter 8 a first-generation glucose sensor is described which is constructed using the same matrix as the third-generation biosensor discussed in Chapter 6. This sensor falls somewhat outside the scope of this thesis as detection of glucose occurs via hydrogen peroxide, which is produced during the enzymatic reaction. However, we have included this sensor as its performance is such that it competes favourably with other first-generation glucose sensors reported in the literature.

References

1. *Electronic Instrumentation Laboratory Profile 1992*. 4th Ed. Delft University of Technology, Delft: (1992).
2. Brooks, S.L., Higgins, I.J., Newman, J.D. and Turner, A.P.F., *Enzyme. Microb. Technol.*, (1991) **13**: 946-955.
3. Turner, A.P.F., *Analytical Proceedings*, (1991) **28**: 376-377.
4. Cammann, K., Lemke, U., Rohen, A., Sander, J., Wilken, H. and Winter, B., *Angew. Chem.*, (1991) **103**: 519-541.
5. Cho, Y.K. and Bailey, J.E., *Biotechnol. Bioeng.*, (1978) **20**: 1651-1665.
6. Kozhukharova, A., Kirova, N., Popova, Y., Batsalova, K. and Kunchev, K., *Biotechnol. Bioeng.*, (1988) **32**: 245-248.
7. Sonawat, H.M., Phadke, R.S. and Govil, G., *Biotechnol. Bioeng.*, (1984) **26**: 1066-1070.
8. Bartlett, P.N. and Whitaker, R.G., *J. Electroanal. Chem.*, (1987) **224**: 37-48.
9. Kaetsu, I., Kumakura, M. and Yoshida, M., *Biotechnol.*, (1979) **11**: 847-861.
10. Hsiue, G. and Wang, C., *Biotechnol. Bioeng.*, (1990) **36**: 811-815.
11. Beh, S.K., Moody, G.J. and Thomas, J.D.R., *Analyst.*, (1989) **114**: 1421.
12. Galiatsatos, C., Ikariyama, Y., Mark, J.E. and Heineman, W.R., *Biosensors & Bioelectronics*, (1990) **5**: 47-61.
13. Cremer, M., *Z. Biol.*, (1906) **47**: 562.
14. Cammann, K. *Das Arbeiten mit Ionselektiven Elektroden*. 2nd Ed. Springer, Berlin: (1977).
15. Taguchi, T. and Naoyoshi, K., *Patent*, (1971) **11520**: US-A.
16. Schasfoort, R.B.M., Kooyman, R.P.H., Bergveld, P. and Greve, J., *Biosensors & Bioelectronics*, (1990) **5**: 103-124.
17. Turner, A.P.F., Karube, I. and Wilson, G.S. *Biosensors. Fundamentals and Applications*. Oxford University Press, New York: (1989).
18. Cass, A.E.G. *Biosensors. A Practical Approach*. Oxford University Press, New York: (1990).
19. Cammann, K., *Fresenius Z. Anal. Chem.*, (1977) **287**: 1-9.
20. Clark Jr., L.C. and Lyons, C., *Ann. N. Y. Acad. Sci.*, (1962) **102**: 29-45.
21. Alcock, S., Karayannis, M. and Turner, A.P.F., *Biosensors & Bioelectronics*, (1991) **6**: 647-652.
22. Pickup, J.C. and Alcock, S., *Biosensors & Bioelectronics*, (1991) **6**: 639-646.
23. Renneberg, R., Trottkriegeskorte, G., Lietz, M., Jäger, V., Pawlowa, M., Kaiser, G., Wollenberger, U., Schubert, F., Wagner, R., Schmid, R.D. and Scheller, F.W., *J. Biotechnol.*, (1991) **21**: 173-185.
24. Havinga, E.E., van Horssen, L.W., ten Hoeve, W., Wynberg, H. and Meijer, E.W., *Polymer Bulletin*, (1987) **18**: 277-281.
25. Havinga, E.E., ten Hoeve, W., Meijer, E.W. and Wynberg, H., *Chemistry of Materials*, (1989) **1**: 650-659.
26. Souto-Maior, R.M., Hinkelmann, K., Eckert, H. and Wudl, F., *Macromol.*, (1990) **23**: 1268-1279.
27. Patil, A.O., Ikenoue, Y., Basescu, N., Colaneri, N., Chen, J. and Wudl, F., *Synth. Met.*, (1987) **20**: 151-159.
28. Foos, J.S., Degnan, S.M., Glennon, D.G. and Beebe, X., *J. Electrochem. Soc.*, (1990) **137**: 2530-2533.
29. Roncali, J., Marque, P., Garreau, R., Garnier, F. and Lemaire, M., *Macromol.*, (1990) **23**: 1347-1352.
30. *Sci. Am.*, (1990): 79.
31. Degani, Y. and Heller, A., *J. Am. Chem. Soc.*, (1989) **111**: 2357-2358.
32. Pishko, M.V., Katakis, I., Lindquist, S., Ye, L., Gregg, B.A. and Heller, A., *Angew. Chem.*, (1990) **102**: 109.
33. Foulds, N.C. and Lowe, C.R., *Anal. Chem.*, (1988) **60**: 2473-2478.

2 Literature Survey

2.1 Elements of a biosensor

Biosensors are made up of three different, but closely connected elements: the selector, the transducer, and the detector (Figure 1). The selector is the part that selectively binds the compound to be detected, the transducer transforms the occurring (bio)chemical reaction into a physically measurable signal, and the detector processes this physical signal. The design and construction of biosensors requires the involvement of different disciplines. Biochemistry brings in the knowledge of how to achieve high selectivity and sensitivity, whereas physics provides the information with regard to microelectronics and computers.¹ For a successful development of the transducer these disciplines should be combined. There are numerous transduction methods available today, some of which are named in Table 1.¹ One of the most useful is the transformation of a chemical reaction or a biological event into an electrical potential or current. The electrochemical devices that have been developed based on this kind of transduction method are relatively easy to construct and to handle.² Furthermore, their miniaturization is feasible. In this regard, the fast developments in micro-electronics have made it possible to develop "intelligent" sensors, which are self-testing and self-calibrating.

Table 1. *Examples of the elements in a biosensor.*

Selector	Transducer	Detector
Enzyme	Current	Amperometric electrode
Antibody	Potential	Potentiometric electrode
DNA	Surface plasmon	Laser light reflectometer
Receptor	Impedance	Conductometer

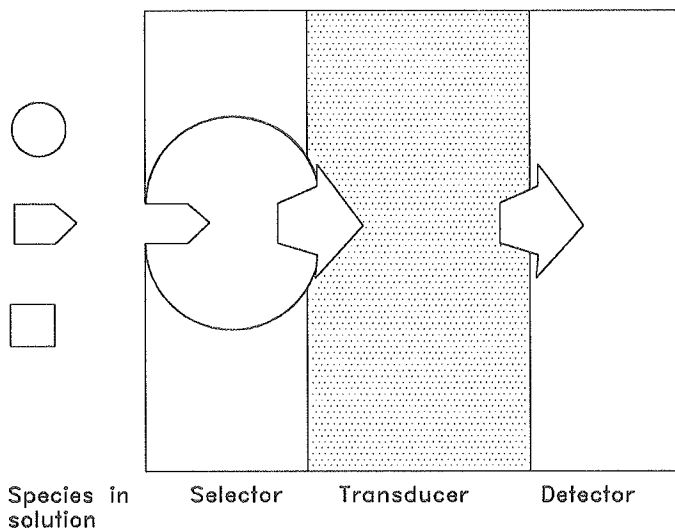


Figure 1. Schematic profile of a traditional amperometric enzyme electrode, which shows the three components of a biosensor.

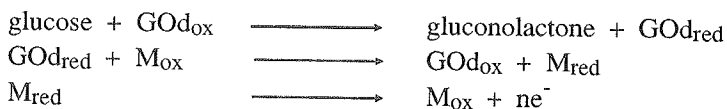
2.2 Biosensors of the first, second, and third generation

First-generation amperometric biosensors³ work by means of the detection of enzymatically produced (or consumed) electroactive species. A good example is the traditional glucose sensor. This sensor amperometrically detects the hydrogen peroxide which is produced in the oxidation of glucose, catalyzed by the enzyme glucose oxidase (GOd):



This sensor has several drawbacks, however. The most important ones are the denaturation of the enzyme by the hydrogen peroxide and the strong dependence of the electrical signal on the oxygen concentration.

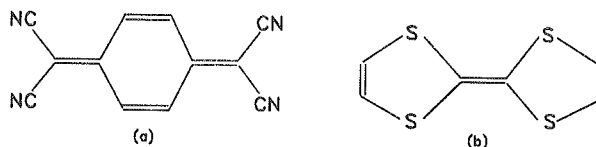
Newer sensor concepts make use of artificial electron carriers. These biosensors are classified as second-generation biosensors.¹ The carrier or mediator (M) shuttles the electrons involved in the redox process from the enzyme to the electrode or vice versa.^{1,4-14} This is exemplified by the following reaction scheme:



Examples of mediators are ferrocene,¹⁵ ferrocene derivatives,¹⁶ and bipyridyl complexes of osmium chloride.^{6,17}

Ideally, one would like to have a material that communicates directly with a redox enzyme. In that case, no co-substrates such as oxygen or mediators are required and the electrons involved in the redox process are measured directly at the electrode. Enzyme electrodes based on this principle are called third-generation biosensors.¹ Only a few years ago it was thought that direct electrochemistry with redox proteins was impossible, but nowadays this opinion has changed.¹⁸⁻²⁰ Early workers in this field made use of mercury electrodes. It is now known that enzyme adsorption on this metal electrode is very strong and leads to denaturation of the enzyme molecules. Evidence has been presented that bare metal electrodes in general are incompatible with redox enzymes.²¹ Surface modification of the electrode is required to make it more compatible with the biological receptor molecule.^{16,22-29} Nevertheless, it has been reported that small redox proteins like cytochrome c can transfer electrons directly to bare electrodes, e.g., glassy carbon.³⁰ For large redox enzymes such as glucose oxidase this is much more difficult to realize as these enzymes have thick insulating protein shells. Their catalytic centers are buried deep inside and are protected from the surroundings.^{31,32} For these large redox enzymes it becomes important that they are immobilized on a compatible electrode surface in a way that makes electron transfer from the catalytic center to the electrode feasible without the occurrence of denaturation.^{29,33,34}

In many research groups work is currently in progress to develop third-generation biosensors. Highly conducting organometallic complexes are one class of materials that are studied for achieving direct electronic contact with redox enzymes. These complexes include charge-transfer salts of tetracyanoquinodimethane (1a) and tetrathiafulvalene (1b).



1

Enzymes like glucose oxidase³⁵ and cholinesterase³⁶ have already been shown to communicate directly with electrode materials based on these complexes.

2.3 Glucose oxidase

Glucose oxidase is the redox enzyme that is used as the selector in the biosensors presented in this study. In this paragraph, some background information will be given on this enzyme. Before oxygen played an important role in life, bio-electrochemical processes took place in the narrow potential range of 700 mV. When oxygen became available as an energy source, this range extended to 1300 mV. Enzymes containing flavins could evolve.^{37,38} Glucose oxidase (β -D-glucose: O₂ oxidoreductase, E.C. 1.1.3.4) from *Aspergillus niger* is such a flavin-containing enzyme. It is an aerobic dehydrogenase, which catalyzes the oxidation of β -D-glucose to D-gluconolactone. Under natural conditions, this oxidation is accompanied by the reduction of molecular oxygen to hydrogen peroxide (see paragraph 2.2). The flavin co-factor (flavine-adenine dinucleotide, FAD) is called the prosthetic group and is responsible for the redox properties of the enzyme (Figure 2). Glucose oxidase contains two FAD-units per molecule.³⁹ These units are firmly bound to the peptide chain, but are not covalently linked. The isoalloxazine system of FAD can exist in three redox states: the oxidized one shown in Figure 2, and in two reduced states which are attained by the uptake of one and two electrons, respectively.³⁷ Despite the fact that glucose oxidase is abundantly used, there is very little structural information available on this enzyme. As with most flavin enzymes,⁴⁰ no X-ray structure has yet been solved. The reason is the large carbohydrate content (16%) of the native molecule,^{39,41} which prevents crystallization of the enzyme.

In large flavin proteins like glucose oxidase the prosthetic group is usually anchored in a crevice formed by the protein structure. It is known that in glucose oxidase the flavin is only partially accessible to water.³² Attempts to accomplish

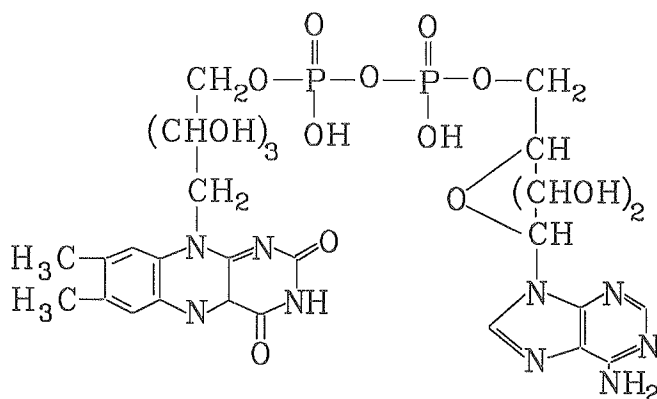


Figure 2. FAD with its isoalloxazine ring system in the oxidized state.

electronic interaction with this redox protein should take into account the orientation and location of the prosthetic group inside the protein molecule. Glucose oxidase has a high affinity for molecular oxygen.⁴² Consequently, oxygen will always be a competing electron acceptor when it is present during experiments in which direct communication is tested. Careful design of the experiments is, therefore, necessary. In Table 2 some physical and chemical parameters of glucose oxidase are presented.^{39,41-43}

Table 2. Some physicochemical properties of glucose oxidase from *A. niger*.

Parameter	Value
Molecular weight	150,000 Dalton
Number of subunits	2
Co-factor	2 FAD
Carbohydrate content	16 %
Isoelectric point (pI)	4.5
Electrophoretic mobility	$2.2 \cdot 10^{-5} \text{ cm}^2 \text{ s}^{-1} \text{ V}^{-1}$
Diffusion coefficient	$4.12 \cdot 10^{-7} \text{ cm}^2 \text{ s}^{-1}$
Turnover number	500 s^{-1}
Michaelis-Menten constant (glucose)	140 mM*
Michaelis-Menten constant (oxygen)	0.33 mM

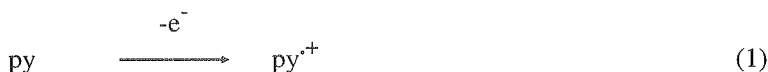
*Highest value reported

2.4 Conducting polymers

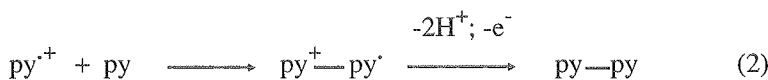
The type of conducting polymers used in this study are poly-aromatic polymers, synthesized from pyrrole and thiophene. Normally, organic polymers are considered to be insulators. However, in poly(pyrrole) and poly(thiophene) it is possible to create electron conduction by doping. In general, during doping the polymers are reduced or oxidized, leading to an excess of electrons or electron holes.⁴⁴⁻⁴⁶ These charge carriers can move along the polymer chain.⁴⁷ Ideally, linear chains of the monomers form a polymer with infinite conjugation length which can lead to electronic conductivity in the metallic region.⁴⁸ In the following paragraphs we will discuss in more detail the synthesis and electrochemistry of poly(pyrrole) as this polymer has been used as the main conducting matrix in our biosensors.

2.4.1 Synthesis of poly(pyrrole)

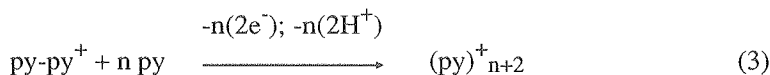
Poly(pyrrole) can be synthesized both electrochemically and by chemical oxidation.⁴⁹ In the case of electrochemical polymerization, the initial step is the removal of an electron from the pyrrole ring at the anode.⁵⁰ The pyrrole monomer is oxidized to its corresponding π -radical cation:



As suggested by Wegner this radical cation may react with another radical cation to form a dimer.⁵⁰ However, according to Asavapiriyant *et al.*⁴⁹ dimerization of small radical species is unusual. These authors have suggested that dimer formation follows a so-called ECE mechanism.⁵¹ This means that a heterogeneous electron transfer step at the electrode surface (E) is followed by a homogeneous chemical reaction (C) and the chemical reaction in its turn is followed by another heterogeneous electron transfer step. Reaction (1) is then succeeded by:



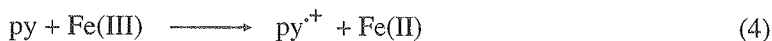
At the electrode surface the dimer, which is also electroactive at the poised electrode potential, is subsequently oxidized and converted to the trimer and eventually to the polymer (3).



As the polymer is produced in its oxidized (and conducting) state, counter-ions are taken up into the polymer structure to maintain electroneutrality. It is generally found that approximately 1 counter-ion (supplied by the electrolyte) is built in for every 4 repeat units.^{49,50} From the reaction scheme it can be seen that protons are produced during the polymerization. As the polymerization potential is independent of pH, the reaction scheme must involve a completely irreversible step involving the ejection of protons. The identity of this step has not yet been clarified in the case of poly(pyrrole).⁴⁹ For thiophene polymerization the elimination of protons is the rate determining step in the coupling reaction.⁵²

The synthesis of poly(pyrrole) by chemical oxidation is a way to produce the polymer when the electrochemical method is not feasible (see for instance Chapter 4). Chemical oxidation is similar to electrochemical oxidation. Frequently used

oxidants like Fe(III) and the hexacyanoferrate(III)-anion attack the pyrrole ring and oxidize it. This resembles the oxidation at an electrode surface.^{49,53} As in electrochemical polymerization, the anion of the oxidant is incorporated into the partly oxidized polymer structure. In the case of chemical oxidation by Fe(III) the polymerization reaction is believed to begin as follows:⁵⁴



The propagation with concomitant elimination of protons has been suggested to follow the same route as for the electrochemical polymerization (*vide supra*). Reaction (4) was found to be the rate determining step.⁵⁴ In other words, the oxidation of the monomer determines the reaction rate. This oxidation is supposed to proceed by an outer-sphere mechanism which means that the rate of reaction will depend on how effectively the pyrrole moiety can approach the solvated Fe(III)-anion.⁵⁵ Pyrrole is a weak base and it can approach Fe(III) solvated by water much better than Fe(III) solvated by one or two OH⁻-groups. Therefore, the rate of reaction (4) increases on decreasing the pH of the solution.⁵⁴

The deposition of conducting polymers on an electrode usually follows a mechanism of nucleation and growth.⁵⁶ Little is known about the structure of the complete conducting polymer films. The simple growth model which is implicated by reaction (3) cannot hold as this accounts for one-dimensional growth and concomitant one-dimensional conductivity only. The resulting films, however, display three-dimensional growth and conductivity (see references 49,57, and 58 and also Chapter 3). The observed high conductivity suggests that the polymer film has a rather organized structure (see Asavapiryanont *et al.*⁴⁹ and Chapter 5).

2.4.2 Charge transport in poly(pyrrole)

When two atoms combine to form a molecule, their atomic orbitals overlap to give a bonding and an anti-bonding molecular orbital. The energy level of the anti-bonding orbital is higher than the level of the bonding orbital. In metals many atoms strongly interact and each combination of atoms passes into its own set of molecular orbitals. The differences in energy level for each bonding and for each anti-bonding orbital are very small. Therefore, when a large number of atoms are combined, a continuous band of bonding and anti-bonding orbitals is formed. In this way, the so-called valence band is generated from s-orbitals, and the so-called conduction band from p-orbitals. This band picture is frequently used to explain the difference in electronic conductivity between metals, insulators, and semi-conductors.⁵⁹ In the case of conducting polymers, the band picture is essentially that

The change in band structure during the oxidation process is illustrated in Figure 3b. This figure shows the transition of the insulating polymer (a) to a state of low (b) and finally high (c) oxidation. State (b) represents the polaron. New electronic levels are introduced between the conduction band and the valence band. The lower level is occupied by one electron. This corresponds to the radical cation in eq. (5). The new levels lead to newly allowed electronic transitions. This explains the higher electrical conductivity. State (c) is the bipolaron state. The unpaired electron has been removed and a dication is formed. The bipolaron has been demonstrated to be the species responsible for charge storage in poly(thiophene).⁶⁴ Overoxidation of conducting polymers like poly(pyrrole) and poly(thiophene) leads to structures that carry one positive charge on every monomeric unit (Figure 3a). This situation makes the polymer insulating again.^{46,53}

Conducting polymers can display both faradaic and capacitive charging behaviour.⁶⁵⁻⁶⁷ It has been shown that these two processes cannot be separated.⁶⁷⁻⁶⁹ Capacitive charging leads to large currents when the conducting polymer is electrochemically characterized, e.g., by cyclic voltammetry (*vide infra*). The electrochemical process of interest, viz. the faradaic process, may be completely obscured by the capacitive currents. By utilizing thin polymeric films, which are in good electrical contact with the underlying electrode, it is possible to suppress the capacitive current to a large extent.⁵¹

2.5 Electrochemical techniques

A number of electrochemical analytical methods have been used in this investigation, viz. amperometry, chronoamperometry, cyclic voltammetry, and the rotating disk electrode (RDE) technique. These methods will be discussed briefly in the following paragraphs.

2.5.1 Amperometry

The measurement of a current at a constant potential is called amperometry. Under favourable conditions, this technique allows the detection of molecules or ions at concentrations as low as 10^{-9} M and it has a dynamic range of 3 to 4 orders of magnitude.¹ Amperometry is often applied in electrolysis. The current is measured as a function of the fraction of converted material.⁵¹ In analytical measurements, however, very little material is consumed and the bulk concentration of the electroactive species of interest does not change. Therefore, steady state conditions can be assumed. In amperometric analysis of biosensor response the current is

measured at various substrate concentrations and compared with the current when no substrate is present. The difference between these two situations is an indication of the biosensor activity.

2.5.2 Chronoamperometry

Chronoamperometry is a technique that measures the current as a function of time, directly after the introduction of a change in potential. This is illustrated in Figure 4a and 4b, where the potential is increased from E_1 to E_2 at time t_0 . At E_1 no faradaic processes occur. The potential E_2 is in the diffusion controlled regime. As a result, the concentration of the electroactive species at the surface of the electrode goes nearly to zero. Diffusion limitation causes a concentration gradient at the electrode surface. The slope of the current-time curve follows the shape of this concentration gradient. The diffusion limited current, i_d , can be calculated with the Cottrell equation (see also 2.7.1.):^{51,70}

$$i_d(t) = nF.A.D^{1/2}c_b / \pi^{1/2}t^{1/2} \quad (6)$$

in which n is the number of electrons, F is the Faraday constant, A is the electrode surface area, D is the diffusion coefficient, and c_b is the bulk concentration of the electroactive species. Equation (6) shows that the diffusion limited current is

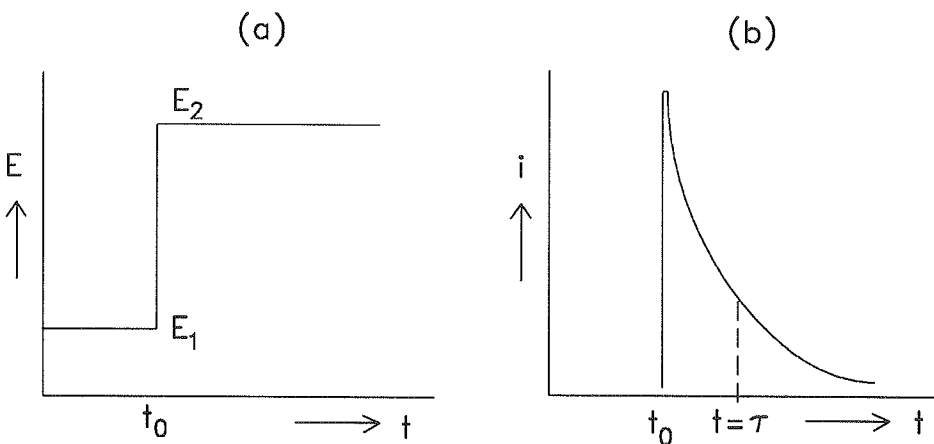


Figure 4. Illustration of the chronoamperometric technique; (a) potential profile, (b) current response as a function of time.

proportional to the bulk concentration of the electroactive species and inversely proportional to $t^{1/2}$. Measuring the current after a potential step under various bulk concentrations, c_b , will lead to different decay curves. Sampling the magnitude of the current at a fixed time, $t = \tau$, will give information about the current dependence on c_b . Chronoamperometry under "Cottrell conditions" must be carried out carefully for several reasons. Very high currents are required at the moment of the potential step. If such high currents cannot be produced, the measured current is different from the current predicted by (6). Also, the recording device might not be able to follow the sudden current increase at the start of the experiment. In that case, the recorder will be overdriven and accurate readings are not possible directly after the potential step. Furthermore, current flows due to capacitive processes. Non-faradaic currents also decay exponentially in time.⁵¹ Finally, at the moment of the potential step the solution must be quiescent. Convection will disturb the measurement.

2.5.3 Cyclic voltammetry

Much information can be obtained in an electrochemical experiment when a potential sweep is applied, e.g., as in cyclic voltammetry. In this technique the potential is raised from a starting potential E_0 to an end potential E_1 and subsequently lowered back to E_0 . This is done at a constant sweep rate (Figure 5). When in the presence of an oxidizable species the potential scan is started at a point well below the oxidizing potential E^0 of the species, only non-faradaic current flows for a while (Figure 5b). When the potential reaches E^0 oxidation starts and current flows (raising part in Figure 5b). At the potential E^0 the surface concentration of the oxidizable species is decreased. This leads to an increase in flux from the bulk solution to the electrode surface and consequently to an increase in current. Raising the potential further leads to a surface concentration near zero. As a consequence, mass transfer to the surface reaches a maximum rate and subsequently declines due to depletion. The result is the peaked current shown in Figure 5b. At E_1 the potential scan is reversed. At the electrode surface a large concentration of oxidized material is present at that moment. When the potential reaches E^0 reduction starts to take place and a cathodic current flows. The cathodic peak has the same form as the anodic peak for basically the same reasons as mentioned above. It is outside the scope of this study to derive an equation for the dependence of the current on the conditions applied in cyclic voltammetry. The current is proportional to the bulk concentration of the redox species and to the square root of the scan rate.⁵¹ In a reversible (Nernstian) system, the difference in potential between the oxidation and the reduction peak is close to $2.3 RT/nF$ (59 mV at 25 °C for a one-electron process). This difference in peak potential is a useful test of a reversible reaction. Irreversible systems will show a larger potential difference between the two current peaks and possibly also a less symmetric shape (see Bard and Faulkner⁵¹ and also Chapter 3).

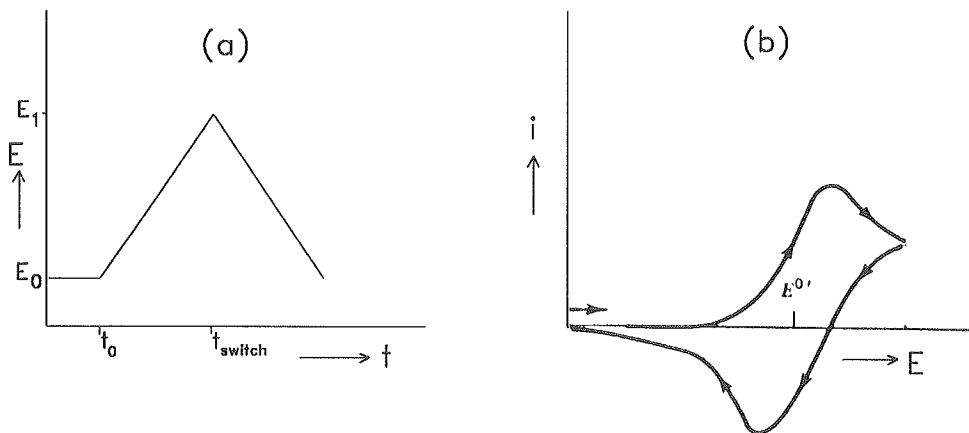


Figure 5. Illustration of cyclic voltammetry; (a) profile of the potential sweep, (b) resulting current as a function of the potential sweep.

Cyclic voltammetry is useful if one wants to obtain information on the redox behaviour of simple ions and molecules as well as on complicated electrode processes in a single experiment (Chapter 3). For this reason cyclic voltammetry has become a very popular technique.⁵¹

2.5.4 Rotating disk electrode technique

In the rotating disk electrode (RDE) technique the working electrode moves with respect to the solution. This electrode is a small disk, which is rotated at such a rate that a smooth flow is obtained at the surface without the occurrence of turbulence (Figure 6). The electrode is connected to a potentiostat by means of a brush contact.

The RDE-technique is a hydrodynamic method and has the advantage that a steady-state condition is reached rather quickly. To attain this steady-state, a minimum angular velocity of the disk is required. On the other hand, the angular velocity should not be so high that vortex formation occurs. In the correct velocity range fast and accurate electrochemical measurements are possible. Double layer charging and concentration polarization does not occur. As a result of high mass transport rates, the contribution of mass transfer to the overall electrode process is much smaller. The electron transfer processes may, therefore, be studied more closely.

The RDE set-up can be used to measure the activity of immobilized enzymes. Briefly, the so-called RDE enzymatic assay for glucose involves the amperometric detection of hydroquinone which is generated in the enzymatic reaction. The RDE

method is a good choice for the activity measurement of immobilized enzymes because it is based on forced convection (see above). Under forced convection

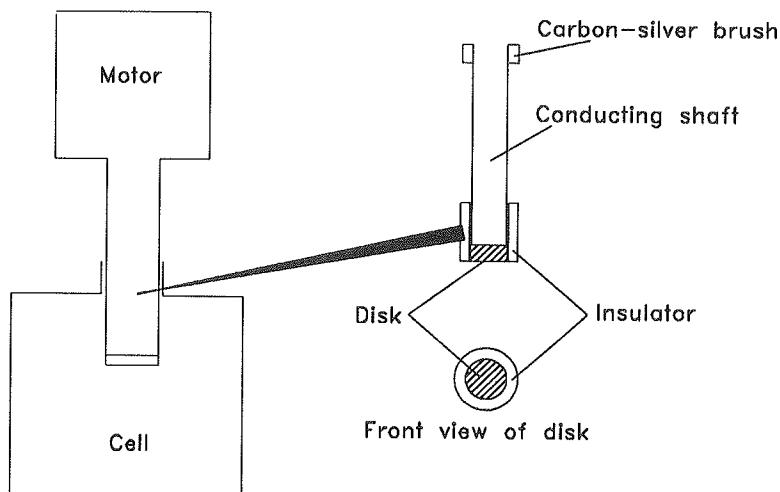


Figure 6. Illustration of the rotating disk electrode set-up.

conditions the transport of the species which is to be detected at the electrode, viz. the enzymatically generated hydroquinone, and the subsequent electrode reaction are very fast. As a result, the enzymatic reaction will be the rate determining step. This means that the slopes of current-time plots for the immobilized enzyme and for the enzyme in solution can be correlated. The measured current at the RDE is, therefore, directly proportional to the enzyme activity, irrespective of whether the enzyme is in solution or is immobilized. For the activity measurements of enzyme samples with the RDE set-up, the cell shown in Figure 6 allows for the introduction of these samples. The samples may contain, e.g., glucose oxidase in solution or glucose oxidase immobilized on some carrier material (e.g. conducting polymers, latex, or hydrogels). A more detailed description of the measurement of glucose oxidase activity with the RDE-technique will be given in Chapter 4.

2.6 Scanning tunneling microscopy

With scanning tunneling microscopy (STM) it is possible to image surfaces with atomic or molecular resolution. We have used this technique to study the surface of conducting polymer structures and to image individual glucose oxidase molecules (see Chapter 5).

STM is based on the tunneling of an electric current from a metallic tip to the surface of a sample (Figure 7).⁷¹ The tip is scanned over the surface of the sample. During this scanning process, the tunnel current is held constant by adjusting the distance between the tip and the surface. The degree of adjustment gives information on the surface morphology. This information is computerized and an image of the surface structure is generated. A critical condition for STM is the fact that the sample must be electrically conducting. Up to now only a limited number of polymers have been studied by STM. Most of these are conducting polymers.⁷²⁻⁷⁷ When the sample

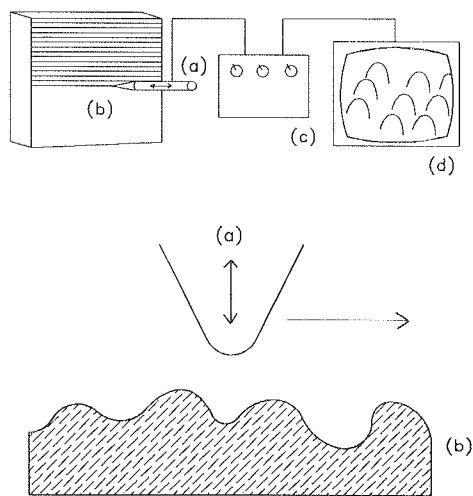


Figure 7. Set-up for scanning tunneling microscopy; (a) needle tip, (b) sample surface, (c) electronics, (d) monitor.

is non-conducting it is still possible to obtain STM-images, viz. by depositing a thin layer of the sample material on a conductive substrate. Atomically flat substrates like highly oriented pyrolytic graphite (HOPG) or a noble metal surface can be used for this. In this way it has been possible to obtain STM images of, e.g., lipids,^{78,79} DNA,⁸⁰ and of n-alkanes.⁸¹

2.7 Theoretical aspects of amperometric biosensors

In an amperometric biosensor the following processes are important and should be considered when designing such a sensor: (i) transport of the analyte to the surface of the sensor, (ii) binding of the analyte to the redox enzyme incorporated in the sensor, and (iii) conversion of the analyte by the redox enzyme and transfer of the electrons involved to the electrode.² A theoretical description of the response of a biosensor has a predictive character. It can be used for the analysis of the experimental data and, more importantly, for effectively optimizing the biosensor. In the following some theoretical aspects related to items (i) - (iii) will be discussed.

2.7.1 Mass transport

In order to be detected by the receptor molecule the analyte must be transported from the bulk solution to the biosensor. Consumed analyte must be replenished to maintain steady-state conditions. There are three modes of transport, viz., migration, diffusion, and convection.

Migration is the movement of a charged species due to the presence of a gradient in the electrical potential. In well-defined electrochemical set-ups these potential gradients do not exist. Biosensor measurements are generally carried out in solutions, containing an excess of supporting electrolyte. The electrolyte suppresses any potential gradients that might be formed. Consequently, migration is not a significant mechanism to be discussed here.

Diffusion is the movement of particles as a result of a concentration gradient. Diffusion is dependent on the random motion of molecules. Therefore, this process is relatively slow.

The formal description of diffusion is given by the first and second law of Fick (7,8).^{51,59}

$$j = -D(dc/dx) \quad (7)$$

$$dc/dt = D(d^2c/dx^2) \quad (8)$$

In equation (7) j is the net flux of matter, dc/dx is the concentration gradient, and D is the diffusion coefficient (expressed in m^2s^{-1}). These laws hold for movement in one dimension. They are, however, sufficient for describing transport to a biosensor surface. As we are interested in the concentration of a chemical compound at a given place on the biosensor surface at the time of measurement, we need to know the rate

of transport of the analyte towards the surface, described by (7), and the build-up (and consumption) of the substrate at the biosensor surface, described by (8). To solve (8) we must define initial and boundary conditions. An appropriate initial condition is the bulk substrate concentration, c_b . When the enzymatic reaction is sufficiently fast the surface concentration, c_0 , reduces effectively to zero and this gives a boundary condition. The difference $c_b - c_0$ is the concentration gradient leading to mass transport by diffusion. As long as there are no other means of transport (e.g. convection, *vide infra*) the reaction rate is diffusion controlled. Equation (8) can now be solved to give the following equation:⁵¹

$$c = c_\infty \operatorname{erf}(x/2D^{1/2}t^{1/2}) \quad (9)$$

in which c_∞ is the concentration at an infinite distance from the electrode surface and *erf* stands for the error function. In the treatment of diffusional problems, the error function or integrated normal error curve is often encountered.^{2,51} The function describes the advancement to a unit limit as the distance x reaches infinity. Equation (9) describes the increase of analyte concentration at increasing distance from the surface (x in numerator), as well as its decrease at increasing reaction time (t in denominator). The practical meaning of this expression in the case of a biosensor is

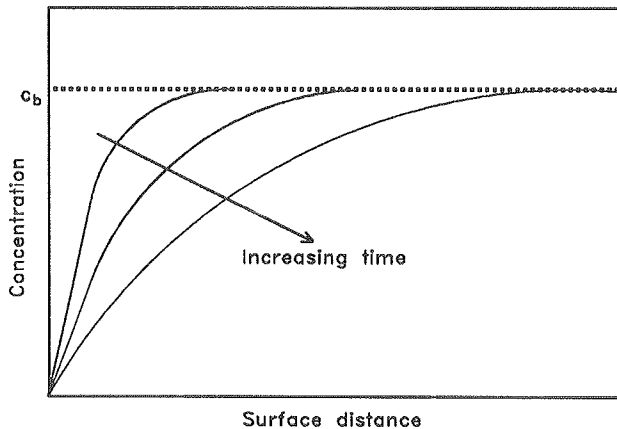


Figure 8. Concentration profiles in a stagnant solution for a reaction of which the velocity is dependent on diffusional mass transport.

that under diffusion controlled conditions a decaying response can be expected (Figure 8). The derivative of (9) with regard to the distance, x , can be substituted in

(7), to give the Cottrell equation for the chronoamperometric response of a biosensor (see 2.5.2, eq. (6)).

Applying convection is very favourable for the biosensor analysis. In many cases it results in enhancement of the sensitivity and in a more stable and reproducible response. Convective mass transport is achieved by moving the electrode with respect to the solution (e.g. the rotating disk electrode, see 2.5) or by forcing the solution to move past the electrode. Convection maintains the concentration of all species at the

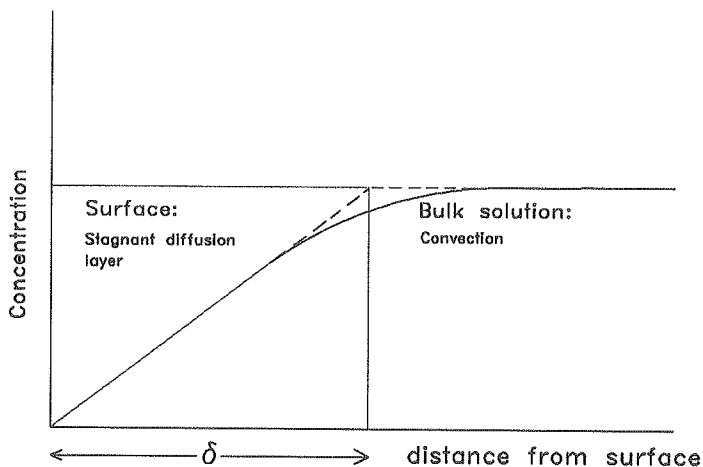


Figure 9. Concentration profile under convective control. Dashed line: theoretical profile; solid line: experiment.

bulk concentration value. A quick and stable response rather than a decaying response is achieved. Only in a very thin layer on the surface of the electrode, is convection not possible and mass transfer is controlled by diffusion. This stagnant layer is called the diffusion layer, δ . In this layer a steady-state concentration profile exists in which the surface reaction is in equilibrium with mass transport (Figure 9). Biosensors often contain some kind of membrane with thickness l_m . If care is being taken to keep l_m as small as possible, concentration polarization can be kept to a minimum, simply by applying convection during the measurements. For a typical substrate like glucose, the diffusion coefficient D approximates $10^{-9} \text{ m}^2 \text{ s}^{-1}$, so a membrane layer in the order of a few micrometers is sufficiently thin. In general, this is easily achievable.

In Figure 10 it is shown how long it takes for a molecule with $D = 5 \times 10^{-10} \text{ m}^2 \text{ s}^{-1}$ to travel a distance x in a non-stirred solution. It can be concluded that convection is of paramount importance for a biosensor.

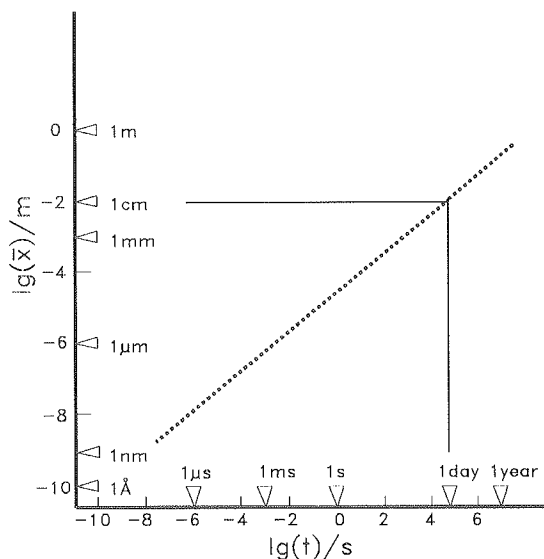
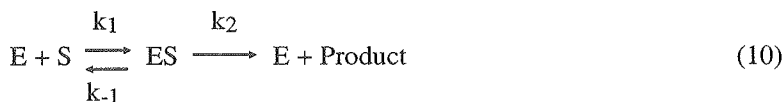


Figure 10. Mean distance travelled by a small molecule with a diffusion coefficient of $5 \cdot 10^{-10} \text{ m}^2 \text{ s}^{-1}$.

2.7.2 Binding and conversion

An important step that takes place in a biosensor is the recognition of the analyte or substrate (S) by the biological receptor molecule, e.g., an antibody or an enzyme (E). Formation of the complex E-S generally is very fast and limited by diffusion. When the receptor is a redox enzyme (e.g. glucose oxidase), the complex formation is followed by a redox reaction (e.g. the oxidation of glucose). In third generation amperometric biosensors, no co-substrate is involved and the enzyme reaction can be described by a simple Michaelis-Menten model:⁵⁹



$$v = \frac{k_2[E]_0[S]}{K_M + [S]} \quad (11)$$

$K_M = (k_{-1} + k_2)/k_1$, E_0 is the total concentration of enzyme. The Michaelis-Menten constant K_M reflects to some extent the affinity of the enzyme for its substrate. A reciprocal form of the Michaelis-Menten equation (Lineweaver-Burk plot^{82,83}):

$$\frac{1}{v} = \frac{K_M}{k_2[E]_0[S]} + \frac{1}{k_2[E]_0} \quad (12)$$

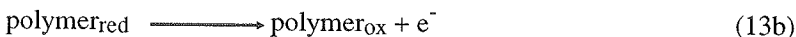
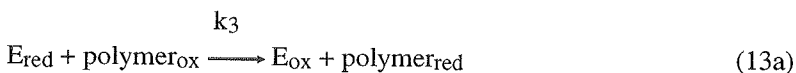
is often used to plot the rate data in a linear way. Deviation from linearity of this plot reveals whether mass transport is important.⁸⁴

The model described above is very simple and not always valid.¹ It applies to systems wherein the concentration of S is sufficiently higher than the concentration of the complex ES. In amperometric biosensor systems this generally is true.²

2.7.3 Conversion and electron transfer

The reaction sequence for a third generation amperometric biosensor (see 2.2) based on a redox enzyme and a conducting polymer is given in Figure 11. The oxidized enzyme E_{Ox} converts the analyte S into product P and gets reduced to its reduced form E_{red} . The enzyme is reoxidized by the conducting polymer, which in turn donates the involved electrons to the electrode. The corresponding kinetic scheme is the following:

Scheme 1. Kinetic scheme of a third generation biosensor.



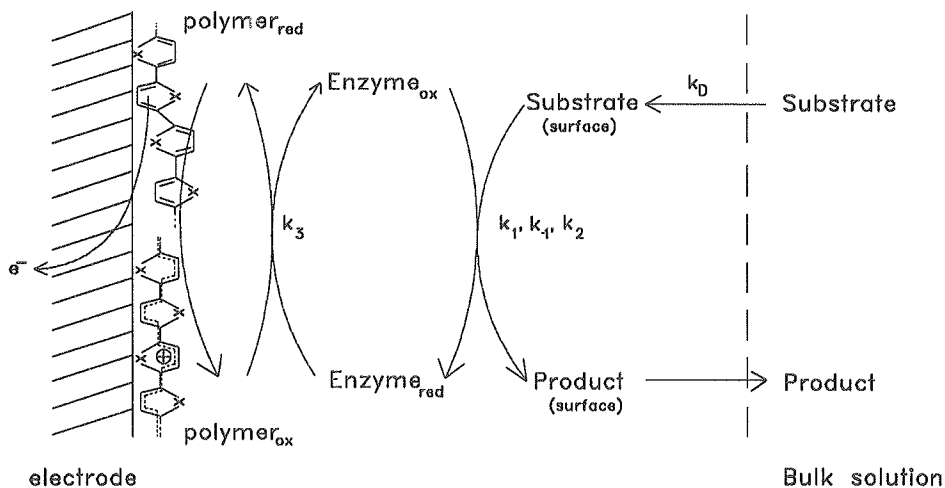


Figure 11. Schematic representation of the reaction sequence in a third-generation biosensor.

In this scheme the rate constants k_1 , k_{-1} , and k_2 are those for Michaelis-Menten kinetics, and k_3 is the rate constant for heterogeneous electron transfer. For a mathematical description of the process some assumptions need to be made. First the conducting polymer is considered to be a solid mediator which shuttles electrons from the enzyme to the electrode by changing its redox state (equation 13a & b). Secondly, it is assumed that the redox capacity of the conducting polymer is sufficiently high. This means that the number of redox-sites on the polymer must be in excess over the number of enzyme molecules bound.⁴⁹ Finally, it is assumed that no concentration polarization occurs. That is, in a certain layer of measuring fluid near the electrode, the concentrations of the various involved species are uniform. This approximation is allowed when this layer is sufficiently thin.^{2,59} Alberly and coworkers have worked out a model for the operation of an amperometric enzyme electrode based on Figure 11 and Scheme 1. In their case the conducting layer on the electrode was an organic salt.^{1,85-87} Taking into account the assumptions mentioned above and setting the activity of the electron mediating sites on the polymer to unity, the result is as follows (eq. 14a):²

$$\frac{[E]_{tot}}{j} = \frac{KM}{lk_2([S]_{\infty} - \frac{j}{k_D})} + \frac{1}{lk_2} + \frac{1}{lk_3} \quad (14a)$$

In equation (14a) $[E]_{\text{tot}}$ is the total concentration of enzyme, j is the flux, l is the biosensor membrane thickness, $[S]_{\infty}$ is the analyte concentration at infinite distance from the biosensor surface, and k_D is the rate constant for analyte transport across the membrane. Equation (14a) separates (to some extent) the possible rate limiting processes.⁸⁸ First, the process may be controlled by the enzyme kinetics. Secondly, mass transfer to the biosensor surface may be the rate limiting process. Third, the kinetics of the electron transfer between conducting polymer and enzyme (described by k_3) can be the rate determining step.

The first right hand term of (14a) reflects the Michaelis-Menten enzyme kinetics, and the transport of the analyte to the electrode surface. Formation and decomposition of the enzyme-product complex is represented by the second term of equation (14a). The third term accounts for the electron transfer between enzyme and conducting polymer.

Two important limiting cases can now be considered. When the enzyme-product complex dissociates fast and when also the reoxidation of the enzyme is a rapid process compared with the preceding steps of mass transport and binding of analyte to the enzyme, the latter two processes become rate determining (k_2 and $k_3 > k_D$ and k_1). The reciprocal expressions for the fast processes (second and third right-hand

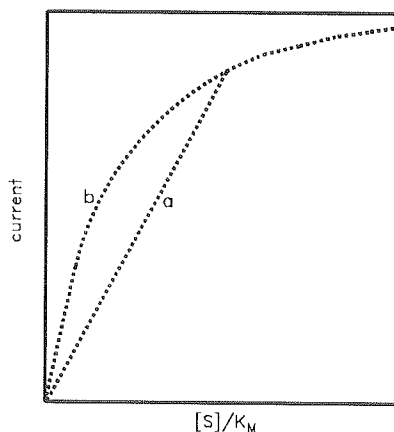


Figure 12. Response curves for an amperometric biosensor under different conditions. Curve a: substrate transport limitation; curve b: no substrate transport limitation.

term of 14a) are correspondingly small and their contribution to the limitation of the overall reaction rate can be neglected. Equation (14a) can in this case be rearranged to (14b).

$$\frac{1}{j} = \frac{K_M}{lk_2 [E]_{tot} [S]_{\infty}} + \frac{1}{k_D [S]_{\infty}} \quad (14b)$$

In this expression, enzyme kinetics and substrate transport are separated. This limiting case is of special interest when analyzing the biosensor response. A biosensor which behaves according to (14b) should display a linear dependence of the current on the analyte concentration. This is shown graphically in Figure 12, curve a. Variation of the enzyme loading, $[E]_{tot}$, or the diffusion layer (for example, by changing the thickness of the enzyme membrane) can reveal to what proportion the two different processes contribute to the overall rate. When the enzyme loading is sufficiently high, the overall rate is determined by the mass transfer. Under these conditions, the inevitable denaturation of enzyme does not immediately affect the biosensor response. Only after a certain amount of time has elapsed, does the biosensor response suddenly drop.

The second limiting case is when the enzymatic reactions or the reoxidation of the enzyme by the conducting polymer are slow processes when compared to the mass transfer step (k_D is large in comparison to k_1 , k_2 , k_3). In this case, the second and third term of (14a) cannot be neglected. The transport of analyte to the biosensor surface is rapid and in no way limits the overall reaction rate. The analyte concentration at the sensor surface remains essentially equal to the bulk concentration and equation 14a reduces to:

$$\frac{[E]_{tot}}{j} = \frac{K_M}{lk_2 [S]_{\infty}} + \frac{1}{lk_2} + \frac{1}{lk_3} \quad (14c)$$

The first two terms on the right-hand side of equation (14c) now describe Michaelis-Menten enzyme kinetics and are analogous to the terms describing the Lineweaver-Burk plot. The last term in (14c) represents the reaction of the reduced enzyme with the conducting polymer. Curve b in Figure 12 represents this limiting case. The response is no longer linear with substrate concentration.

When the electric potential is too low, the biosensor will display so-called Tafel behaviour,^{11,51} i.e., the response current becomes dependent on the applied potential. This current limitation by interfacial kinetics was first described by Tafel (1905). He showed that in many electrochemical experiments the current is exponentially related to the overpotential η (15). The latter potential is the sum of all potentials involved in the redox process, e.g., concentration polarization, energy of activation, and reaction polarization. This overpotential must be added to the formal electrochemical

potential E^0 , for the redox reaction to occur. In the Tafel equation (15) a and b are constants:

$$\eta = a + b \log i \quad (15)$$

In the so-called Tafel-region of an electrochemical process a plot of $\log i$ versus the work electrode potential gives a straight line. Testing for Tafel behaviour of badly performing biosensor systems may give valuable information with regard to the optimization of parameters like the applied potential and mass transfer limitations. Tafel plots will reveal whether the current is controlled by mass transfer limitations, interfacial dynamics, or a combination of both.

From a thermodynamic point of view, a mediator for a redox enzyme must have the proper redox potential in order to exchange electrons with the redox-active center of the enzyme. The formal potential of redox enzymes is usually rather critical. An advantage of conducting polymers is that they are electrochemically active and able to show interfacial electron exchange over a rather large potential interval.⁸⁹

It may be concluded that it is possible to get a properly functioning (third-generation) biosensor when the mass transport is not too fast in comparison with the kinetics of the enzymatic reaction. When this condition is not met, a poor biosensor performance and a low dynamic range will result. It is of paramount interest to keep this condition in mind in the design of biosensor geometry.

References

1. Turner, A.P.F., Karube, I. and Wilson, G.S. *Biosensors. Fundamentals and Applications*. Oxford University Press, New York: (1989).
2. Cass, A.E.G. *Biosensors. A Practical Approach*. Oxford University Press, New York: (1990).
3. Clark Jr., L.C. and Lyons, C., *Ann. N. Y. Acad. Sci.*, (1962) **102**: 29-45.
4. Bidan, G., Deronzier, A. and Moutet, J.C., *J. Chem. Soc., Chem. Commun.*, (1984): 1185.
5. Hale, P.D., Inagaki, T., Karan, H.I., Okamoto, Y. and Skotheim, T.A., *J. Am. Chem. Soc.*, (1989) **111**: 3482-3484.
6. Degani, Y. and Heller, A., *J. Am. Chem. Soc.*, (1989) **111**: 2357-2358.
7. Pishko, M.V., Katakis, I., Lindquist, S., Ye, L., Gregg, B.A. and Heller, A., *Angew. Chem.*, (1990) **102**: 109.
8. Dicks, J.M., Hattori, S., Karube, I., Turner, A.P.F. and Yokozawa, T., *Ann. Biol. Clin.*, (1989) **47**: 607-619.
9. Cass, A.E.G., Davis, G., Francis, G.D., Hill, H.A.O., Aston, W.J., Higgins, I.J., Plotkin, E.V., Scott, L.D.L. and Turner, A.P.F., *Anal. Chem.*, (1984) **56**: 667-671.
10. Pishko, M.V., Michael, A.C. and Heller, A., *Anal. Chem.*, (1991) **63**: 2268-2272.
11. O'Hare, D., Parker, K.H. and Winlove, C.P., *Bioelectrochem. Bioenerg.*, (1990) **23**: 203-209.
12. Bartlett, P.N., Bradford, V.Q. and Whitaker, R.G., *Talanta*, (1991) **38**: 57-63.
13. Schuhmann, W., Ohara, T.J., Schmidt, H. and Heller, A., *J. Am. Chem. Soc.*, (1991) **113**: 1394-1397.
14. Bourdillon, C. and Majda, M., *J. Am. Chem. Soc.*, (1990) **112**: 1795-1799.
15. Beh, S.K., Moody, G.J. and Thomas, J.D.R., *Analyst.*, (1991) **116**: 459-462.
16. Yokoyama, K., Tamiya, E. and Karube, I., *Anal. Lett.*, (1989) **22**: 2949-2959.
17. Pishko, M.V., Katakis, I., Lindquist, S., Ye, L., Gregg, B.A. and Heller, A., *Angew. Chem. Int. Ed. Engl.*, (1990) **29**: 82-84.
18. Betsu, S.R., Klapper, M.H. and Anderson, L.B., *J. Am. Chem. Soc.*, **94**: 8197-8204.
19. Scheller, F., Jänchen, M., Lampe, J., Prümke, H.-J., Blank, J. and Palecek, E., *Biochim. Biophys. Act.*, (1975) **412**: 157-167.
20. Frew, J.E. and Hill, H.A.O., *Phil. Trans. R. Soc. Lond.*, (1987) **B 316**: 95-106.
21. Higgins, I.J. and Hill, H.A.O., *Essays in Biochemistry*, (1986) **21**: 119.
22. Bartlett, P.N. and Whitaker, R.G., *J. Electroanal. Chem.*, (1987) **224**: 37-48.
23. Tamiya, E., Karube, I., Hattori, S., Suzuki, M. and Yokoyama, K., *Sensors and Actuators*, (1989) **18**: 297-307.
24. D'Costa, E.J. and Higgins, I.J., *Chimicaoggi*, (1990): 9-12.
25. Schuhmann, W., *Synth. Met.*, (1991) **41-430**: 429-432.
26. Kajiya, Y., Sugai, H., Iwakura, C. and Yoneyama, H., *Anal. Chem.*, (1991) **63**: 49-54.
27. Janda, P. and Weber, J., *J. Electroanal. Chem.*, (1991) **300**: 119-127.
28. Crumbliss, A.L., McLachlan, K.L., O'Daly, J.P. and Henkes, R.W., *Biotechnol.*, (1988) **31**: 796-801.
29. Armstrong, F.A., Cox, P.A., Hill, H.A.O., Lowe, V.J. and Oliver, B.N., *J. Electroanal. Chem.*, (1987) **217**: 331-366.
30. Hagen, W.R., *Eur. J. Biochem.*, (1989) **182**: 523-530.
31. Heller, A., *Acc. Chem. Res.*, (1990) **23**: 128-134.
32. Schopfer, L.M., Massey, V. and Claiborne, A., *J. Biol. Chem.*, (1981) **256**: 7329-7337.
33. Armstrong, F.A., Hill, H.A.O. and Walton, N.J., *Acc. Chem. Res.*, (1988) **21**: 407-413.
34. De Taxis Du Poet, P., Miyamoto, S., Murakami, T., Kimura, J. and Karube, I., *Anal. Chim. Act.*, (1990) **235**: 255-263.
35. Boutelle, M.G., Stanford, C., Fillenz, M., Albery, W.J. and Bartlett, P.N., *Neurosci. Lett.*, (1986) **72**: 283-288.
36. Kulys, J. and D'Costa, E.J., *Biosensors & Bioelectronics*, (1991) **6**: 109-115.
37. Schmidt, H.-L. and Günther, H., *Phil. Trans. R. Soc. Lond.*, (1987) **B 316**: 73-84.

38. Visser, C.M., *Naturwissenschaften*, (1980) **67**: 549-555.
39. Swoboda, B.E.P. and Massey, V., *J. Biol. Chem.*, (1965) **240**: 2209-2215.
40. Wingard, L.B. and Narasimhan, K., *Meth. Enzymol.*, (1988) **137**: 103-111.
41. Kalisz, H., Hecht, H., Schomburg, D. and Schmidt, R.D., *J. Mol. Biol.*, (1990) **213**: 207-209.
42. Frederick, K.R., Tung, J.T., Emerick, R.S., Masiarz, F.R., Chamberlain, S.H., Vasavada, A., Rosenberg, S., Chakraborty, S., Schopfer, L.M. and Massey, V., *J. Biol. Chem.*, (1990) **265**: 3793-3802.
43. Barker, S.A. and Shirley, J.A. . In: *Economic Microbiology, Vol. 5*. edited by Rose, A.H. Academic Press, New York: (1980) pp. 455-465.
44. Caspar, J.V., Ramamurthy, V. and Corbin, D.R., *J. Am. Chem. Soc.*, (1991) **113**: 600-610.
45. Nowak, M.J., Rughooputh, S.D.D.V., Hotta, S. and Heeger, A.J., *Macromol.*, (1987) **20**: 965-968.
46. Ofer, D., Crooks, R.M. and Wrighton, M.S., *J. Am. Chem. Soc.*, (1990) **112**: 7869-7879.
47. *Sci. Am.*, (1990) 79.
48. Roncali, J., Yassar, A. and Garnier, F., *J. Chem. Soc., Chem. Commun.*, (1988): 581.
49. Asavapiriyant, S., Chandler, G.K., Gunawardena, G.A. and Pletcher, D., *J. Electroanal. Chem.*, (1984) **177**: 229-244.
50. Wegner, G., *Angew. Chem.*, (1981) **93**: 352-371.
51. Bard, A.J. and Faulkner, L.R. *Electrochemical Methods. Fundamentals and Applications*. John Wiley & Sons, New York: (1980).
52. Takakubo, M., *J. Electroanal. Chem.*, (1989) **258**: 303-311.
53. Rosseinsky, D.R., Morse, N.J., Slade, R.C.T., Hix, G.B., Mortimer, R.J. and Walton, D.J., *Electrochim. Act.*, (1991) **36**: 733-738.
54. Bjorklund, R.B., *J. Chem. Soc. Faraday Trans. 1.*, (1987) **83**: 1507.
55. Basolo, F. and Johnson, R.C. In: *Coordination Chemistry*. W.A. Benjamin, Menlo Park: (1964).
56. Harrison, J.A. and Thirsk, H.R. The Fundamentals of Metal Deposition. In: *Electroanalytical Chemistry, Vol. 5*. edited by Bard, A.J Marcel Dekker, New York: (1971) pp. 67-146.
57. Hillman, A.R. and Mallen, E.F., *J. Electroanal. Chem.*, (1987) **220**: 351-367.
58. Miller, L.L., Zinger, B. and Zhou, Q.X., *J. Am. Chem. Soc.*, (1987) **109**: 2267-2272.
59. Atkins, P.W. *Physical Chemistry*. 2nd Ed. Oxford University Press, London: (1982).
60. Genies, E.M. and Pernaut, J.M., *J. Electroanal. Chem.*, (1985) **191**: 111.
61. Brédas, J.L. and Street, G.B., *Acc. Chem. Res.*, (1985) **18**: 309.
62. Nechtsheim, M., Devreux, F., Genoud, F., Vieil, E., Pernaut, J.M. and Genies, E., *Synth. Met.*, (1986) **15**: 59.
63. Zhong, C.J., Tian, Z.Q. and Tian, Z.W., *J. Phys. Chem.*, (1990) **94**: 2171-2175.
64. Chung, T., Kaufman, J.H., Heeger, A.J. and Wudl, F., *Physical Review B*, (1984) **30**: 702-710.
65. Kobayashi, M., Yoneyama, H. and Tamura, H., *J. Electroanal. Chem.*, (1984) **177**: 281.
66. Bull, R.A., Fan, F.F. and Bard, A.J., *J. Electrochem. Soc.*, (1982) **129**: 1009.
67. Feldberg, S.W., *J. Am. Chem. Soc.*, (1984) **106**: 4671.
68. Meerholz, K. and Heinze, J., *Angew. Chem.*, (1990) **102**: 695-697.
69. Zotti, G., Schavion, G. and Comisso, N., *Electrochim. Act.*, (1990) **35**: 1815-1819.
70. Cottrell, F.G., *Z. Physik. Chem.*, (1902) **42**: 385.
71. Binnig, G., Rohrer, H., Gerber, C. and Weibel, E., *Phys. Rev. Lett.*, (1982) **49**: 57-60.
72. Magonov, S.N. and Cantow, H-J. *Applications of scanning tunneling microscopy to layered materials, organic charge transfer complexes and conductive polymers*. In: *Scanning Tunneling Microscopy and Related Methods*. edited by Behm, R., Garcia, N. and Rohrer, H. Kluwer Academic Publishers, Dordrecht: (1990) pp. 367-376.
73. Caple, G., Wheeler, B.L., Swift, R., Porter, T.L. and Jeffers, S., *J. Phys. Chem.*, (1990) **94**: 5639-5641.
74. Everson, M.P. and Helms, J.H., *Synth. Met.*, (1991) **40**: 97-109.

75. Yang, R., Dalsin, K.M., Evans, D.F., Christensen, L. and Hendrickson, W.A., *J. Phys. Chem.*, (1989) **93**: 511-512.
76. Kempf, S., Rotter, H.W., Magonov, S.N., Gronski, W. and Cantow, H-J., *Polymer Bulletin*, (1990) **24**: 325-332.
77. Jandt, K.D., Buhk, M., Petermann, J., Eng, L.M. and Fuchs, H., *Polymer Bulletin*, (1991) **27**: 101-107.
78. Smith, D.P.E., Brayant, A., Quate, C.F., Rabe, J.B., Gerber, C. and Swalen, J.D., *Proc. Natl. Acad. Sci. USA*, (1987) **84**: 969-972.
79. Heckl, W.M., Kallury, K.M.R., Thompson, M., Gerber, C., Horber, H.J.K. and Binnig, G., *Langmuir*, (1989) **5**: 1433-1435.
80. Cricenti, A., Selci, S., Felici, A.C., Gerzerosi, R., Gori, E., Diaczenko, W.D. and Chiarotti, G., *Science*, (1989) **245**: 1226-1227.
81. Travaglini, G., Amrein, M., Michel, B. and Gross, H. *Imaging and conductivity of biological and organic materials*. In: *Scanning Tunneling Microscopy and Related Methods*. edited by Behm, R., Garcia, N. and Rohrer, H. Kluwer Academic Publishers, Dordrecht: (1990) pp. 335-347.
82. Lineweaver, H. and Burk, D., *J. Am. Chem. Soc.*, (1934) **56**: 658-666.
83. Cornish-Bowden, A. *Fundamentals of Enzyme Kinetics*. Butterworths, London: (1979).
84. Horvath, C. and Engasser, J., *Biotechnol. Bioeng.*, (1974) **16**: 909-923.
85. Albery, W.J. and Bartlett, P.N., *J. Electroanal. Chem.*, (1985) **194**: 211-222.
86. Albery, W.J., Bartlett, P.N. and Craston, D.H., *J. Electroanal. Chem.*, (1985) **194**: 223-235.
87. Albery, W.J. and Knowles, J.R., *Biochem.*, (1976) **15**: 5631-5640.
88. Albery, W.J. and Knowles, J.R., *Biochem.*, (1976) **15**: 5588-5600.
89. Atta, N.F, Galal, A., Karagözler, A.E., Russell, G.C., Zimmer, H. and Mark Jr, H.B., *Biosensors & Bioelectronics*, (1991) **6**: 333-341.

3 Synthesis and characterization of polymer modified electrodes for possible use in amperometric biosensors

3.1 Introduction

In this thesis electron conducting polymers are studied as a matrix for the immobilization of redox enzymes. The ultimate goal is to achieve direct electronic communication between the enzyme and an electrode on which the conducting polymer is deposited.¹⁻³ It has been shown that a conducting polymer can improve the stability of the immobilized enzyme.⁴ Furthermore, such a polymer can introduce kinetic selectivity on the electrode surface and can prevent fouling of the electrode.⁴⁻⁶

Deposition of conducting polymers on electrode surfaces can be achieved by electro-oxidation of the corresponding monomers. When these monomers have hydrophilic sidegroups (e.g. sulphonate or hydroxyl functions) electrochemical oxidation may lead to electroconductive hydrogels.⁷⁻⁹ Such hydrogels might be very favourable matrices for enzyme immobilization.

In this chapter we describe the electrochemical polymerization of a series of hydrophobic and hydrophilic pyrrole and thiophene monomers on platinum coated glassy carbon electrodes. The resulting polymer-covered electrodes are characterized by infrared spectroscopy, scanning electron microscopy, and cyclic voltammetry and subsequently tested for their enzyme immobilization properties. This investigation was undertaken as a possible first step towards the development of a third-generation biosensor.

3.2 Synthesis of monomers

Ten different monomers were studied in this work. They are presented in Chart 1. Compounds 1, 3, and 4 are commercially available. The other monomers were synthesized following literature procedures,⁹⁻¹⁸ which had to be improved in some cases.

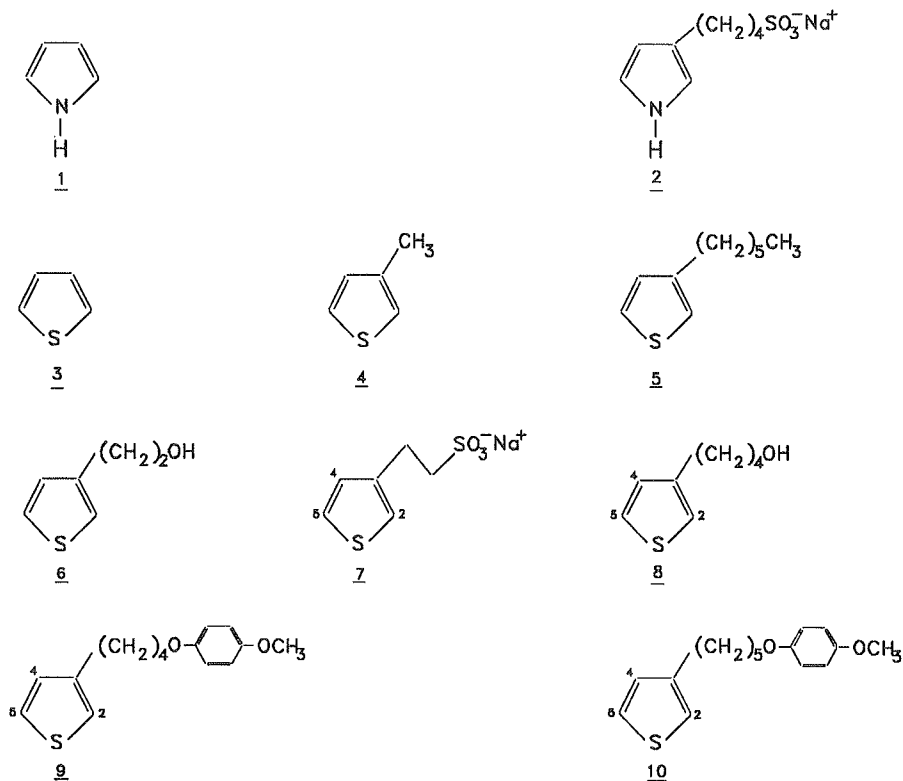
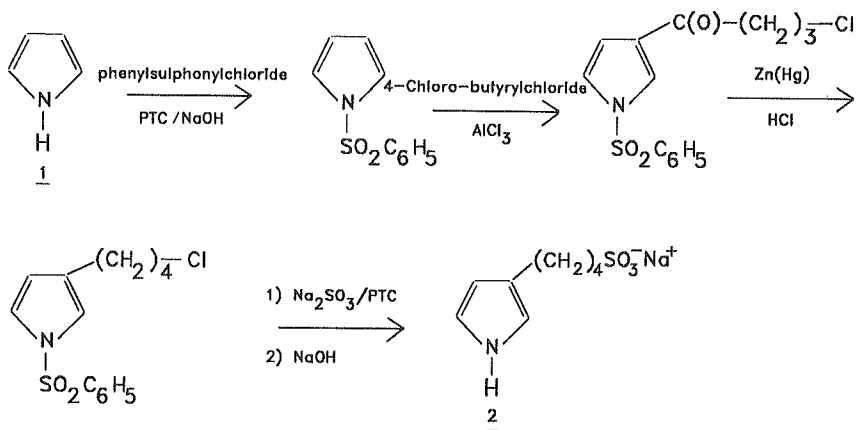


Chart 1.

The synthesis of 2 involves 4 steps, starting from pyrrole (1) (Scheme 1).^{9,11,13} The latter compound was first protected on nitrogen by treatment with phenylsulphonyl chloride using phase transfer-conditions. The N-protected pyrrole was provided with a 4-chlorobutyryl substituent at the 3-position by a Friedel-Crafts reaction with 4-chlorobutyryl chloride and AlCl_3 followed by a Clemmensen reduction. Treatment of the resulting compound with Na_2SO_3 (Strecker reaction) and N-deprotection with NaOH yielded 2 in a pure form (12.5 % yield). In the Strecker

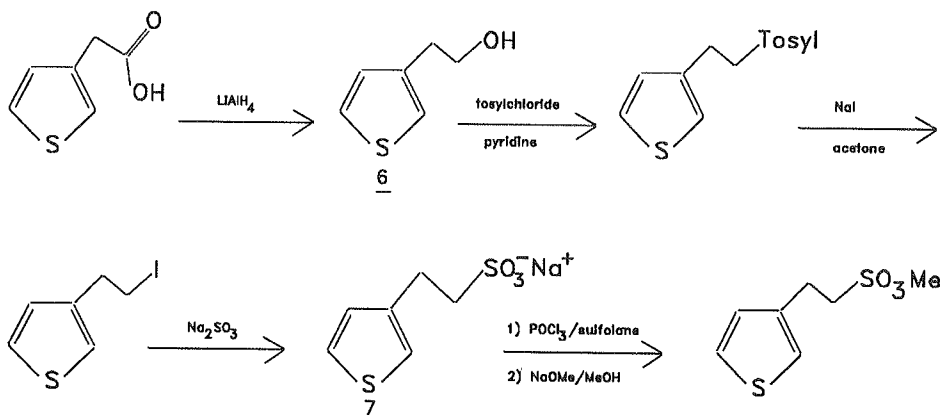


Scheme 1.

reaction a phase transfer catalyst was used. The need for this catalyst was not evaluated.

Monomer 5 was synthesized by a nickel catalyzed cross-coupling reaction from 3-bromothiophene and hexylbromide.^{12,15,19}

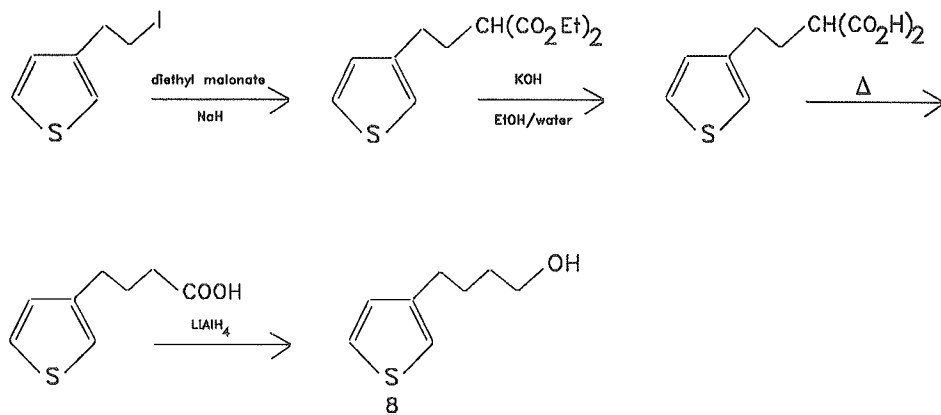
The syntheses of 6 and 7 are presented in Scheme 2. The reactions start with the reduction of 3-thiophene acetic acid with LiAlH₄ to give the alcohol 6.¹⁰ The latter compound was converted into the tosylate using standard conditions.²⁰ This route is to be preferred over a literature method which uses the mesylate.^{7,18} The tosylate is a crystalline solid which can be isolated by filtration. The mesylate derivative can



Scheme 2.

only be purified by tedious chromatographic procedures. The tosylate was converted into the iodide with NaI in dry acetone at room temperature. This reaction proceeded quantitatively. Finally, the iodide was transformed into **7** by a Strecker reaction with a slight excess of an aqueous solution of Na₂SO₃ in an autoclaved vessel at 140 °C (yield 70-80%).²¹ It is known from the literature that sulphonate **7** is difficult to polymerize, in contrast to its methyl ester.⁷ Therefore, we also prepared the latter compound as shown in Scheme 2. The above-mentioned sulphonate was converted to the sulphonyl chloride by treatment with POCl₃ in acetonitrile and sulfolane. This method is more convenient than the literature procedure, which uses thionyl chloride in dimethylformamide, as no complexes of the product with the solvent are formed.²² In our case the sulphonyl chloride could be obtained by crystallization from hot hexane. Treatment of the sulphonyl chloride with sodium methoxide in methanol at 0 °C yielded the ester in nearly quantitative yield as white crystals.²³

1-iodo-2-(3-Thienyl)ethane was used as the starting material for the synthesis of **8** (Scheme 3). Alkylation of the former compound with diethyl malonate and NaH in DMF,¹⁸ followed by hydrolysis and decarboxylation at 180 °C afforded 4-(3-thienyl)butanoic acid as a brown oil. This oil was treated with LiAlH₄ in dry diethyl ether to give **8** in 47 % yield.¹⁰



Scheme 3.

Monomers **9** and **10** were synthesized by a nickel catalyzed cross-coupling reaction from 3-bromothiophene and 1-bromo-4-(4-methoxyphenoxy)butane and 1-bromo-5-(4-methoxyphenoxy)pentane, respectively.^{15,16}

3.3 Synthesis of polymers

Electrochemical polymerization of monomers **1** - **10** was performed under potentiostatically as well as galvanostatically controlled conditions. In general, the latter procedure gave polymer films of higher quality. However, polymerization under potentiostatic control offered the possibility to record current-potential curves during the reaction. The onset potentials (oxidation potential of the monomer) for the various polymerizations were obtained by linear sweep voltammetry (LSV). These onset values as well as the other polymerization conditions are presented in Table 1. As expected from data in the literature, the onset potential for the thiophene-based monomers was much higher than for the pyrrole-based monomers as the oxidation of the pyrrole ring proceeds at a lower potential than the oxidation of the thiophene ring.²⁴⁻²⁷ The redox behaviour of the resulting conducting polymers was evaluated by cyclic voltammetry (CV). The oxidation (Ox) and reduction (Red) potentials of the polymers are given in Table 1. Electrochemical polymerization of monomers **6** and **8** led to blueish paste-like deposits on the electrode. This material did not adhere sufficiently to the electrode surface and as a result determination of the redox behaviour was not possible. The hydroxylic functions probably caused the polymer

Table 1. Experimental conditions for the polymerization of different pyrrole and thiophene monomers and redox potentials of the corresponding polymers.

Monomer ^a	Onset potential/V ^b	Solvent	Electrolyte ^a	Polymer	
				Oxidation potential/V ^b	Reduction potential/V ^b
1	0.56	water	NaCl	0.85/1.20	-
2	0.99	water	NaCl	0.96/1.10	-
3	1.75	acetonitrile	Bu ₄ NClO ₄	1.15	1.00
4	1.58	acetonitrile	Bu ₄ NClO ₄	0.89	0.77
5	1.64	acetonitrile	Bu ₄ NClO ₄	1.41	0.80
6	1.14	acetonitrile	Bu ₄ NBF ₄	-	-
7	c	acetonitrile	Bu ₄ NBF ₄	0.84	0.61
8	1.08	acetonitrile	Bu ₄ NBF ₄	-	-
9	1.17	acetonitrile	Bu ₄ NClO ₄	-	-
10	1.13	acetonitrile	Bu ₄ NClO ₄	1.81	1.05

^a Monomer concentration 0.3 M; electrolyte concentration 0.15 M; T = 25 °C.

^b All potentials are versus an Ag/AgCl reference.

^c Not determined. The literature value for the corresponding methylester is 1.80 V.^{7,28}

to be soluble in the polymerization medium, preventing the formation of a continuous film. In the case of monomer **9** no electrode deposit was obtained at all. We tentatively ascribe this to steric factors. Electropolymerization of monomer **10**, however, did yield a continuous film, both under potentiostatic and galvanostatic conditions. A possible explanation might be that the bulky ether substituent in **10** is farther away from the thiophene ring, creating the proper conditions for film growth.

It has been reported in the literature that monomer **7** and its sulphonic acid derivative cannot be polymerized electrochemically.⁷ Because of this, we initially used the methyl ester of **7** in the electrochemical polymerization. The reaction was conducted in dry acetonitrile and yielded a blue continuous film.^{18,28,29} We hoped that it would be possible to convert the methyl ester to the polyelectrolyte¹⁸ and still be left with a continuous film on the electrode. We found this not to be the case:

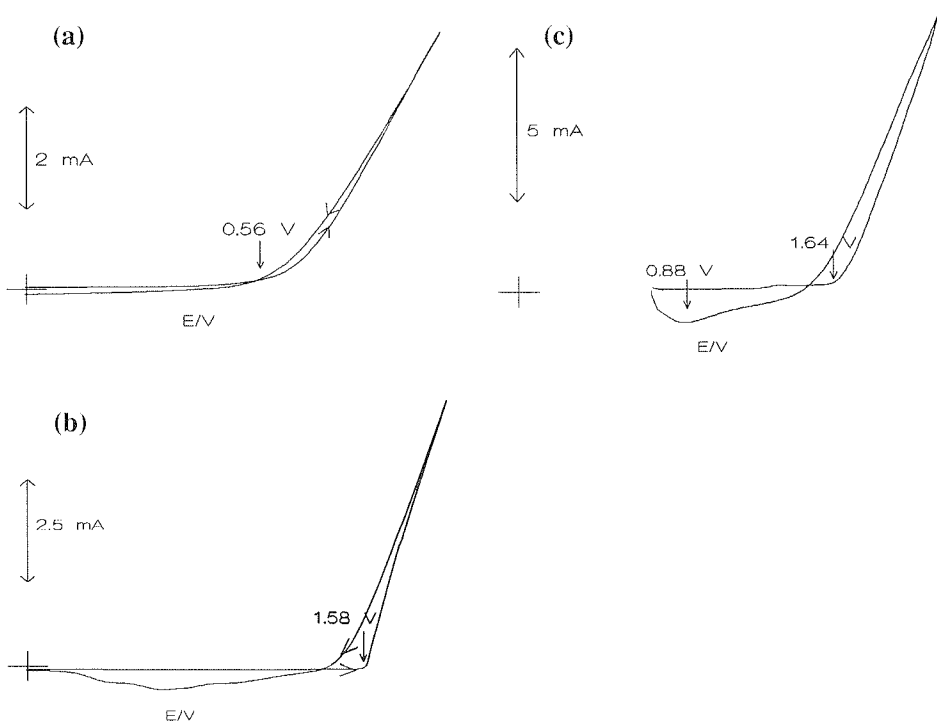


Figure 1. Cyclic voltammograms recorded during the polymerization of: (a) pyrrole in water containing 0.15 M sodium chloride, (b) (3-methyl)thiophene in acetonitrile with 0.15 M tetrabutylammonium perchlorate, and (c) (3-hexyl)thiophene in acetonitrile with 0.15 M tetrabutylammonium perchlorate. Monomer concentration 0.3 M. Scanning rate 50 mV/s, potentials are given versus Ag/AgCl.

dipping the polymer coated electrode into a solution of for instance sodium iodide in acetone⁷ led to dissolution of the polymer film. Later we found that it is possible to polymerize **7** in a direct manner, therefore further attempts to use the methyl ester of **7** were discontinued. Electrochemical polymerization of **7** appeared to be successful in CH_3CN solution with our standard monomer concentration of 0.3 M. This monomer concentration apparently is high enough to create conditions in which the growth rate of the polymer is sufficiently high to compete with deactivation by overoxidation.³⁰

An attempt was made to co-polymerize monomer **7** with the acrylic acid ester of **6** in order to obtain a conducting polymer that could be cross-linked by irradiation with UV-light after electropolymerization. The idea was to perform this cross-linking reaction in the presence of glucose oxidase. This enzyme would then become entrapped in the resulting polymer structure. However, this copolymerization reaction was not successful: no deposit was formed on the electrode when the acrylate of **6** was present in the electropolymerization solution. When this acrylate was electropolymerized separately, a dark-blue deposit was obtained. This deposit appeared to be insoluble and inprocessable and it was concluded that cross-linking of the acrylic functions with the growing polymer chains had occurred during the electrochemical polymerization. This was confirmed by infrared spectroscopy which revealed the disappearance of the acrylic functions in the solid product.

With the exception of **10**, all monomers polymerized by a nucleation and growth mechanism,³¹ indicated by the cyclic voltammograms that were recorded during the polymerization. The anodic current in the first part of the reverse scan in the cyclic voltammograms of pyrrole, 3-methylthiophene, and 3-hexylthiophene was larger

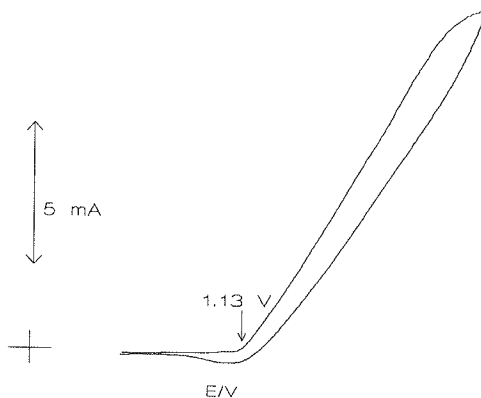


Figure 2. Cyclic voltammogram recorded during the polymerization of **10** in acetonitrile with 0.15 M tetrabutylammonium perchlorate. Monomer concentration 0.3 M. Scanning rate 50 mV/s, potentials are given versus Ag/AgCl.

than the current in the forward scan, resulting in a crossover (Figure 1a - c). This phenomenon has been observed before for a number of conducting polymers.^{27,30,32,33} The cyclic voltammogram of **10** did not show such a crossover (Figure 2). The formation of the polymer of **10** probably proceeds through a more regular growth mechanism. Scanning electron micrographs of the polymer films

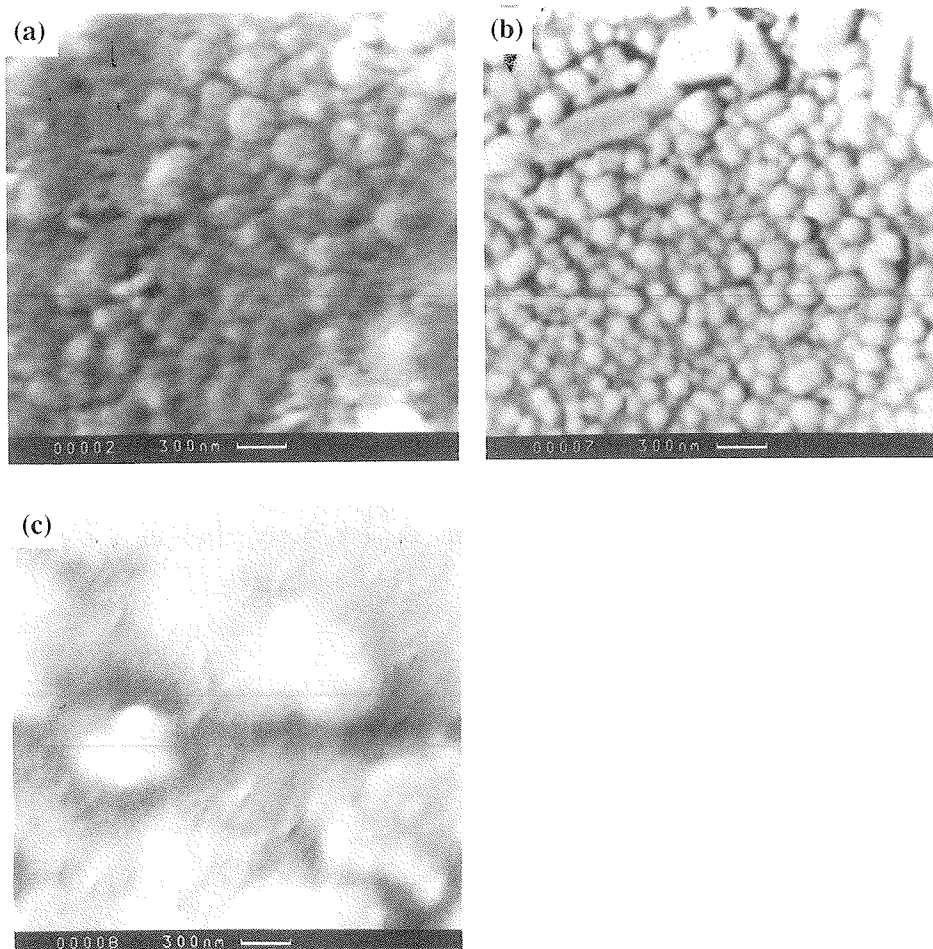


Figure 3. Scanning electron micrographs of electrochemically synthesized polymer films: (a) poly(pyrrole), (b) poly-[(3-hexyl)thiophene], (c) poly-[1-(4-methoxyphenoxy)-5-(3-thienyl)pentane]. Polymerization conditions: monomer concentration 0.3 M, electrolyte concentration 0.15 M, galvanostatic polymerization at 20 mA/cm² during 60 s. The magnification is 30,000.

confirmed the existence of different growth mechanisms. In the case of poly(**10**) a rather smooth and continuous surface morphology is observed (Figure 3c), whereas the morphology of the other polymers (Figure 3a and b) is typified by individual nuclei of various dimensions. The deviating behaviour of **10** may partly be explained from the fact that the onset potential of this monomer is relatively low as compared to the other thiophene derivatives (Table 1). As a result, many individual chains start to grow on the electrode surface, giving rise to a smooth structure. The oxidation potential of these regularly growing chains changes only very slowly. This leads to a normal cyclic voltammogram (Figure 2). Most likely, the other conducting polymers are initially formed in the solution very near the electrode surface. When the concentration of the polymer molecules reaches a certain value, the molecules precipitate onto the electrode. Nuclei are formed, which grow farther into a bulk film structure. At the moment of nucleation, the oxidation potential suddenly drops. In practice, this is revealed by the enhanced anodic current in the cyclic voltammogram during the backward scan and the mentioned current crossover (Figure 1).

Cyclic voltammetry on the synthesized polymers in monomer free electrolyte solutions yielded characteristic current-potential profiles (fingerprints, Table 1).³⁴ As an illustration the cyclic voltammograms of poly(**4**) and poly(**5**) are shown in Figure 4a and 4b, respectively. In the voltammograms the oxidation and reduction waves are clearly visible, which means that the polymers are electroactive in the indicated potential region. At higher anodic potentials some overoxidation of the polymers is observed.^{27,35,36} Both poly(**4**) and poly(**5**) show overoxidation at a potential that is

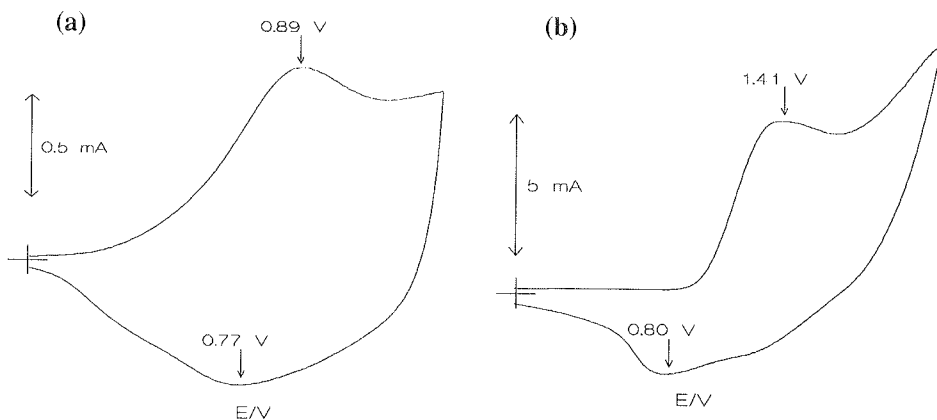


Figure 4. Cyclic voltammograms of conducting polymers in monomer free solution of tetrabutylammonium perchlorate in acetonitrile: (a) poly-[(3-methyl)thiophene], (b) poly-[(3-hexyl)thiophene]. Electrolyte concentration 0.15 M. Scan rate 50 mV/s, potentials are given versus Ag/AgCl.

lower than the onset potential of the corresponding monomers (Table 1). These polymers, therefore, are not stable at the potential they are synthesized. However, when excess of monomer is present this overoxidation must compete with polymerization and is suppressed. This phenomenon is called the poly(thiophene) paradox.^{26,37}

Fourier transform infrared spectroscopy (FTIR) was used to characterize the polymers further. As compared to the monomers the IR-spectra of the polymers displayed a diminished absorption at the frequency corresponding to the CH-stretch of the aromatic heterocycle (3125 cm^{-1}). This is a strong indication that polymerization of the heterocycles has taken place at the α,α -position. Some other relevant IR data of the polymers are summarized in Table 2.

Table 2. IR data of conducting polymer electrodes.^{38,39}

Polymer of	Absorption band cm^{-1}	Assignment
1	3225; 1550	N-H; C=C
2	1175; 1040	SO_3^-
3	1495	C=C
4	2850-2950 (medium)	methyl
5	2850-2950 (strong)	hexyl
7	1170; 1060	SO_3^-
10	1230; 1115; 1040	$-\text{OC}_6\text{H}_4\text{OCH}_3$

As already mentioned, polymerization under potentiostatic control produced films of rather low quality. Especially in the case of the hydrophobic monomers 1, 3, 4, & 5 the coverage of the electrode was non-continuous and the polymers were very brittle. Polymerization under galvanostatic control gave conducting films of much higher quality. In all cases, except for monomers 6, 8, and 9 where no polymer film was formed, nicely adhering layers were obtained. These polymer-modified electrodes were tested for enzyme adsorption.

3.4 Enzyme adsorption

Adsorption of glucose oxidase on the polymer-modified electrodes was investigated by dipping these electrodes into a phosphate buffered saline (PBS, pH 7.4) solution, containing the enzyme (5 mg/ml). The enzyme was allowed to adsorb

for time periods varying between 1 hour and several days. Both stirred and unstirred solutions were used. After this treatment the electrodes were either directly rinsed with PBS solution or dried first and rinsed with PBS afterwards. Drying was carried out by storing the electrodes at 4 °C for at least 17 hours either over CaCl₂ or without this drying reagent.

The various enzyme modified electrodes were tested for enzyme activity by an electrochemical assay in which the natural co-substrate of the enzyme is replaced by the artificial electron acceptor benzoquinone.^{40,41} The hydroquinone formed is measured by the rotating disk electrode technique. The procedure is described in more detail in Chapter 4. None of the enzyme treated polymer electrodes displayed any significant enzymatic activity. Apparently, adsorption of active glucose oxidase molecules either does not take place on the electrodes or the enzyme becomes denatured during the immobilization. Because of this negative result no further efforts were undertaken to test the various conducting polymer electrodes as amperometric biosensors.

3.5 Conclusions

We may conclude from the results presented in this chapter that enzyme immobilization by physical adsorption on planar conducting polymer electrodes is unsuccessful. Similar conclusions were drawn by others and a number of alternative methods for glucose oxidase immobilization on conducting polymers have appeared in the literature.⁴²⁻⁵⁰ In the course of our investigations we realized that the microstructure of the conducting polymer matrix is an important parameter. Planar electrodes modified with hydrophobic or hydrophilic conducting polymers apparently cannot create the proper environment for immobilizing an enzyme while retaining its biological activity. In the following chapters, two different microporous conducting polymer matrices which can be successfully used to construct a third-generation biosensor are described.

3.6 Experimental

Refractive indices were measured with a Haake FE refractometer. Melting points were measured with a Reichert Thermopan optical microscope and are uncorrected. IR spectra were recorded on a Perkin Elmer model 298 spectrophotometer. FTIR spectra were taken on a Perkin Elmer model 1750 Infrared Fourier Transform spectrometer. ¹H NMR spectra were recorded on a Bruker WH-90 (90 MHz) or a

Bruker AM-400 (400 MHz) spectrometer. Mass spectra were taken on a VG 7070E spectrometer.

Monomer synthesis

When necessary, syntheses were conducted under a nitrogen atmosphere using standard Schlenk apparatus. Pyrrole was purchased from Merck, thiophene and 3-methylthiophene were purchased from Sigma. These monomers were distilled under nitrogen before use. 3-Hexylthiophene was synthesized according to a literature procedure¹² and was stored at -20 °C under argon after distillation. 3-Thienylacetic acid was purchased from Janssen Chimica and was used without further purification. Benzoquinone was purchased from Aldrich and was sublimed at 100 °C prior to use.

1-(Phenylsulphonyl)pyrrole

This compound was synthesized according to a method described in the literature.¹³

1-Chloro-3-[(1-(phenylsulphonyl)-3-pyrrolyl)carbonyl]propane

To a stirred and cooled mixture of 25.3 g (0.19 mol) of AlCl_3 in 125 ml of CH_2Cl_2 was added slowly a solution of 28 g (0.199 mol) of 4-chloro-butylchloride in 25 ml of dichloromethane. After 30 min. 31.05 g (0.15 mol) of 1-(phenylsulphonyl)pyrrole in 100 ml of dichloromethane was added. Stirring was continued for one hour, whereafter the reaction mixture was poured into 500 ml of water. After extraction with chloroform (300 ml), washing of the organic layer with aqueous NaOH (400 ml, 0.6 N) and water, drying over MgSO_4 , and concentration 45.3 g (100 %) of crude 1-chloro-3-[(1-(phenylsulphonyl)-3-pyrrolyl)carbonyl]propane was obtained. This material was used as such in the next synthesis. ^1H NMR (CDCl_3) of the crude product was satisfactory.

1-chloro-4-[1-(phenylsulphonyl)-3-pyrrolyl]butane

The crude material from the above mentioned synthesis (46.9 g, 0.15 mol) was dissolved in 200 ml of toluene. To this solution was added a mixture of zinc powder (120 g) and HgCl_2 (10 g) in 200 ml of aqueous HCl (0.5 N) followed by 200 ml of concentrated HCl. The reaction mixture was heated under reflux for 2 h., while stirring. During this period three times an additional amount of 25 ml of concentrated

hydrochloric acid was added. The progress of the reaction was followed by ^1H NMR. At the end of the reaction the mixture was allowed to cool to room temperature, whereafter the organic layer was separated. The water layer was extracted with toluene (2 x 50 ml). The combined organic layers were washed with water, dried (MgSO_4) and concentrated to yield 34.83 g of a brown oil (0.12 mol; 78 %). This crude material was used in the next synthesis without further purification. ^1H NMR (CDCl_3) of this product was satisfactory.

4-(3-Pyrrolyl)butanesulphonic acid sodium salt (2)

To 17.6 g (59 mmol) of the product from the above described synthesis, 175 ml of water and 70 ml of ethanol were added. Tetrabutylammonium chloride (2 g) and 2.6 g (17 mmol) of sodium iodide were added and the mixture was heated under reflux for 18 h. To the still hot reaction mixture, 17.6 g of NaOH was added and refluxing was continued for an additional 1.5 h. Subsequently, 10 ml of a saturated aqueous NaCl solution was added and the reaction mixture was extracted with chloroform (2 x 100 ml). The chloroform layer was washed with water (50 ml), and the combined aqueous layers were collected and concentrated under vacuum. The resulting brown paste was boiled in 170 ml of distilled water and then partially concentrated until the solution became turbid. The mixture was allowed to cool to room temperature, the resulting light-brown paste was filtered off, and washed twice with saturated aqueous NaCl. The filtrate, which contained benzenesulphonic acid (^1H NMR) was discarded. The solid material was extracted with a hot mixture of 250 ml of ethanol (96 %) and 10 ml of 2-chloroethanol followed by 100 ml of hot ethanol (90 %). The ethanolic extracts were combined and evaporated to dryness. The resulting solid was extracted again with 250 ml of hot ethanol (90 %). The ethanol was evaporated and the residue was recrystallized from ethanol (150 ml, 96 %) to give 4.27 g of light-brown crystalline 2. Yield 32 %. The material decomposed before melting. The product was hygroscopic and slightly contaminated with benzene sulphonic acid sodium salt as proved by elemental analysis. IR (KBr): 3535 (N-H), 1205 & 1050 (SO) cm^{-1} ; ^1H NMR (D_2O) δ 7.4 (m, 2 H, pyrrolylH-2,5), 6.8 (m, 1 H, pyrrolylH-4), 3.6, 3.2, and 2.4 (3m, 8 H, alkylH); Anal. Calcd for $\text{C}_8\text{H}_{12}\text{NNaO}_3\text{S}\cdot\text{H}_2\text{O}\cdot 0.05\text{C}_6\text{H}_5\text{NaO}_3\text{S}$: C, 38.08; N, 5.56; H, 5.59. Found: C, 37.83; N, 5.06; H, 5.32.

2-(3-Thienyl)ethanol (6)

This compound was synthesized according to a literature procedure.¹⁰

1-Iodo-2-(3-thienyl)ethane

To 10.6 g (82.2 mmol) of 6 in dry pyridine (60 ml) was added at -15°C 19 g (100 mmol) of *p*-toluenesulphonyl chloride. The mixture was allowed to warm up to 4°C and was subsequently stored in the refrigerator overnight. Water (10 ml) was added and the resulting solution was poured into a mixture of ice water (300 ml) and concentrated HCl (100 ml). The precipitated material was isolated by filtration and recrystallized from diethyl ether. Yield 21.9 g (94 %) of white 2-(3-thienyl)ethyl tosylate.

The above mentioned compound (33.9 g, 0.12 mol) was added to a solution of dried NaI (22.5 g, 0.15 mol) in dry acetone and stirred at ambient temperature for 45 h. After the solid (sodium tosylate) had been removed by filtration, the solvent was evaporated. To the resulting material 150 ml of brine was added. The mixture was extracted with diethyl ether (3 x 100 ml) and the extracts were washed with an aqueous solution of 1 % sodium thiosulphate to reduce traces of iodine. The combined extracts were dried (MgSO_4) and concentrated to yield 28.3 g (99 %) of 1-iodo-2-(3-thienyl)ethane. $n_D^{22} = 1.623$; $^1\text{H NMR}$ (CDCl_3) δ 7.25 - 7.10 (m, 1 H, thienylH), 6.95 - 6.75 (m, 2 H, thienylH), 3.40 - 2.95 (m, 4 H, CH_2CH_2); MS m/z 238 (26 %, M^+), 111 (100 %, $\text{C}_4\text{H}_3\text{S}-\text{CH}_2-\text{CH}_2$), 97 (22 %, $\text{C}_4\text{H}_3\text{S}-\text{CH}_2$).

2-(3-Thienyl)ethanesulphonic acid sodium salt (7)

A mixture of 2.5 g (10.5 mmol) of 1-iodo-2-(3-thienyl)ethane and 1.51 g (12 mmol) of sodium sulphite in distilled water (15 ml) was heated in an autoclave at 140°C for 6 h. while stirring. The water was evaporated in vacuum and the resulting off-white solid was washed with diethyl ether and acetone to remove unreacted starting material and any sodium iodide formed. Recrystallization from water yielded 1.98 g of 7. The product was slightly contaminated with inorganic impurities (sodium sulphite) as proved by elemental analysis. The compound decomposed before melting. IR (KBr) 1215, 1180, and 1050 (S-O), 1170 (C-O); $^1\text{H NMR}$ (D_2O) δ 7.26 (dd, $J(5,4) = 4.9$, $J(5,2) = 2.9$ Hz, 1 H, thienylH-5), 7.04 (dd, $J(2,5) = 2.2$, $J(2,4) = 0.9$ Hz, 1 H, thienylH-2), 6.92 (dd, $J(4,5) = 4.8$, $J(4,2) = 1.2$ Hz, 1 H, thienylH-4), 3.06 - 3.01 (m, 2 H, CH_2), 2.94 - 2.90 (m, 2 H, CH_2); Anal. Calcd. for $\text{C}_6\text{H}_7\text{NaO}_3\text{S}_2 \cdot 0.02\text{Na}_2\text{SO}_3$: C, 33.25; H, 3.26. Found: C, 33.30; H, 3.21.

2-(3-Thienyl)ethanesulphonyl chloride

A mixture of 2.14 g of 7, acetonitrile (10 ml), sulfolane (5 ml) and POCl_3 (3.65 ml) was stirred at 70°C for 1 h. The resulting brown mixture was poured into ice

water (30 ml) and extracted with diethyl ether (4 x 50 ml). The combined extracts were washed with water (5 x 100 ml), dried (MgSO_4) and concentrated in vacuum. The yellow residue was recrystallized from hot hexane to yield white needles of 2-(3-thienyl)ethanesulphonyl chloride (1.71 g, 80 %), mp 58-59 °C. ^1H NMR (CDCl_3) δ 7.35 (dd, $J(5,4) = 4.9$, $J(5,2) = 2.9$ Hz, 1 H, thienylH-5), 7.11 (dd, $J(2,5) = 2.8$, $J(2,4) = 1.0$ Hz, 1 H, thienylH-2), 6.98 (dd, $J(4,5) = 4.9$, $J(4,2) = 1.3$ Hz, 1 H, thienylH-4), 3.94 - 3.90 (m, 2 H, CH_2), 3.40 - 3.36 (m, 2 H, CH_2); Anal. Calcd. for $\text{C}_6\text{H}_7\text{ClO}_2\text{S}_2$: C, 34.20; H, 3.35. Found: C, 34.40; H, 3.39.

2-(3-Thienyl)ethanesulphonic acid methyl ester

To a suspension of the above mentioned compound (1 g, 4.75 mmol) in methanol (2.5 ml) was slowly added at 0 °C sodium methoxide until the apparent pH of the mixture reached neutrality. After allowing the mixture to warm up to ambient temperature, the solvent was evaporated. The residue was disrupted by sonic treatment in dichloromethane and the resulting suspension was suction filtered. The filtrate was concentrated and the residue was recrystallized from carbon tetrachloride. Yield of pure white product 0.96 g (98 %); mp 27.0-27.5 °C. IR (KBr): 1170 (C-O), 1215, 1185, and 1050 (S-O) cm^{-1} ; ^1H NMR (CDCl_3) δ = 7.31 (dd, $J(5,4) = 5.0$, $J(5,2) = 2.9$ Hz, 1 H, thienylH-5), 7.07 (dd, $J(2,5) = 2.9$, $J(2,4) = 1.1$ Hz, 1 H, thienylH-2), 6.96 (dd, $J(4,5) = 5.0$, $J(4,2) = 1.3$ Hz, 1 H, thienylH-4), 3.88 (s, 3 H, OCH_3), 3.40 - 3.36 (m, 2 H, CH_2), 3.21 - 3.17 (m, 2 H, CH_2); MS m/z 206 (33 %, M^+), 110 (100 %, $\text{M} - \text{SO}_3\text{-CH}_3$); Anal. Calcd. for $\text{C}_7\text{H}_{10}\text{O}_3\text{S}_2$: C, 40.76; H, 4.89. Found: C, 40.69; H, 4.88.

2-(3-Thienyl)ethylacrylate

To a mixture of 2 g (15.6 mmol) of **6** and 2.1 g (20.3 mmol) of triethylamine in 25 ml of dry THF was added dropwise at 0 °C under a nitrogen atmosphere 1.84 g (20.3 mmol) of acryloylchloride in 10 ml of THF. Ionol (1 wt%; radical scavenger) was added and the mixture was stirred in the dark at room temperature for 18 h. The resulting off-white suspension was poured into 150 ml of aqueous HCl (0.25 N) and extracted with diethylether (2 x 50 ml). The combined extracts were washed with 100 ml of saturated aqueous NaHCO_3 and dried (MgSO_4). Yield: 2.77 g (98 %) of yellow oil. IR (KBr): 1725 (C=O), 1620 (C=C), 815 (=C-H) cm^{-1} ; ^1H NMR (CDCl_3) δ 7.35 - 7.25 (m, 1 H, thienylH), 7.1 - 6.9 (m, 2 H, thienylH), 6.3 (dd, $J_{\text{trans}} = 16$, $J_{\text{gem}} = 2$ Hz, 1 H, $-\text{C}(\text{O})\text{-CH}=\text{CH}_2$), 5.9 (dd, $J_{\text{trans}} = 16$, $J_{\text{cis}} = 10$ Hz, 1 H, $-\text{C}(\text{O})\text{-CH}=\text{CH}_2$), 5.5 (dd, $J_{\text{cis}} = 10$, $J_{\text{gem}} = 2$ Hz, 1 H, $-\text{C}(\text{O})\text{-CH}=\text{CH}_2$), 3.7 (t, $J(1,2) = 7$ Hz, 2 H, CH_2), 2.0 (t, $J(2,1) = 7$ Hz, 2 H, CH_2); MS m/z 111 (13 %, $\text{C}_4\text{H}_3\text{S-CH}_2\text{CH}_2$) 110 (100 %, $\text{C}_4\text{H}_3\text{S-CH}_2\text{CH}$) 97 (42 %, $\text{C}_4\text{H}_3\text{S-CH}_2$) 55 (40 %, $\text{C}(\text{O})\text{CH}=\text{CH}_2$).

2-Carboxy-4-(3-thienyl)butanoic acid

Diethyl malonate (11.2 g, 70 mmol) was dissolved in 60 ml of distilled DMF. To this solution 2.09 g (70 mmol) of sodium hydride (80 % dispersion in oil) was added. After stirring for 20 min. a solution of 15.8 g (66.5 mmol) of freshly prepared 1-iodo-2-(3-thienyl)ethane in 20 ml of dry DMF was added dropwise over a 10 min. period. Stirring was continued for 45 min. at room temperature, whereafter the reaction mixture was heated to 140 °C for 4 hrs. Hereafter, it was poured into ice-cold diluted hydrochloric acid. The organic layer was separated and the aqueous layer was extracted with diethyl ether (6 x 100 ml). The combined organic layers were dried (MgSO₄) and concentrated to give 5.1 g of product. The latter was added to a solution of 9 g of KOH in 350 ml of 50 % aqueous ethanol.⁵¹ The mixture was heated under reflux until TLC indicated complete saponification of the malonic ester (17 h). The reaction mixture was poured into 350 ml of ice-cold 10 % aqueous HCl and was extracted with diethyl ether (4 x 100 ml). The organic phase was washed with 1 % sodium thiosulphate, dried (MgSO₄), and concentrated. This yielded a mixture of a white solid and a yellow oil. Recrystallization (CHCl₃/hexane) yielded 2.72 g (12.7 mmol, 69 % based on the starting material) of white crystalline 2-carboxy-4-(3-thienyl)butanoic acid. Mp: 121 - 122 °C. ¹H NMR (CDCl₃ + CD₃OD) δ 7.28 - 7.25 (m, 1 H, thienylH), 7.00 - 6.95 (m, 2 H, thienylH), 3.37 (t, J(1,2) = 7.3 Hz, 1 H, HC(COOH)₂), 2.77 - 2.72 and 2.27 - 2.21 (2 m, 4 H, CH₂CH₂).

4-(3-Thienyl)butanol (8)

The above mentioned diacid (2.47 g, 11.5 mmol) was thermally decarboxylated on an oil bath of 180 °C. Yield 1.46 g (75 %) of 4-(3-thienyl)butanoic acid as a brown oil. ¹H NMR (CDCl₃) δ 7.27 - 7.23 (m, 1 H, thienylH), 6.98 - 6.93 (m, 2 H, thienylH), 4.24 - 4.11 (m, 2 H, CH₂COOH), 2.72 - 2.67 and 2.36 - 2.19 (2 m, 4 H, CH₂CH₂).

The combined material of several decarboxylation experiments (3.36 g) was dissolved in 50 ml of dry diethyl ether and added dropwise to a suspension of 1.5 g of LiAlH₄ in 100 ml of dry diethyl ether. Excess LiAlH₄ was destroyed with water and hydrochloric acid (10%) was added until two clear layers appeared. The organic layer was separated and the water layer was extracted with diethyl ether (3 x 100 ml). The combined extracts were washed with water and dried (MgSO₄). After evaporation of the solvent, the residue was distilled (110 °C, 11 mm Hg) yielding 1.93 g (47 %, based on the diacid) as a colorless oil. IR (KBr) 3350 (OH), 2950 and 2850 (CH₂), 1150 (C-O); ¹H NMR (CDCl₃) δ 7.35 - 7.25 (m, 1 H, thienylH), 7.1 - 6.9 (m, 2 H, thienylH), 3.1 (t, J(1,2) = 6.0 Hz, 2 H, CH₂), 2.8 (t, J(4,3) = 6.1 Hz, 2 H, CH₂), 2.1 - 1.6 (broad s, 4 H, CH₂CH₂); MS m/z 156 (39 %, M⁺) 110 (31 %, C₄H₃S-CH₂CH) 97 (100 %, C₄H₃S-CH₂).

1-Bromo-4-(4-methoxyphenoxy)butane

A solution of 20.3 g of KOH in 60 ml of methanol was added to a solution of 37.2 g (0.3 mol) of *p*-methoxyphenol in 15 ml of methanol. The resulting yellow solution was added slowly over a 1 h. period to a solution of 126.9 g (0.6 mol) of 1,4-dibromobutane in 40 ml of acetone. The reaction mixture was refluxed for 1 h., cooled, and extracted with diethylether (3 x 100 ml). The combined extracts were washed with aqueous 1 N NaOH (2 x 100 ml) and water (1 x 100 ml), dried (Na₂SO₄) and concentrated. The resulting crude yellow material was distilled under vacuum. The product was collected at 111 °C (0.4 mm Hg). It solidified in the distillation setup. Yield 52.3 g (67 %) of 1-bromo-4-(4-Methoxyphenoxy)butane. Mp 42 °C. IR (KBr) 2920 (CH₂-O, CH₃-O), 1235 and 1110 (C-O) cm⁻¹; ¹H NMR (CDCl₃) δ 6.83 (s, 4 H, ArH), 3.94 (t, J(4,3) = 6.1 Hz, 2 H, CH₂Oph), 3.77 (s, 3 H, OCH₃), 3.48(t, J(1,2) = 6.7 Hz, 2 H, CH₂Br), 2.09 - 2.02 and 1.94 - 1.87 (2 m, 4 H, CH₂CH₂); MS m/z 258 (21 %, M⁺), 135 (47%, Br(CH₂)₄), 124 (100 %, (O-C₆H₄-O-CH₃) + H⁺), 109 (58 %, C₆H₄-O-CH₃).

1-Bromo-5-(4-methoxyphenoxy)pentane

This compound was synthesized from 230 g (1 mol) of 1,5-dibromopentane and 31 g (0.24 mol) of *p*-methoxyphenol as described for 1-bromo-4-(4-methoxyphenoxy)butane. The product was distilled under vacuum at 120 °C (0.2 mm Hg) and collected as a colorless oil. Yield 46.1 g (70.4 %); $n_D^{22} = 1.5370$; IR (KBr) 2925 (CH₂-O, CH₃-O), 1230 and 1105 (C-O) cm⁻¹; ¹H NMR (CDCl₃) δ 6.82 (s, 4 H, ArH), 3.91 (t, J(5,4) = 6.3 Hz, 2 H, CH₂Oph), 3.76 (s, 3 H, OCH₃), 3.42 (t, J(1,2) = 6.8 Hz, 2 H, BrCH₂), 1.96 - 1.89, 1.80 - 1.74, and 1.65 - 1.58 (3 m, 6 H, CH₂CH₂CH₂); MS m/z 272 (14 %, M⁺), 149 (4%, Br(CH₂)₅), 124 (100%, (O-C₆H₄-O-CH₃) + H⁺), 109 (35 %, C₆H₄-O-CH₃).

1-(4-Methoxyphenoxy)-4-(3-thienyl)butane (9)

To 3.16 g (0.13 mol) of magnesium flakes in 10 ml of dry diethylether was added slowly a solution of 30.4 g (125 mmol) of 1-bromo-4-(4-Methoxyphenoxy)butane in 40 ml of dry diethylether. After refluxing for 6 h. the mixture was filtered and the filtrate was slowly added at 0 °C to 17.2 g (0.106 mol) of 3-bromothiophene and 70 mg (0.1 mol%) of dichloro[1,3-bis(diphenylphosphino)propane]nickel(II).¹⁹ The mixture was refluxed overnight and subsequently poured into 150 ml of ice-cold aqueous HCL (0.25 N). The organic layer was separated and the water layer was extracted with diethyl ether (3 x 100 ml). The combined extracts were washed with

water, dried (Na_2SO_4), and concentrated. The resulting brown oil (28.11 g) was crystallized by the addition of methanol (200 ml). Recrystallization from hexane (250 ml) yielded 12 g (43 %) of off-white **9**. The product was slightly contaminated with 1,8-bis(*p*-methoxyphenoxy)octane¹⁵; mp 31-33 °C. IR (KBr) 3100 (ArH), 2965 ($\text{CH}_2\text{-O}$, $\text{CH}_3\text{-O}$), 1240 and 1110 (C-O) cm^{-1} ; ¹H NMR (CDCl_3); δ 7.19 (dd, $J(5,4) = 5.0$, $J(5,2) = 3.0$ Hz, 1 H, thienylH-5), 6.91 (dd, $J(4,5) = 5.0$, $J(4,2) = 1.1$ Hz, 1 H, thienylH-4), 6.89 (dd, $J(2,5) = 2.9$, $J(2,4) = 1.0$ Hz, 1 H, thienylH-2), 6.81 - 6.78 (m, 4H, ArH), 3.92 - 3.85 (m, 2 H, CH_2), 3.7 (s, 3 H, OCH_3), 2.7 - 2.6 (m, 2 H, CH_2), 1.8 - 1.7 (m, 4 H, CH_2CH_2); MS m/z 262 (43 %, M^+) 139 (37 %, $\text{C}_4\text{H}_3\text{S-(CH}_2)_4$) 124 (100%, ($\text{O-C}_6\text{H}_4\text{-O-CH}_3$) + H^+), 109 (20 %, $\text{C}_6\text{H}_4\text{-O-CH}_3$) 97 (85 %, $\text{C}_4\text{H}_3\text{S-CH}_2$); Anal. Calcd for $\text{C}_{15}\text{H}_{18}\text{O}_2\text{S}\cdot 0.015\text{C}_{22}\text{H}_{30}\text{O}_4$: C, 67.28; H, 6.78. Found: C, 67.56; H, 6.77.

1-(4-Methoxyphenoxy)-5-(3-thienyl)pentane (10)

This compound was synthesized from 34.1 g (0.125 mol) of 1-bromo-5-(4-methoxyphenoxy)pentane 5-(*p*-Methoxyphenoxy)pentylbromide and 17.2 g (0.106 mol) of 3-bromothiophene as described for **9**. Crystallization of the crude oil was achieved by the addition of hot hexane. Yield 21.1 g (72 %) white solid **10**. The product was slightly contaminated with 1,10-bis(*p*-methoxyphenoxy)decane¹⁵; mp 48-49 °C. IR (KBr) 3100 (ArH), 2965 ($\text{CH}_2\text{-O}$, $\text{CH}_3\text{-O}$), 1240 and 1110 (C-O) cm^{-1} ; ¹H NMR (CDCl_3) δ 7.23 (dd, $J(5,4) = 4.9$, $J(5,2) = 2.9$ Hz, 1 H, thienylH-5), 6.94 (dd, $J(4,5) = 4.8$, $J(4,2) = 1.2$ Hz, 1 H, thienylH-4), 6.92 (dd, $J(2,5) = 2.6$, $J(2,4) = 0.9$ Hz, 1 H, thienylH-2), 6.84 - 6.81 (m, 4 H, ArH), 3.92 - 3.88 (m, 2 H, CH_2), 3.76 (s, 3 H, OCH_3), 2.69 - 2.64 (m, 2 H, CH_2), 1.83 - 1.75 (m, 2 H, CH_2), 1.73 - 1.65 (m, 2 H, CH_2), 1.54 - 1.46 (m, 2 H, CH_2); MS m/z 276 (51 %, M^+) 153 (11 %, $\text{C}_4\text{H}_3\text{S-(CH}_2)_5$) 124 (100%, ($\text{O-C}_6\text{H}_4\text{-O-CH}_3$) + H^+), 109 (22 %, $\text{C}_6\text{H}_4\text{-O-CH}_3$) 97 (76 %, $\text{C}_4\text{H}_3\text{S-CH}_2$); Anal. Calcd for $\text{C}_{16}\text{H}_{20}\text{O}_2\text{S}\cdot 0.05\text{C}_{24}\text{H}_{34}\text{O}_4$: C, 64.98; H, 6.82. Found: C, 64.57; H, 6.73.

Polymer synthesis and characterization

Electrochemical polymerizations as well as characterizations were performed in a one compartment three-electrode glass cell (RDE 0018 analytical cell kit, EG&G PARC). The cell was kept at room temperature and was equipped with a device to purge the solution inside the cell and to blanket it with inert gas. A platinum plate was used as the auxiliary electrode and an Ag/AgCl electrode (K801, Metrohm) was used as the reference electrode. The potentiostatic polymerizations were carried out using an Autolab potentiostat (Eco Chemie, The Netherlands). The potentiostat was controlled by an Olivetty M24 personal computer. Galvanostatic polymerizations

were conducted with a home-built galvanostat. A digital multimeter (Fluke 45) was used to register the output current and potential. Glassy carbon disks of 8 mm diameter (Antec Leyden, The Netherlands) were used as the working electrode. The electrodes were polished with Alpha Micropolish Alumina No. 1C (1.0 micron, Buehler LTD., U.S.A.). Platinum was applied on the polished surface with an Edwards sputtercoater S150B. A platinum target of 8 cm diameter and 0.5 mm thickness was used as the platinum source. The layer thickness was monitored with an Edwards FTM5 unit. Sputtering was continued until the thickness of the platinum layers was 300 nm.

The electropolymerization solutions contained 0.3 M of monomer and 0.15 M of electrolyte. Nitrogen was first bubbled through these solutions (10 min.) to purge oxygen and was then used to blanket the solution during the polymerization experiment. After polymerization the polymer-modified electrodes were rinsed thoroughly with distilled water.

Enzyme immobilization and measurement of enzyme activity

Enzyme immobilization on the polymer films was achieved by agitating (Gyrotory Shaker model G2, New Brunswick Scientific, USA) the electrodes in 3 ml of 5 mg/ml of glucose oxidase (E.C. 1.1.3.4, type II from *Aspergillus niger*, Sigma company; 25,000 U/g) in phosphate buffered saline (PBS) pH 7.4 at 4 °C for at least 1 h. The membranes were successively dried overnight at 4 °C in a desiccator either over CaCl₂ or without this drying agent.

Enzyme activity was assayed with a three electrode cell containing 20 ml of phosphate buffered saline (PBS) pH 7.4, 5 mM of benzoquinone, and 0.5 M of glucose. Prior to use, the glucose solution was allowed to mutarotate for at least 24 h. The assay was performed with a platinum rotating disk electrode (6 mm diameter) equipped with an Electrocraft corporation model E550 motor and E552 speed control unit. The platinum working electrode was set at a potential of 0.350 V (Ag/AgCl reference) and was rotated at a speed of 2000 rpm. A platinum wire was used as auxiliary electrode. The solution was flushed with argon before each experiment. During the assay argon was blanketed over the solution. The actual assay was performed by monitoring the current output of the potentiostatted RDE while immersing an enzyme-conducting polymer sample into the solution.

References

1. Garnier, F., *Angew. Chem.*, (1989) **101**: 529.
2. Atta, N.F., Galal, A., Karagözler, A.E., Russell, G.C., Zimmer, H. and Mark Jr., H.B., *Biosensors & Bioelectronics*, (1991) **6**: 333-341.
3. Schuhmann, W., Lammert, R., Hämmerle, M. and Schmidt, H.-L., *Biosensors & Bioelectronics*, (1991) **6**: 689-697.
4. Sasso, S.V., Pierce, R.J., Walla, R. and Yacynych, A.M., *Anal. Chem.*, (1990) **62**: 1111-1117.
5. Hillman, A.R., Loveday, D.C., Bruckenstein, S. and Wilde, C.P., *J. Chem. Soc. Faraday Trans. 1.*, (1990) **86**: 437-438.
6. Geise, R.J., Adams, J.M., Barone, N.J. and Yacynych, A.M., *Biosensors & Bioelectronics*, (1991) **6**: 151-160.
7. Patil, A.O., Ikenoue, Y., Wudl, F. and Heeger, A.J., *J. Am. Chem. Soc.*, (1987) **109**: 1858-1859.
8. Havinga, E.E., van Horssen, L.W., ten Hoeve, W., Wynberg, H. and Meijer, E.W., *Polymer Bulletin*, (1987) **18**: 277-281.
9. Havinga, E.E., ten Hoeve, W., Meijer, E.W. and Wynberg, H., *Chemistry of Materials*, (1989) **1**: 650-659.
10. Campaigne, E. and Yokley, O.E., *J. Org. Chem.*, (1963) **28**: 914-917.
11. Gilbert, E. *Sulfonation and related reactions*. Interscience Publ., New York: (1965).
12. Pham, C., Mark, H.B. and Zimmer, H., *Synthetic Comm.*, (1986) **16**: 689-696.
13. Anderson, H.J., Loader, C.E., Xun Xu, R., Le, N., Gogan, N.J., McDonald, R. and Edwards, L.G., *Can. J. Chem.*, (1985) **63**: 896-902.
14. Vogel, A.I. *Textbook of practical organic chemistry*. 5th Ed. John Wiley & Sons, New York: (1989).
15. Bäuerle, P., Würthner, F. and Heid, S., *Angew. Chem.*, (1990) **102**: 414-415.
16. Ashley, J.N., Collins, R.F., Davis, M. and Sirett, N.E., *J. Chem. Soc.*, (1958): 3298.
17. Nineham, A.W., *J. Chem. Soc.*, (1953): 2601.
18. Ikenoue, Y., Uotani, N., Patil, A.O., Wudl, F. and Heeger, A.J., *Synth. Met.*, (1989) **30**: 305-319.
19. Hecke, G.R. and Horrocks Jr., W.DeW., *Inorg. Chem.*, (1966) **5**: 1968.
20. Rallings, R.J. and Smith, J.C., *J. Chem. Soc.*, (1953): 618-622.
21. Reed, R.M. and Tartar, H.V., *J. Am. Chem. Soc.*, (1935) **57**: 570-571.
22. Fujita, S., *Synthesis*, (1982) **39**: 423-424.
23. Distler, H., *Angew. Chem.*, (1965) **77**: 291-302.
24. Ikenoue, Y., Saida, Y., Kira, M., Tomozawa, H., Yashima, H. and Kobayashi, M., *J. Chem. Soc., Chem. Commun.*, (1990): 1694-1695.
25. Takakubo, M., *J. Electroanal. Chem.*, (1989) **258**: 303-311.
26. Gratzl, M., Hsu, D., Riley, A.M. and Janata, J., *J. Phys. Chem.*, (1990) **94**: 5973-5981.
27. Asavapiriyant, S., Chandler, G.K., Gunawardena, G.A. and Pletcher, D., *J. Electroanal. Chem.*, (1984) **177**: 229-244.
28. Ikenoue, Y., Chiang, J., Patil, A.O., Wudl, F. and Heeger, A.J., *J. Am. Chem. Soc.*, (1988) **110**: 2983-2985.
29. Patil, A.O., Ikenoue, Y., Basescu, N., Colaneri, N., Chen, J. and Wudl, F., *Synth. Met.*, (1987) **20**: 151-159.
30. Albery, W.J., Li, F. and Mount, A.R., *J. Electroanal. Chem.*, (1991) **310**: 239-253.
31. Harrison, J.A. and Thirsk, H.R. *The Fundamentals of Metal Deposition*. In: *Electroanalytical Chemistry, Vol. 5*, edited by Bard, A.J., Marcel Dekker, New York: (1971) pp. 67-146.
32. Hillman, A.R. and Mallen, E.F., *J. Electroanal. Chem.*, (1987) **220**: 351-367.
33. Miller, L.L., Zinger, B. and Zhou, Q.X., *J. Am. Chem. Soc.*, (1987) **109**: 2267-2272.
34. Krishna, V., Ho, Y.-H., Basak, S. and Rajeshwar, K., *J. Am. Chem. Soc.*, (1991) **113**: 3325-3333.
35. Ofer, D., Crooks, R.M. and Wrighton, M.S., *J. Am. Chem. Soc.*, (1990) **112**: 7869-7879.

36. Rosseinsky, D.R., Morse, N.J., Slade, R.C.T., Hix, G.B., Mortimer, R.J. and Walton, D.J., *Electrochim. Act.*, (1991) **36**: 733-738.
37. Krische, B. and Zagorska, M., *Synth. Met.*, (1989) **28**: c263.
38. Phillips, J.P. *Spectra-structure correlation*. Academic Press, New York: (1964).
39. Pretsch, E., Clerc, T., Seibl, J. and Simon, W. *Tabellen zur Strukturaufklärung organischer Verbindungen mit spektroskopischen Methoden*. 3rd Ed. Springer-Verlag, Berlin: (1986).
40. Aubré-Lecat, A., Hervagault, C., Delacour, A., Beaudé, P., Bourdillon, C. and Remy, M., *Anal. Biochem.*, (1989) **178**: 427-430.
41. Bourdillon, C. and Majda, M., *J. Am. Chem. Soc.*, (1990) **112**: 1795-1799.
42. Bartlett, P.N. and Whitaker, R.G., *J. Electroanal. Chem.*, (1987) **224**: 37-48.
43. Tamiya, E., Karube, I., Hattori, S., Suzuki, M. and Yokoyama, K., *Sensors and Actuators*, (1989) **18**: 297-307.
44. Yokoyama, K., Tamiya, E. and Karube, I., *Anal. Let.*, (1989) **22**: 2949-2959.
45. Janda, P. and Weber, J., *J. Electroanal. Chem.*, (1991) **300**: 119-127.
46. Guo, L.H. and Hill, H.A.O., *Adv. Inorg. Chem.*, (1991) **36**: 341-375.
47. Aizawa, M., Yabuki, S., Shinohara, H. and Ikariyama, Y., *Ann. N. Y. Acad. Sci.*, (1990) **613**: 827-831.
48. Fortier, G. and Bélanger, D., *Biotechnol. Bioeng.*, (1991) **37**: 854-858.
49. Bartlett, P.N., Tebbutt, P. and Tyrrell, C.H., *Anal. Chem.*, (1992) **64**: 138-142.
50. De Taxis Du Poet, P., Miyamoto, S., Murakami, T., Kimura, J. and Karube, I., *Anal. Chim. Act.*, (1990) **235**: 255-263.
51. Souto-Maior, R.M., Hinkelmann, K., Eckert, H. and Wudl, F., *Macromol.*, (1990) **23**: 1268-1279.

4 Amperometric glucose sensor based on glucose oxidase immobilized within poly(pyrrole) microtubules

Abstract

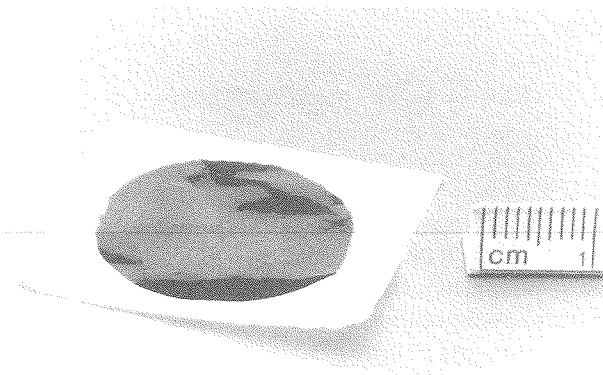
Template synthesis inside track-etch membranes is employed to create conducting microtubules of poly(pyrrole). Within these tubules, glucose oxidase can be adsorbed irreversibly, while retaining its catalytic activity. A glucose sensor is described in which the poly(pyrrole) microtubules are used as a mediator. With this sensor glucose concentrations ranging from 1-40 mM can be measured amperometrically under steady-state conditions. By applying flow injection conditions this range can be extended to 250 mM. Chronoamperometric determination of glucose is possible in the concentration range of 2.5-15 mM. The sensor is highly selective for glucose and the response is independent of oxygen concentration. Evidence is presented that in the biosensor direct electron transfer occurs between glucose oxidase and the poly(pyrrole).

4.1 Introduction

Creating an environment where a redox enzyme, despite its insulating protein shell,^{1,2} can communicate directly with an electronically conducting material, opens the possibility to construct a reagentless biosensor. In this chapter we describe such a biosensor. We have immobilized the redox enzyme glucose oxidase on poly(pyrrole), which is located within the pores of a track-etch membrane (Nuclepore[®] or Cyclopore[®]). Such pores can act as a template to synthesize microtubules from polyconjugated conducting materials like poly(pyrrole) and poly(thiophene), as was shown earlier by Cai and Martin.³ These microtubules display enhanced electronic conductivity. Our rationale was that the microscopic space inside the pores of the track-etch membranes, together with the morphology of

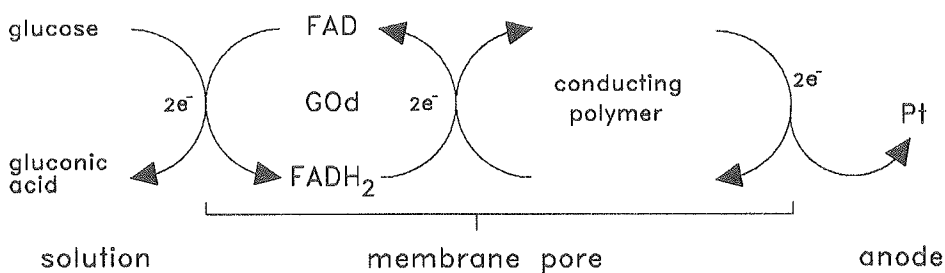
the conducting polymer might allow immobilization of glucose oxidase (GOd) and would favour direct electron transfer between the redox enzyme and the conducting polymer.

It is most preferable to perform enzyme immobilization without additional reagents. Simple adsorption on the conducting polymer surface will allow the enzyme to remain catalytically active. We expected that the confined space in the pores would



Photograph of the track-etch membrane biosensor.

contribute to this desired property. Not only will the protein molecules inside the pores have a better chance to retain their active structure, but also these molecules will be protected from the bulk solution. Sheer forces and sensor manipulation will have a less damaging effect. We will show that the immobilization of glucose oxidase on poly(pyrrole) inside the pores of track-etch membranes indeed gives rise to a stable



Scheme 1. *Electron shuttle, showing the path of the electrons involved in the enzymatic oxidation of glucose, mediated by the poly(pyrrole) microtubules.*

and reagentless biosensor. This sensor is able to detect glucose in an amperometric way. The reduced enzyme becomes reoxidized by donating its electrons directly to the conducting polymer (Scheme 1). Optimal interaction between glucose oxidase and the conducting polymer results in an oxygen independent detection. A photograph of the sensor membrane is shown on page 56.

4.2 Results and discussion

4.2.1 Synthesis of microtubules

Track-etch membranes were modified with poly(pyrrole) by means of an oxidative polymerization reaction (see also Chapter 2). The polymerization equipment is shown in Figure 1. Poly(pyrrole) polymerization was effected by allowing the track-etch membrane to separate an aqueous 0.6 M pyrrole solution from

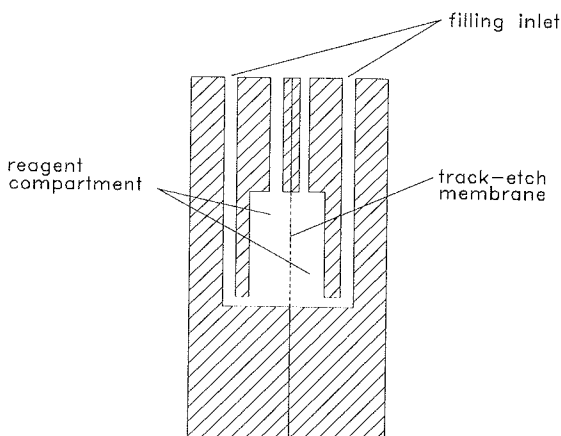


Figure 1. Schematic representation of the apparatus used in the poly(pyrrole) microtubules synthesis.

an aqueous 2.0 M FeCl_3 solution. In the pores of the membrane the pyrrole monomer and the oxidizing solution meet, whereupon polymerization takes place. In this way we were able to modify membranes with original pore sizes ranging from 200 nm to 8 μm . We managed to immobilize GOd in conducting polymer modified membranes with 400, 600, 800, and 1000 nm pores (*vide infra*). Membranes with larger pores were not used for enzyme immobilization, because modification of these larger pores

with conducting polymer does not lead to enhanced conductivities.³ Therefore, it was not expected that such membranes would lead to working biosensors.

The porosity of the modified membranes was varied by allowing the polymerization reaction to take place for increasing periods of time. Scanning electron microscopy (SEM) showed how the pores of the track-etch membranes became filled

Table 1. Mean pore size, electrical resistance, and enzyme immobilization capacity of poly(pyrrole) microtubules as a function of polymerization time.^a

Time/min.	Mean pore size/nm	Resistance/ Ω	Enzyme immobilization
untreated	985	∞	-
0.5	889	52.0	+
1.0	603	13.1	+++
2.0	315	3.9	+
3.0	264	2.1	+
4.0	212	1.9	+
5.0	0	1.9	-
10.0	0	1.9	-

^a Cyclopore[®] membrane with originally 1000 nm pores, treated with 0.6 M of pyrrole and 2.0 M of FeCl₃ in water.

with conducting polymer when the polymerization time increased (Figure 2). In Table 1 the mean pore size as measured by differential flow porosimetry is given as a function of the polymerization time. The results in this table are for a membrane with an original pore size of 1 μm . There is a correlation between the pore size of the membrane after polymerization and the electrical resistance of the conducting polymer inside the pores (Figure 3). When the pores become smaller, the amount of conducting polymer inside the pores increases and the resistance becomes lower. After 4 minutes, the porosity became insignificantly low and the resistance reached a constant value of 1.9 Ω . Longer polymerization times gave non-porous membranes (Table 1). Enzyme treatment of these membranes did not produce a working biosensor (see section 4.2.2).

The membranes that were polymerized until they became non-porous showed a conductivity of approximately 20 Scm^{-1} .^{*} As the surface area of the microscopic

^{*} This is the conductivity (S/cm) of a poly(pyrrole) microtubule which was calculated from the resistance (Ω) of the pores according to the formula: $\sigma = l/R.A$. In this formula σ is the conductivity, R is the resistance, l is the length, and A is the surface area of a microtubule. The resistance of a microtubule is estimated from the measured resistance by correcting for the number of pores that contribute to the electrical conductivity during the measurement. The number of pores is known from scanning electron micrographs.

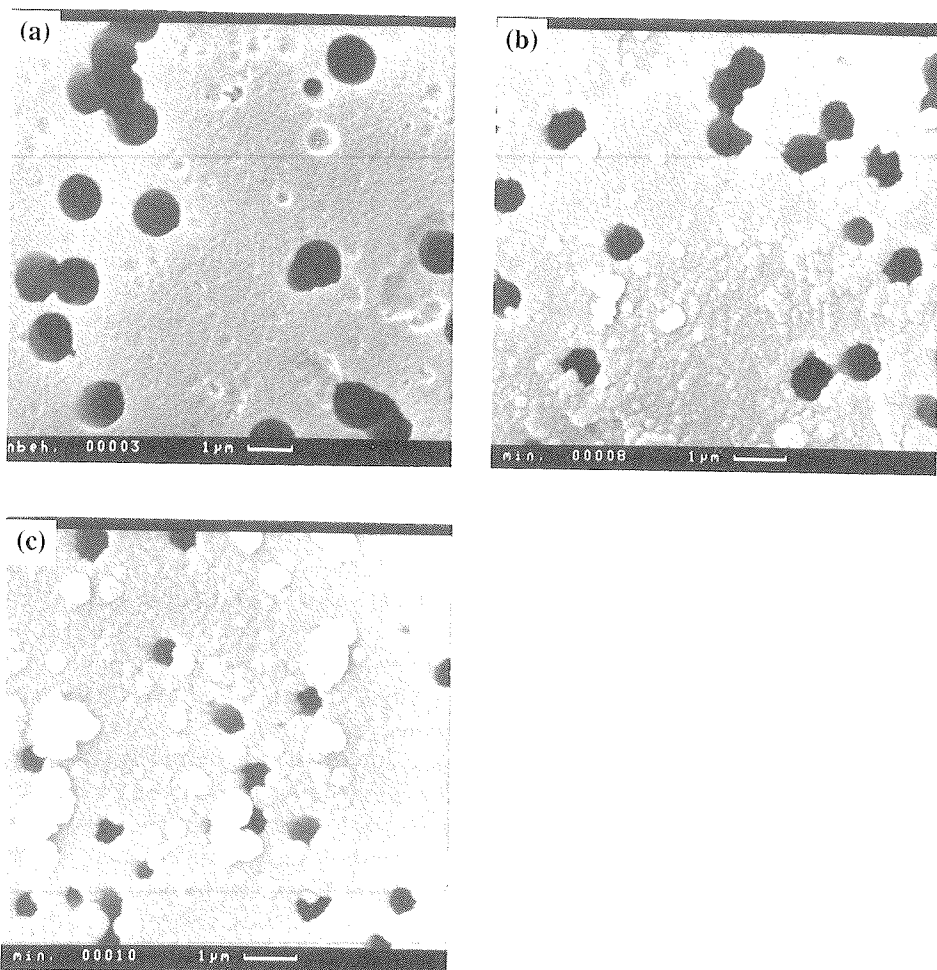


Figure 2. Scanning electron micrographs of track-etch membranes with an original pore size of 800 nm at various polymerization times: (a) untreated membrane; (b) 2 min.; (c) 5 min.

hollow cylinders cannot be determined precisely, it is not possible to give exact conductivity values. The electrical resistances in Table 1, however, are accurate.

4.2.2 Immobilization of glucose oxidase

Immobilization of glucose oxidase inside the conducting microtubules was achieved by soaking a modified membrane in an aqueous, buffered solution,

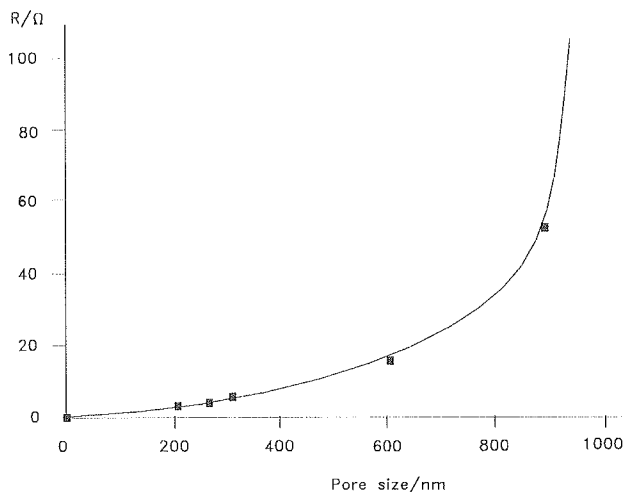


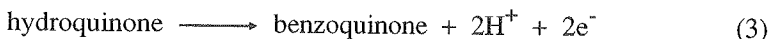
Figure 3. Resistance of a track-etch poly(pyrrole) membrane with originally 1000 nm pores as a function of the pore size after treatment with pyrrole and FeCl_3 .

containing the enzyme, for at least 0.5 hour and successively drying overnight at 4 °C.

The membranes, modified with conducting polymer and treated with GOD-solution, were tested for enzymatic activity by means of an electrochemical assay based on the rotating disk electrode technique (Chapter 2).⁴ It is important to have an indication of the amount of biochemically active redox enzyme present in the biosensor. The actual current response of an amperometric biosensor may be obscured by, e.g., interfering electroactive species in the sample solution, the solution impedance, and capacitive charging of the electrode. An independent assay of the enzyme activity would be helpful in the biosensor analysis. In the electrochemical assay the natural cosubstrate of the enzyme (oxygen) was replaced by the artificial electron acceptor benzoquinone. This molecule was chosen because it had been used previously with good results.⁵ The formation of hydroquinone, its reduced form, can be measured amperometrically at a rotating disk electrode (RDE, see section 2.5.4.). The following reactions take place:



At the rotating disk electrode, the enzymatically produced hydroquinone is reoxidized to benzoquinone:



This process can be measured amperometrically. The angular velocity of the rotating electrode was chosen such that no diffusion limitation took place. The measurements were conducted at pH 7.4, which is not the optimum value for glucose oxidase (optimum activity at pH 5.5 - 6).^{6,7} However, we calibrated the activity of the immobilized enzyme with the activity of the enzyme in solution at exactly the same pH value. The glucose concentration was chosen as high as possible, viz. 0.5 M, which is far above the K_M value.⁶ Higher values cannot be used, because of substrate inhibition.⁴ The benzoquinone concentration was 5 mM. This value was a compromise: on the one hand it is desirable to use a high concentration to avoid reaction rate variation due to cosubstrate consumption, on the other hand it is required to minimize the current increase due to the spontaneous oxidation of glucose by benzoquinone.⁴ For this a low concentration of co-substrate is desired. The measurements were conducted in an anaerobic three electrode cell to exclude the mediation of oxygen (see also Chapter 2). Under the above mentioned conditions the oxidation of benzoquinone by the enzyme will be the rate determining step. This means that the slopes of current-time plots from experiments with immobilized and free enzyme can be correlated, at least in a semi-quantitative way. The measured current is, therefore, directly proportional to the enzyme activity, irrespective of whether the enzyme is in solution or is immobilized.

In Figure 4 the rotating disk electrode assay of a GOD-treated poly(pyrrole) membrane is shown. The shown response curve is for an 800 nm pore size membrane introduced into the assay cell. As can be seen, the current increases immediately after introduction of the membrane. Membranes with 400, 600, and 1000 nm pores also showed this behaviour, whereas membranes with pores smaller than 400 nm did not display any enzyme activity. The fact that after withdrawal of the membrane the activity returns to its initial value, is an indication that the enzyme is properly immobilized. Not properly immobilized material would have stayed in solution and the slope of the line after point 2 in the figure would have been higher. This was actually found for membranes treated with GOD without conducting polymer present in the pores. In the latter case any enzyme present in the pores is washed out.

Drying of the membrane after adsorption of the enzyme appeared to be essential. Enzyme was washed out completely when membranes were used directly after enzyme treatment. We may conclude, therefore, that drying results in proper immobilization on the conducting polymer surface inside the pores of the membrane.

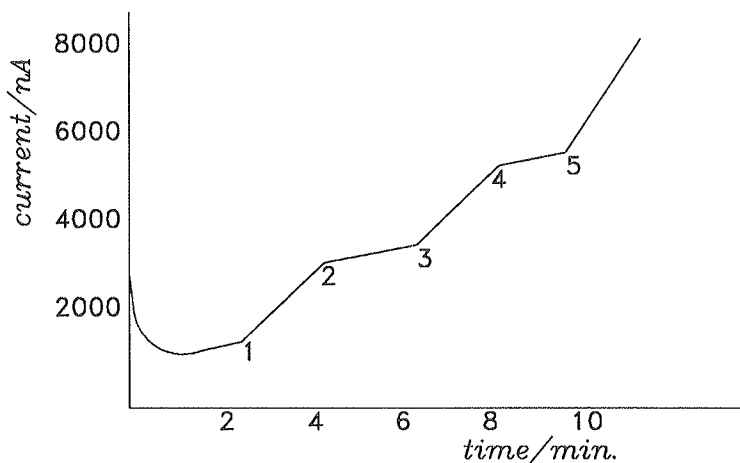


Figure 4. Measurement of enzyme activity by monitoring enzymatically produced hydroquinone at a rotating disk electrode. (1) & (3): introduction of membrane; (2) & (4): withdrawal of membrane; (5): introduction of 0.125 U of glucose oxidase in solution.

From Table 1 (last column) it is evident that the enzymatic activity of the polymer modified membrane disappears when it is no longer porous. Different polymerization times gave different enzyme activities. For the membrane in Table 1 the highest activity was reached at a polymerization time of one to two minutes. Figure 4 shows that repeated introduction and withdrawal of the poly(pyrrole) membrane does not change the amount of active, immobilized enzyme (points 1-4). At the end of the measurement, a known quantity (5 μg ; 0.125 U) of enzyme was added to calibrate the activity (point 5 in Figure 4). From this calibration it was concluded that approximately 0.125 U of active GOd is present in the membrane of Figure 4.

A poly(pyrrole) modified (1 minute polymerization time) membrane with originally 1000 nm pores was treated with fluorescein-labeled⁸ glucose oxidase. This labeled enzyme was synthesized according to a literature procedure (reaction of GOD with fluorescein isothiocyanate in borate buffer, pH 9, for 2 hours at 4 °C). The membrane treatment was exactly the same as for the unlabeled glucose oxidase. After enzyme adsorption, the membrane was imaged with a confocal laser scan microscope in the fluorescence mode (Figure 5). From Figure 5, it is clear that only the poly(pyrrole) walls within the membrane pores contain glucose oxidase. Enzyme adsorption on the membrane surface hardly occurs. There are only a few clusters of -probably denatured- protein molecules present on the surface. Therefore, we may conclude that the enzyme immobilization is most effective inside the pores and not on the membrane surface. This is in line with the results described in Chapter 3.

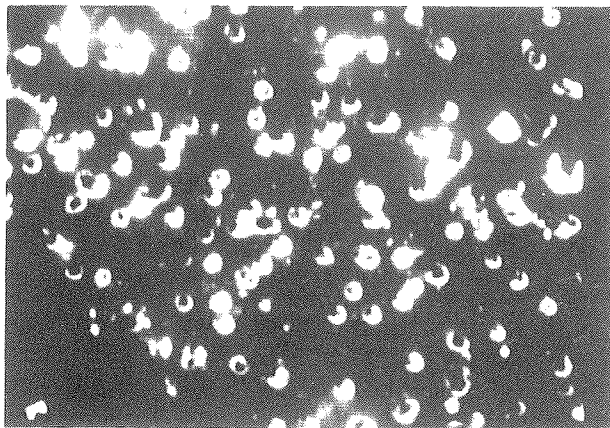


Figure 5. Convocal laser scan microscopy image of a track-etch membrane treated with fluorescein-labeled glucose oxidase. Original pore size 800 nm, poly(pyrrrole) treatment 1 min.

4.2.3 Amperometric analysis

Continuous flow analysis in combination with amperometry is the most frequently used analysis method in this thesis. This combination allows for easy, fast, and accurate measurements of the current response of an amperometric biosensor at various substrate concentrations.

In continuous flow analysis, the detector unit is situated in a flow cell and a continuous flow of either a carrier solution or a solution containing the analyte of interest, is conducted along the detector. In our case the detector unit is the biosensor membrane and the analyte is the substrate for the applied enzyme. With the continuous flow technique steady-state currents are measured. This means that the concentration of analyte at the surface of the biosensor is not changing at the moment the current response is recorded.

The principle of amperometry was discussed in Chapter 2.5.1. In amperometric biosensor analysis, the current of a given sensor is measured under the steady-state conditions mentioned above, in the presence of various substrate concentrations and compared with the current that flows when no substrate is present (background current). The difference in current between these two situations is an indication of the biosensor activity and will be dependent on the substrate concentration as described in Chapter 2.

In order to construct electrodes from our poly(pyrrrole) modified membranes, we coated one of the membrane sides with a platinum layer. A layer thickness of 50 nm

proved to be sufficient. Subsequent to coating, the membranes were treated with GOD-solution. The platinum coated electrodes did not respond to glucose when the membranes had not previously been treated with enzyme. Therefore, it can be concluded that non-specific oxidation of glucose at the platinum surface does not take place.

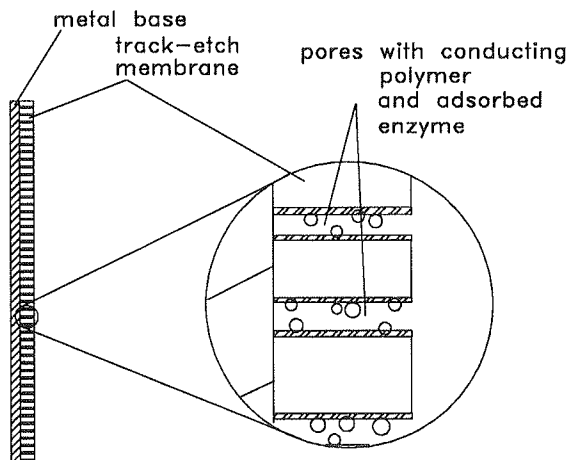


Figure 6. Schematic representation of the track-etch membrane biosensor.

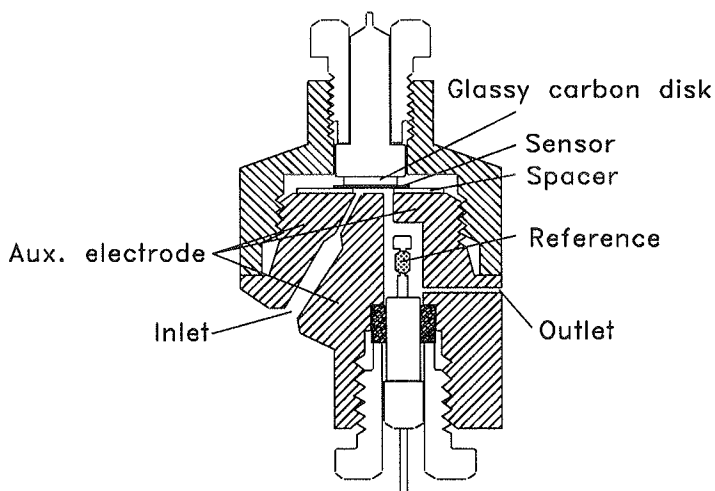


Figure 7. Layout of the flow cell used in the biosensor activity measurements.

The biosensor thus constructed is shown in Figure 6. The membrane was placed in a three electrode cell and acted as the working electrode (Figure 7). The cell was taken up in a continuous flow system, with the possibility to switch between a buffer solution and a solution which contained a known amount of glucose. All experiments were carried out under an argon atmosphere and at least 25 units/ml of catalase present in all solutions. The latter enzyme was added to destroy any H_2O_2 produced. In Figure 8 the increase in current upon the addition of 10 mM glucose is shown. The

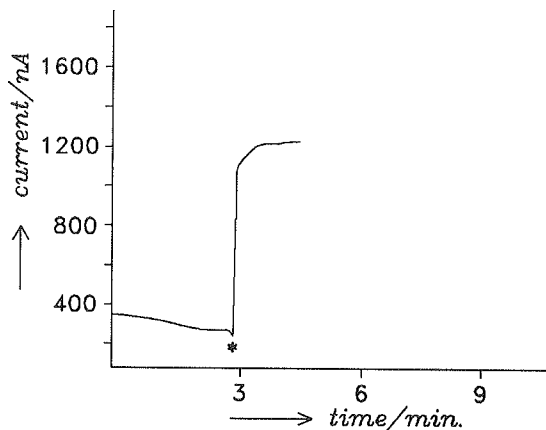


Figure 8. Response of the track-etch membrane biosensor to 10 mM glucose under continuous flow conditions. Applied potential 0.350 V (vs. Ag/AgCl). Phosphate buffered saline solution (pH 7.4), 25 U/ml catalase. Measurements under an argon atmosphere. (*) Addition of glucose.

electrochemical response to glucose in this figure is representative for membranes containing 400, 600, 800, and 1000 nm pores. A calibration curve was made by successively measuring various amounts of glucose with the same sensor (Fig. 9). The current response to glucose was more or less linear up to 10 mM. Measurements could be performed up to 40 mM of glucose.

When oxygen is present, it may become a competing species for the poly(pyrrole) in accepting electrons from the flavin units of glucose oxidase. In that case not only the current due to the direct electron transfer to the polymer becomes smaller, but also hydrogen peroxide will be formed. We observed no difference in response to glucose between sensors operating under an argon and under an oxygen atmosphere. To assure that absolutely no oxygen was present during the experiments the solutions were purged continuously with argon gas for several days and the response to glucose was measured at fixed intervals during this period. No decrease in response was

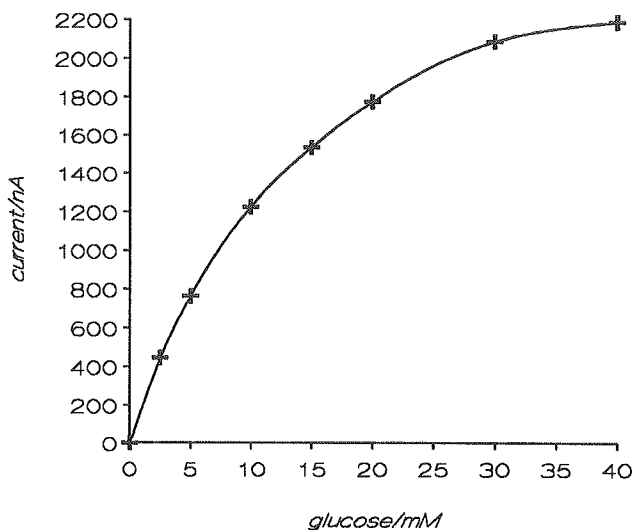


Figure 9. Plot of the steady-state current measured at 0.350 V (vs. Ag/AgCl) as a function of glucose concentration. Track-etch membrane with 800 nm pores, treated with pyrrole/iron(III) chloride for 1 min, and incubated with 5 mg/ml of glucose oxidase and subsequently dried for 18 h. Measured in phosphate buffered saline solution pH 7.4 with 25 U/ml of catalase under an argon atmosphere.

observed in this case. Further proof that the response current indeed is independent of oxygen comes from the experiments discussed below.

The potential we applied routinely in our measurements was 0.350 V vs. Ag/AgCl reference, which is very low. Even lower potentials were possible. We were able to measure the response of the biosensor to glucose at a potential as low as 100 mV vs. Ag/AgCl (Figure 10a). In order to test whether there was any mediation by oxygen we also measured the response of the same sensor to H_2O_2 separately. At a potential of 100 mV vs. Ag/AgCl the current due to the addition of glucose was positive, whereas even small amounts of purposely added H_2O_2 (0.0025 wt% in phosphate buffer, pH 7.4) gave a strongly negative response (Figure 10b).^{9,10} This confirms that no hydrogen peroxide is formed in our track-etch membrane sensor.

The positive response to glucose at the low potential of 100 mV is possible because the redox potential of the flavin unit is still much more negative. FAD, free in solution has a redox potential of -480 mV vs. Ag/AgCl.¹¹ The actual redox potential of FAD inside our biosensor will be different, but is probably of the same order of magnitude as in solution. Electron transfer from the FAD centers in glucose oxidase to an (aminophenyl)boronic acid modified glassy carbon electrode has been reported to take place at a potential of -505 mV vs. Ag/AgCl.¹²

In our opinion, electron mediation by FAD, which is released from the enzyme, can be excluded. The flavin co-factor is essentially irreversibly bound to the protein.¹³ Our measurements were performed in a flow-system. Any released FAD would have been immediately washed out and could not accidentally have mediated the electron transfer. Therefore, we may be reasonably sure that the enzyme transfers its electrons directly to the conducting polymer. The confined space in the pores, together with the amorphous structure of the poly(pyrrrole) interior¹⁴ apparently brings the active centers of the enzyme molecules in close contact with the conducting polymer. In its oxidized state poly(pyrrrole) is a polycation.⁶ Glucose oxidase, on the other hand has at least net 10 negative charges on its surface.¹⁵ The interaction between polymer and enzyme, therefore, is expected to be electrostatic in nature and may be very strong (see also below).

After enzyme treatment the track-etch biosensors were dried over CaCl_2 in a desiccator. Drying of the membrane after enzyme treatment appeared to be essential for good enzyme immobilization and for the communication between the enzyme and the conducting polymer. We believe that water and enzyme are competing species with regard to binding to the polymer. When water is removed by evaporation, enzyme adsorption is favoured¹⁶ and the active centers of the enzyme can approach the conducting polymer sufficiently to make direct electron transfer possible. The possibility of realizing direct electron transfer from biocatalysts to electrodes has been mentioned in the literature¹⁷ and direct electron transfer between glucose oxidase and poly(pyrrrole) has been described before.^{18,19} However, no glucose dependent current values were reported and it was said that the direct interaction of glucose oxidase with poly(pyrrrole) is weak.²⁰ Electron transfer between glucose oxidase and an

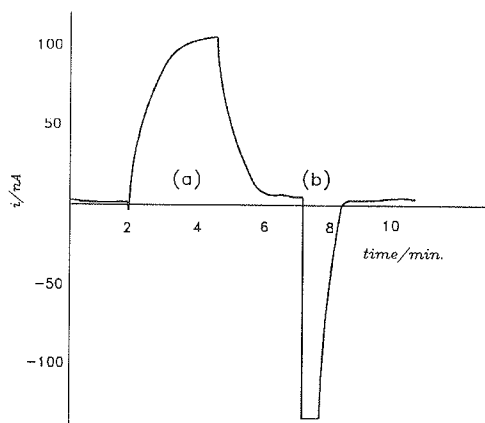


Figure 10. Current response of a track-etch membrane biosensor (same sensor as in Figure 9) at a measuring potential of 0.100 V vs. Ag/AgCl : (a) 5 mM glucose; (b) 0.0025 wt% of H_2O_2 .

(aminophenyl)boronic acid modified glassy carbon electrode has been described but measurements of glucose concentrations were not reported.¹² The direct interaction of glucose oxidase with conducting organic salt electrodes has been claimed by Albery and coworkers,^{21,22} but their results are not unambiguous.²³ We observed a distinct current response and the possibility of mediated electron transfer can probably be excluded as discussed above.

The response time of the sensor is the time necessary to reach 95% of the steady-state current. This response time was measured for 5 mM glucose concentrations and appeared to be 40 ± 2 s, which is fast considering the geometry of the sensor. External and internal substrate diffusion resistances contribute to this response time (see Chapters 2 & 7).

4.2.4 Response under increased salt concentrations

The response of the sensor to 10 mM glucose was investigated under various salt (NaCl) concentrations. When the ionic strength of the solution was increased, the electron transfer from the enzyme to the electrode became diminished as is shown by the decreased current response in Figure 11. However, the process is reversible as the response fully recovered upon switching back to the initial salt concentration (0.15 M; Figure 11). We believe that at high ionic strength the charges involved in the

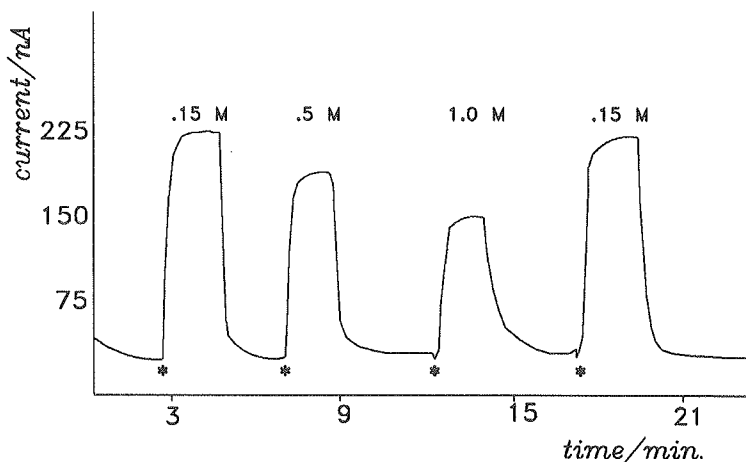


Figure 11. Response of a track-etch membrane biosensor to 10 mM glucose at different NaCl concentrations. The conditions were as indicated in Figure 9. (*) Addition of glucose.

electrostatic interaction between enzyme and conducting polymer are screened, thereby suppressing the transfer of electrons (see also Chapter 5).

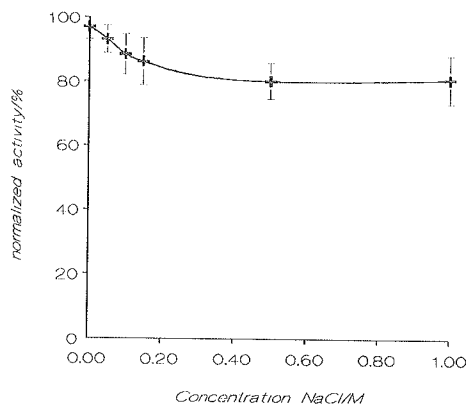


Figure 12. Relative activity of glucose oxidase in solution in the presence of various concentrations of NaCl.

To exclude the possibility that the diminished current response is due to inhibition of the enzyme activity by Cl^- ,²⁴ we tested the enzyme activity of glucose oxidase in solution in the presence of NaCl by means of a spectrophotometric assay.²⁵ This assay is based on a coupled reaction of the enzymes glucose oxidase and horseradish peroxidase. The peroxidase catalyses the reaction of a reduced chromogen (*o*-dianisidine) with H_2O_2 , which is produced by glucose oxidase. The oxidized form of *o*-dianisidine is subsequently measured spectrophotometrically at 450 nm. The chloride concentration in the activity measurements was varied from 0 to 1 M. An enzyme concentration corresponding to 5 mU/ml and a glucose concentration of 100 mM were used. The concentration of *o*-dianisidine was 10 mM and the peroxidase activity was approximately 0.6 U/ml. In the relevant NaCl concentration range (0.15–1.0 M) the enzyme activity did not decrease significantly (Figure 12), showing that the enzyme activity is not dependent on the Cl^- concentration.

4.2.5 Selectivity and lifetime

The sensitivity of the sensor to fructose, citrate, lactate, urea, uric acid, gluconate, and pyruvate was tested separately. No significant response was observed to any of these components when they were present at mM concentrations. Ascorbate (vitamin C), a common interferent in amperometric biosensors, however, interfered strongly when present at 5 mM concentration. However, in real samples the ascorbate concentration is usually much lower²⁶ (e.g. milk; 0.1 mM).

The response of a freshly made biosensor to 10 mM glucose was tested over a period of 5 weeks in the presence of 25 units/ml of catalase. The response was not stable during the first days of operation (Figure 13). In the beginning, the current

response to 10 mM glucose decreased to 50 % of the value measured on the first day. Similar lifetime curves have been reported before in the literature for other biosensors.²⁷ We presume that in the beginning an amount of enzyme, which is less

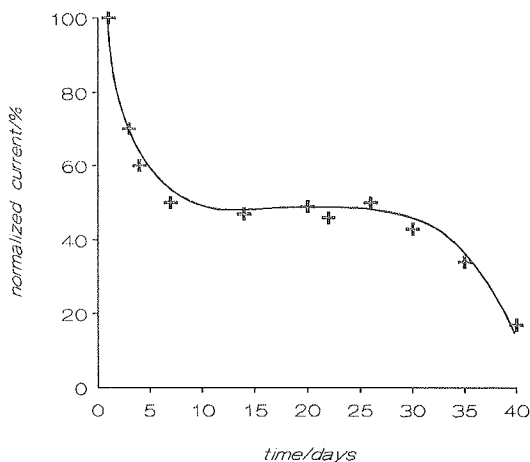


Figure 13. Plot of the current response due to 10 mM glucose for the track-etch membrane biosensor of Figure 10 as a function of time. Between the measurements the biosensor was kept in the flow cell while the flow was maintained at 1.75 ml/min. $T = 25^{\circ}\text{C}$.

firmly bound, is slowly washed out. After a few days, only firmly bound enzyme is left and a stable current response is obtained over an extended period of time. The response of the sensor remained nearly the same for more than 3 weeks (Figure 13). In this period measurements of glucose were performed for prolonged periods of time and different experiments were conducted with the sensor membrane. For instance, between day 20 and 22, 10 mM glucose was measured continuously for 18 hours. The current did not decrease significantly during this measurement.

We also measured glucose for extended periods of time under ambient atmosphere without catalase present. No significant loss of membrane sensitivity was observed in this case. If the reoxidation of GOD had been mediated by oxygen, this would have resulted in denaturation of the enzyme by hydrogen peroxide.

4.2.6 Flow injection analysis technique

In the flow injection analysis technique (FIA) a small volume of a sample solution is introduced into the carrier stream of a flow system. In this way a well defined and reproducible concentration transient is produced at the detector. The current response

of an amperometric biosensor in a flow injection system is the sum of various parameters, e.g., the injection volume, the analyte (substrate) dispersion during transport from the injection site to the sensor surface, and the mass transfer parameters of the biosensor.²⁸ The best results are obtained when the sample volume leads to a current response with a peak height of half the value of the steady-state response.²⁸ For an enzyme based biosensor this means that in FIA measurements not all the enzyme molecules are occupied with substrate. As a result, current limitation by the enzyme reaction kinetics will not occur, even not at high substrate concentrations. Therefore, it may be expected that under FIA conditions the dynamic range of the biosensor will be larger.

A track-etch membrane with originally 800 nm pores which had been treated with pyrrole and FeCl₃ for one minute, followed by glucose oxidase adsorption and drying, was used as the enzyme electrode in the FIA experiments. The electrode was poised at a potential of 0.35 V versus Ag/AgCl. Measurements were conducted under argon with 25 U/ml catalase present in all solutions. The same flow system was used as for the continuous flow measurements (section 4.2.3). In the FIA experiments the buffer

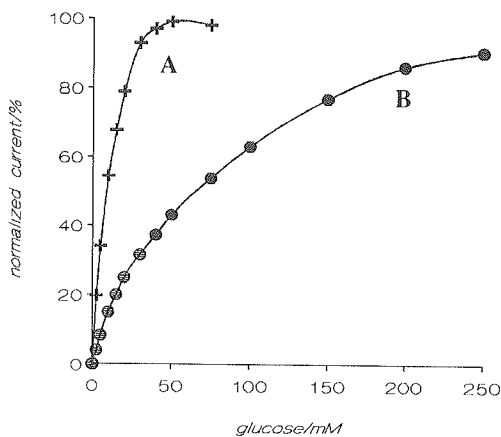


Figure 14. Plot of the current measured at 0.350 V (vs. Ag/AgCl) as a function of glucose concentration. Comparison of the steady-state current (A) with the current measured in the flow injection analysis technique (B). Track-etch membrane with 800 nm pores, treated with pyrrole/iron(III) chloride for 1 min., incubated with 5 mg/ml of glucose oxidase and subsequently dried for 18 hrs. Measured in phosphate buffered saline solution pH 7.4 with 25 U/ml of catalase under an argon atmosphere.

stream was replaced by a glucose solution for a short period of time. In this way, a small amount of glucose solution could be introduced into the carrier stream. The carrier solution was forced through the cell with a flow rate of 1.75 ml/min. A high concentration of glucose (250 mM) was chosen to optimize the conditions (*vide*

supra). The optimum injected volume corresponded with a sampling time of 19 s. In Figure 14 the normalized current response ($i_{\max} = 100\%$) of the sensor is shown under steady-state conditions (A) and FIA conditions (B). From this figure it can be seen that the response in the FIA measurement is very good over a wide range of glucose concentrations. It can be concluded that the dynamic range of the biosensor is much larger in the flow injection mode than in the steady-state condition mode, as was expected. Concentrations up to 250 mM glucose can be determined with good results. This is an improvement of more than 600% in comparison with measurements under steady-state conditions.

4.2.7 Chronoamperometry

The chronoamperometric analysis technique was described in Chapter 2.5.2. From the Cottrell equation (Chapter 2, equation 7) it follows that the diffusion limited current, i_d , is proportional to the bulk analyte concentration and inversely proportional to $t^{1/2}$. Measuring the current as a function of time after a potential step under various bulk analyte concentrations, c_b , will lead to different decay curves. Sampling the current magnitude at a fixed time, $t = \tau$, will give information about the current dependence on the analyte concentration.

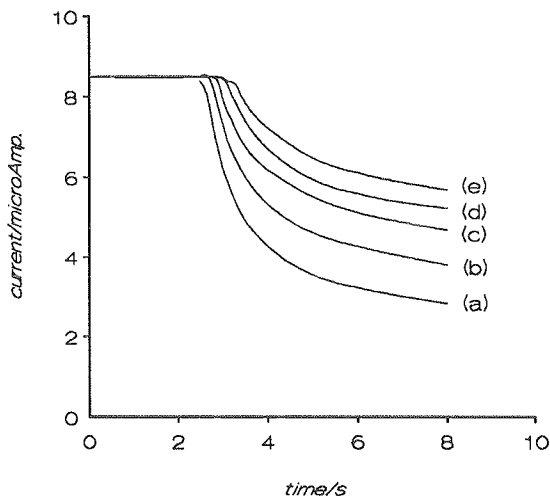


Figure 15. Chronoamperometric measurements of glucose concentrations with the track-etch membrane biosensor described in Figure 9. Degassed stagnant solutions, containing 25 U/ml of catalase, kept under argon. Potential step from 0.150 to 0.350 V versus Ag/AgCl: (a) no glucose, (b) 2.5 mM, (c) 5 mM, (d) 10 mM, and (e) 15 mM of glucose.

It was found that the dynamic range of the track-etch membrane biosensor was very small when the working potential was 0.15 V versus Ag/AgCl. This potential is too low for the poly(pyrrole) tubules to mediate electron transfer and the enzyme molecules probably remain in the reduced state. As a result the latter molecules are all saturated with substrate, even at low glucose concentrations. Consequently, no catalytic current flows at such a low potential. As the current response at low (0.15 V vs. Ag/AgCl) and high (0.35 V vs. Ag/AgCl) potential was very different, it was expected that the membrane sensor could be used to analyze glucose concentrations successfully by chronoamperometry.

Chronoamperometric measurements were performed with a track-etch

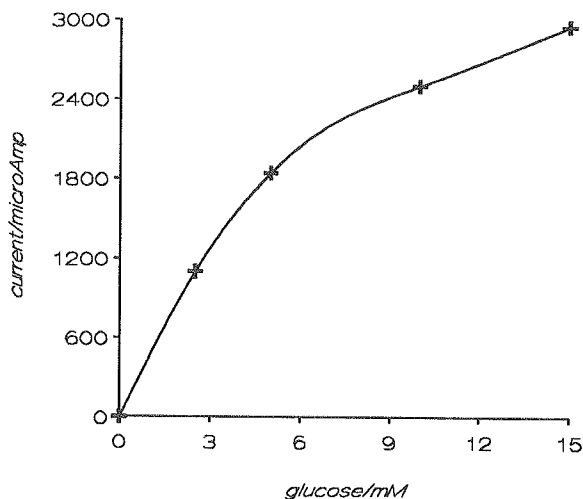


Figure 16. Calibration curve based on the chronoamperometric data in Figure 15; sampling time 3.4 s.

membrane sensor with originally 800 nm pores, treated with pyrrole and FeCl_3 for one minute. Adsorption of glucose oxidase was achieved in the usual way. The applied potential step was from 0.15 to 0.35 V versus Ag/AgCl. All solutions were purged with argon and contained 25 U/ml of catalase. The chronoamperometric curves obtained at various glucose concentrations are shown in Figure 15. A number of sampling times was tested but the best results were obtained with a time of 3.4 s. As is seen in the figure, concentrations up to 15 mM can be measured reproducibly. Higher concentrations of glucose gave curves that could not be distinguished from the curve for 15 mM glucose. In Figure 16 a calibration curve is shown based on the data in Figure 15.

4.3 Conclusions

The biosensor described here can easily be constructed and is a simple device for measuring glucose. It can be used for extended periods of time. The selectivity for glucose is high. Our amperometric measurements were carried out at relatively low potentials, which is very advantageous since interference by non-enzymatically oxidizable species will become less important, thereby improving the selectivity of the biosensor.

Evidence is presented that the response to glucose may be the result of direct electron transfer between enzyme and conducting polymer. The positive current response of the sensor on the addition of glucose even at low measuring potential (100 mV vs. Ag/AgCl), the observed negative response to H_2O_2 at this potential, the reversible quenching of the response current under increased salt concentration, and the oxygen independent signal are indications for this. The fact that no oxygen is required as a mediator has a positive effect on the stability and the lifetime of the biosensor.

4.4 Materials and methods

Materials and apparatus

Glucose oxidase (E.C. 1.1.3.4) type II (25,000 U/g) or type X-S (150,000 U/g) from *Aspergillus niger* and catalase (E.C. 1.11.1.6, 2800 U/mg) from Bovine liver were obtained from Sigma. Horseradish peroxidase (E.C. 1.11.1.7) grade II (180 U/mg) was purchased from Boehringer (Mannheim). Benzoquinone was from Aldrich (FRG) and was sublimed prior to use. Pyrrole was from Merck and was distilled under nitrogen before use. Anhydrous iron(III)chloride (98%) was obtained from Fluka and was used as received. Fluorescein isothiocyanate was from Janssen. The Nuclepore[®] membranes were purchased from Ankersmit (The Netherlands). The Cyclopore[®] membranes were a gift from Cyclopore S.A. (Belgium). All other reagents were commercial products and of analytical grade.

Electrochemical measurements were performed with an Antec CU-04-AZ controller (Antec Leyden, The Netherlands) or an Autolab potentiostat controlled by an Olivetti M24 Personal Computer and General Purpose Electrochemical System (GPES)-software (Eco Chemie, The Netherlands). Current output was recorded on a Yew 3056 pen recorder. The pore size distribution of the filter membranes was measured with a Coulter Porometer II (V3B). Electron micrographs were made on a CAMSCAN scanning electron microscope (Cambridge Instruments). Confocal laser

scan microscopy images were made on a home made instrument (Sensor Group, TNO Environmental and Energy Research).²⁹

Preparation of poly(pyrrole) modified membranes

Pyrrole was chemically polymerized within the pores of Nuclepore[®] or Cyclopore[®] membranes in a specially designed reaction vessel (Figure 1). Polymerization was achieved with freshly made solutions containing 0.6 M of pyrrole and 2 M of iron(III)chloride in distilled water. Membranes with different pore diameters were used. The polymerization time varied between 30 s and 10 min, depending on the diameter of the pores. In the polymerization experiment the membrane separated the pyrrole solution from the oxidizing solution. The reagents met in the pores and reacted to give poly(pyrrole). After the appropriate time, the polymerization reaction was quenched by rinsing the membrane with distilled water. Surface material was removed by carefully wiping the membrane with a tissue.

The resistance of the composite membranes was measured according to a procedure described in the literature.³ A bed of silver powder served as the auxiliary electrode in the resistance measurement. A membrane was placed on this bed and a second electrode, consisting of a platinum wire sealed into a 7 mm diameter glass tube was placed on top of the membrane. A pressure of 1.3 kg/cm² was applied to the latter electrode to ensure a uniform contact. The resistance was measured with a Fluke model 45 digital multimeter.

Coating with metal layer

Platinum was applied to one side of the polymer modified membranes with an Edwards sputtercoater S150B. A platinum target of 8 cm diameter and 0.5 mm thickness was used as the platinum source. The layer thickness was monitored with an Edwards FTM5 unit. The thickness of the platinum layers was varied between 50 and 350 nm.

Immobilization of enzyme

Enzyme immobilization was achieved by agitating (Gyrotory Shaker model G2, New Brunswick Scientific, USA) the polymer and platinum containing membranes in 3 ml of a phosphate buffered saline solution (pH 7.4) containing 5 mg/ml of GOD at a temperature of 4 °C for at least 0.5 h. The membranes were successively dried overnight in a desiccator over CaCl₂.

Measurement of enzyme activity

Enzyme activity was electrochemically assayed with a three electrode cell containing 20 ml of phosphate buffered saline (PBS) pH 7.5, 5 mM of benzoquinone and 0.5 M of glucose. Prior to use, the glucose solution was allowed to mutarotate for at least 24 h. The assay was performed with a platinum rotating disk electrode (6 mm Ø) equipped with an Electrocraft corporation model E550 motor and E552 speed control unit. The platinum working electrode was set at a potential of 0.350 V (Ag/AgCl reference) which is the optimum potential for hydroquinone oxidation.⁴ A platinum working electrode was used, because we found that this metal gave a slightly better signal than glassy carbon. The latter material is often applied in the literature.^{7,30} The angular velocity of the RDE was chosen sufficiently high to avoid the current response from being dependent on the rotation speed. A rotation speed of 2000 rpm proven to be an appropriate value. A platinum wire was used as auxiliary electrode. The solution was flushed with argon before each experiment. During the assay argon was blanketed over the solution. The actual assay was performed by monitoring the current output of the potentiostated RDE while immersing a sample membrane into the solution.

Glucose oxidase activity in solution at various NaCl concentrations was assayed spectrophotometrically. The assay was carried out *in duplo* (50 mM sodium phosphate buffer pH 7.7 at room temperature) in an automated assay system (Titertec multiscan mcc/340 spectrophotometer) at a wave length of 450 nm. In a 96-well microtiter plate each sample was prepared as follows: 0.125 ml of the appropriate NaCl solution in buffer was mixed with 0.100 ml of a buffer solution containing 25 mM of *o*-dianisidine, 250 mM of glucose, and ca. 0.6 U/ml of horseradish peroxidase. A 0.025 ml buffer solution containing 50 mU/ml of glucose oxidase was added, rapidly mixed and the microtiter plate was measured immediately hereafter. The average extinction over a period of 30 s after the addition of GOD was determined. From these measurements the relative glucose oxidase activity of the various samples could be obtained.

Enzyme labeling with fluorescein isothiocyanate

Glucose oxidase was treated with fluorescein isothiocyanate (FITC) in the following way. A 50 mM boric acid solution was adjusted to pH 9 with a 0.2 M solution of NaOH. In 5 ml of this borate buffer 1 mg of glucose oxidase was dissolved. A solution of 1.5 mg FITC in 5 ml of borate buffer was added to the enzyme solution. The reaction was allowed to proceed for two h. at room temperature. Afterwards, the reaction mixture was dialyzed in borate buffer for 48 h. at a temperature of 4 °C. The dialysis solution was refreshed two times during this period. After dialysis, low molecular weight material was separated from the labeled protein by elution with

borate buffer on a G-25 column. The protein fraction was collected, cooled to -196°C (liquid nitrogen), and dried in high vacuum. The greenish modified protein material (0.96 mg) was stored at -20°C when not used.

Fluorescein labeled glucose oxidase was used for adsorption to poly(pyrrole) microtubules in the same way as the non-treated glucose oxidase. The resulting enzyme membranes were imaged with a confocal laser scan microscope in the fluorescence mode.

Amperometric measurements

To perform amperometric measurements, the enzyme membrane was placed as the working electrode in a three electrode flow cell (Antec Leyden, The Netherlands). The metal coated rear of the membrane was pushed against a glassy carbon disk (\varnothing 8 mm). To insulate the active surface of the membrane from the auxiliary electrode, it was covered with a Teflon spacer of 1 mm thickness. In the spacer a duct of 0.15 cm^2 was left, allowing the membrane to make contact with the solution. An Ag/AgCl electrode was used as reference electrode. The base of the flow cell acted as the auxiliary electrode (glassy carbon). Buffer solution was driven through at 1.75 ml/min. (Watson Marlow 101U peristaltic pump). The potential of the membrane was set at 0.350 V. When the background current had diminished ($\leq 200\text{ nA}$), the buffer solution was replaced by the glucose solution and the current response was monitored.

References

1. Degani, Y. and Heller, A., *J. Am. Chem. Soc.*, (1989) **111**: 2357-2358.
2. Heller, A., *Acc. Chem. Res.*, (1990) **23**: 128-134.
3. Cai, Z. and Martin, C.R., *J. Am. Chem. Soc.*, (1989) **111**: 4138-4139.
4. Aubré-Lecat, A., Hervagault, C., Delacour, A., Beaupe, P., Bourdillon, C. and Remy, M., *Anal. Biochem.*, (1989) **178**: 427-430.
5. Bourdillon, C. and Majda, M., *J. Am. Chem. Soc.*, (1990) **112**: 1795-1799.
6. Fortier, G. and Bélanger, D., *Biotechnol. Bioeng.*, (1991) **37**: 854-858.
7. Bourdillon, C., Thomas, V. and Thomas, D., *Enzyme Microb. Technol.*, (1982) **4**: 175-180.
8. Sinsheimer, J.E., Jagodic, V. and Burckhalter, J.H., *Anal. Biochem.*, (1974) **57**: 227-231.
9. Hoare, J.P. Oxygen. In: *Standard Potentials in Aqueous Solution*. edited by Bard, A.J., Parsons, R. and Jordan, J. Marcel Dekker, Inc., New York: (1985) pp. 49-66.
10. Delahay, P. *Voltammetry and Polarography at Constant Potential. Kinetic and Catalytic Processes*. In: *New Instrumental Methods in Electrochemistry*. Interscience Publishers, Inc., New York: (1965) 4th Ed., pp. 87-114.
11. Narasimhan, K. and Wingard Jr., L.B., *J. Mol. Catal.*, (1986) **34**: 263-273.
12. Narasimhan, K. and Wingard Jr., L.B., *Anal. Chem.*, (1986) **58**: 2984-2987.
13. Swoboda, B.E.P. and Massey, V., *J. Biol. Chem.*, (1965) **240**: 2209-2215.
14. Tamiya, E., Karube, I., Hattori, S., Suzuki, M. and Yokoyama, K., *Sensors and Actuators*, (1989) **18**: 297-307.
15. Szucs, A., Hitchens, G.D. and Bockris, J.O., *J. Electrochem. Soc.*, (1989) **136**: 3748-3755.
16. Armstrong, F.A., Cox, P.A., Hill, H.A.O., Lowe, V.J. and Oliver, B.N., *J. Electroanal. Chem.*, (1987) **217**: 331-366.
17. Delaney, G.M., Bennetto, H.P., Mason, J.R., Roller, S.D., Stirling, J.L. and Thurston, C.F., *Anal. Proc.*, (1986) **23**: 143-144.
18. Yabuki, S., Shinohara, H. and Aizawa, M., *J. Chem. Soc., Chem. Commun.*, (1989) 945-946.
19. Aizawa, M., Yabuki, S., Shinohara, H. and Ikariyama, Y., *Ann. N. Y. Acad. Sci.*, (1990) **613**: 827-831.
20. Kajiya, Y., Sugai, H., Iwakura, C. and Yoneyama, H., *Anal. Chem.*, (1991) **63**: 49-54.
21. Albery, W.J. and Bartlett, P.N., *J. Electroanal. Chem.*, (1985) **194**: 211-222.
22. Albery, W.J., Bartlett, P.N. and Craston, D.H., *J. Electroanal. Chem.*, (1985) **194**: 223-235.
23. Cenás, N.K. and Kulys, J.J., *Bioelectrochem. Bioenerg.*, (1981) **8**: 103-113.
24. Weibel, M.K. and Bright, H.J., *J. Biol. Chem.*, (1971) **246**: 2734-2744.
25. Kelley, R.L. and Reddy, C.A. *Glucose Oxidase of Phanerochaete chrysosporium*. In: *Methods in Enzymology. Volume 161. Biomass. Part B. Lignin, Pectin, and Chitin*. edited by Wood, W.A. and Kellogg, S.T. Academic Press, New York: (1988) pp. 307-316.
26. Clark Jr., L.C. *The Hydrogen Peroxide Sensing Platinum Anode as an Analytical Enzyme Electrode*. In: *Methods in Enzymology, Vol. LVI*. Academic Press, New York: (1979) pp. 448-479.
27. Foulds, N.C. and Lowe, C.R., *J. Chem. Soc., Faraday Trans. 1.*, (1986) **82**: 1259-1264.
28. Olsson, B., Lundbäck, H., Johansson, G., Scheller, F. and Nentwig, J., *Anal. Chem.*, (1986) **58**: 1046-1052.
29. Houpt, P.M. and Draaijer, A., *Inst. Phys. Conf. Ser. No 98*, (1989) **Chapter 14**: 639-642.
30. Mikkelsen, S.R. and Lennox, R.B., *Anal. Biochem.*, (1991) **195**: 358-363.

5 Scanning tunneling microscopy study of poly(pyrrole) and of glucose oxidase. A model for the electronic interaction between glucose oxidase and poly(pyrrole) in microtubular form

Abstract

In this chapter the surface morphology of different forms of the organic conductor poly(pyrrole), which serves as the environment for immobilization of the redox enzyme glucose oxidase, is studied. Scanning tunneling microscopy (STM) images of poly(pyrrole) films, obtained electrochemically on highly oriented pyrolytic graphite (HOPG), STM images of poly(pyrrole) microtubules and STM images of glucose oxidase molecules adsorbed on a gold facet are presented and discussed.

The conclusions from this study are: (i) The poly(pyrrole) films, prepared chemically or electrochemically, exhibit disordered non-crystalline structures. (ii) The dimensions of the poly(pyrrole) surface corrugations in the microtubules and the dimensions of the glucose oxidase molecule are of the same order of magnitude, allowing strong adsorption of the enzyme to the conducting polymer. Based on these data a model for the direct interaction between glucose oxidase and poly(pyrrole) in microtubular form is proposed.

5.1 Introduction

Interaction of redox enzymes with bare metal or carbon surfaces is often accompanied with large structural changes in the protein structure and concomitant loss of enzymatic activity. Therefore, protein electrochemistry is usually performed with surface modified electrodes.¹ Many research groups have applied organic conductors as surface modifiers,²⁻⁵ in particular poly(pyrrole).⁶⁻⁹

In the previous chapter we showed that glucose oxidase can be immobilized very efficiently on a new type of poly(pyrrole), viz. in the form of microtubules. These microtubules were synthesized using the pores of a track-etch membrane as templates.^{10,11} With these microtubules we were able to construct a reagentless glucose sensor, which displayed direct electron transfer from the enzyme to the conducting polymer. As the microtubular poly(pyrrole) did not contain additional redox mediators^{3,4,12-15} (neither covalently anchored nor physically adsorbed) the intriguing question arises why direct electron transfer takes place. To answer this question we have undertaken a scanning tunneling microscopy (STM) study of the

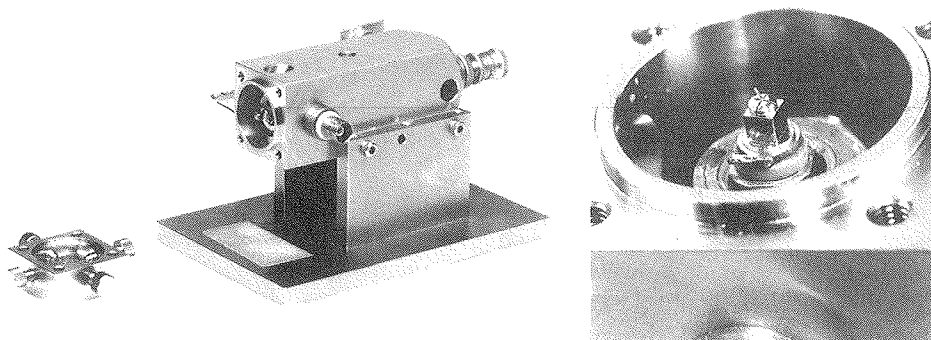


Figure 1. *Photograph of the used STM apparatus.*

two main components of the biosensor, viz. the conducting polymer and the redox enzyme.

For comparison we have also studied by STM the surface morphology of poly(pyrrole) electrochemically deposited on a highly oriented pyrolytic graphite (HOPG) substrate. The results of these studies are used to propose a model for the observed direct interaction between glucose oxidase and the conducting polymer.

The principle of the scanning tunneling microscope has been explained in Chapter 2.6. In Figure 1 a photograph is shown of the STM machine that we used.

5.2 Results and discussion

5.2.1. Poly(pyrrole) on HOPG

Poly(pyrrole) films on HOPG were electrochemically prepared following the method described in the Experimental Section (see also Chapter 2.4.1). The various samples we studied were obtained by applying different numbers of electrochemical cycles to a HOPG electrode in a solution containing 0.3 M of pyrrole and 0.15 M of NaCl. The samples obtained by cycling up to 3 times from 0 to 1 V (vs. Ag/AgCl) at 100 mV/s, were used to study the initial steps of the polymerization reaction. Considering the fact that the onset potential for pyrrole polymerization under these conditions is 0.56 V vs. Ag/AgCl (see Chapter 3), the effective polymerization time is very short. We estimate it to be 9 s/cycle at most, when the potential is cycled from 0 to 1 V at 100 mV/s. The polymerization current was limited to 100 μ A in these experiments. The samples which were polymerized for longer times (approximately 100 s effective polymerization time) were used to study the final surface corrugation of poly(pyrrole) as it is expected to be in the amperometric biosensor described in Chapter 4. The thickness of the poly(pyrrole) microtubules walls is approximately 100 - 200 nm (Chapter 4, Figure 2). The thickness of the electrochemically synthesized films is estimated to be of the same order of magnitude as the microtubules walls. This estimation is based on the fact that 50 mC of charge per cm^2 leads to a film of 100 nm.^{8,16-19}

Figure 2 shows the STM images of poly(pyrrole) deposited on a HOPG surface at the initial stage of the polymerization (after 3 electrochemical cycles). Some individual islands are visible in Figure 2a. In Figure 2b the poly(pyrrole) deposit has a much more dense structure. These STM images were taken from the same sample. Our explanation for the observed different structures is the following. The polymerization reaction occurs at numerous individual sites on the surface of the HOPG electrode. From the locations where the polymer nucleates, the polymer chains grow slowly into dome structures. These domes eventually impinge on each other. When the number of growth sites increases, the overall structure becomes smoother and more parallel to the original electrode surface.^{20,21} This nucleation and growth process for poly(pyrrole) has been reported before.²²⁻²⁵ It is supported by our cyclic voltammetry experiments (Chapter 3) which also showed a nucleation and growth mechanism for this polymer.

The dimensions of the islands in Figure 2a are up to 250 nm in lateral directions and up to 50 nm in height. The domes which impinge upon each other (Figure 2b) are up to several hundreds of nm long and up to 100 nm in height. The structures between the islands in Figure 2a are chain-like with a width of 10 nm at the base and up to 1 nm in height. These chains are presented at higher magnification in Figure

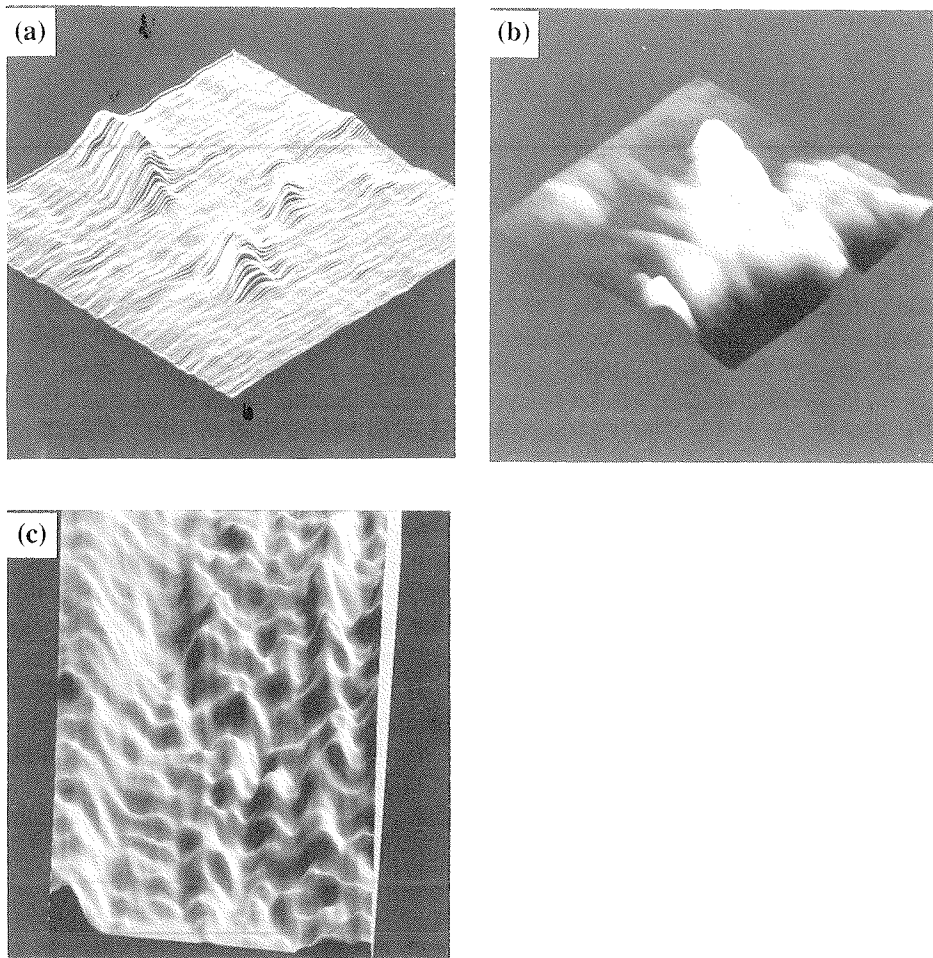


Figure 2. STM images of polypyrrole films deposited on highly oriented pyrolytic graphite (tunnel current = 100 pA, tip voltage = -150 mV): (a and b) 800x 800 nm² image of a polypyrrole film formed in the initial stage of the polymerization. The vertical scale range is 100 nm, (c) 80x80 nm² image of the structures between the islands in (a).

2c. They seem to exhibit randomly distributed zig-zag structures, in accordance with the molecular organization of the films reported by Mitchell *et al.*²¹ We failed to obtain atomic or individual molecular orbital resolution of the STM images with our samples. In all our measurements, the tunnel current was noisy and trials to scan with higher current (the tip closer to the sample surface) led to oscillations or to so-called

dragging effects. This means that the STM needle touched the sample material and successively moved (part of) the sample molecules over the substrate surface during the scanning process. As a consequence, successful STM images could not be obtained.

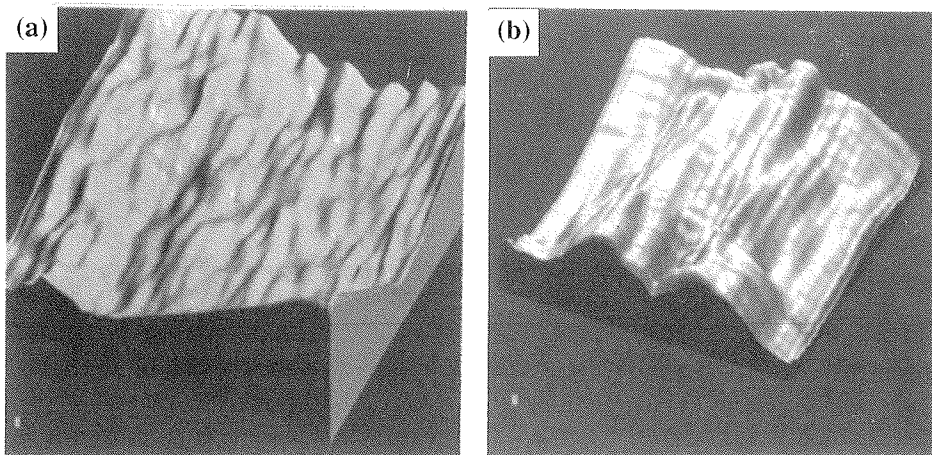


Figure 3. STM images of a polypyrrole film surface with a thickness corresponding to the thickness of the material used in the amperometric track-etch membrane biosensor (tunnel current = 50 pA, tip voltage = -150 mV): (a) 50x50 nm² detail; the vertical full scale is ca. 20 nm, (b) 10x10 nm² detail; the vertical scale is ca. 4 nm.

Figure 3a presents a 50x50 nm² STM image of a poly(pyrrole) film with a thickness corresponding to the poly(pyrrole) material used in the amperometric track-etch membrane biosensor. This image is a representative picture of the structure of the poly(pyrrole) layer. It shows rows of poly(pyrrole) chains elongated in one preferential direction. The individual chains had various widths and heights. Figure 3b shows the image obtained at the highest magnification. The structure observed in Figure 3b is the same when different scanning directions and speeds are used. This picture suggests that two rows, 3 nm wide and 1.5 nm high, are impinging on one another. A cross-section of the image height in Figure 3a is given in Figure 3c. Typical values of the width and height are approximately 5 to 6 nm and up to 2.5 nm, respectively.

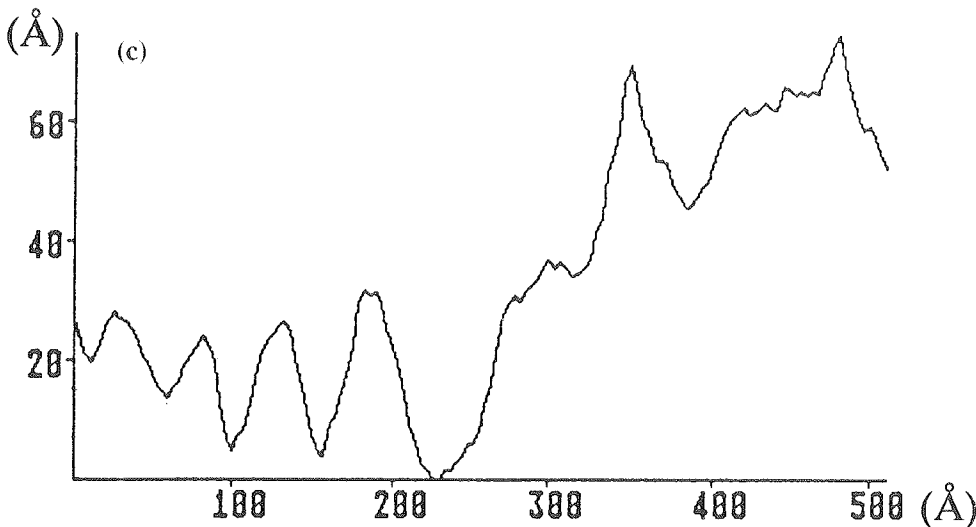


Figure 3. (Continued) (c) cross-section of the image in Figure 3a taken from the lower-right part.

5.2.2 Glucose oxidase

Gold facets with adsorbed glucose oxidase molecules were imaged by both SEM and STM. The enzyme molecules were deposited in a way as is described in detail in the Experimental Section. Solutions with an enzyme concentration of 0.5 and 5 mg/ml were used. These two concentrations were chosen in order to obtain samples with a low as well as a high surface coverage. On the SEM images the adsorbed enzyme layers are clearly visible (Figure 4b & c). The layer has a fuzzy appearance as compared to the smooth gold facet (Figure 4a). The latter facet is atomically flat. As a result, no structure is visible, both on SEM and STM scale.

Figures 5a and 5b show the STM line and intensity images of glucose oxidase molecules on Au facets. The imaged area is $38 \times 38 \text{ nm}^2$ and the vertical range is approximately 3 nm. The picture displays a conglomerate of enzyme molecules. The individual molecules are oval shaped with a dimension of 14-18 nm along the long axis and 5-8 nm along the short axis. These structures were reproducibly present in both scanning directions. Their heights are approximately 1-2 nm. The molecules have the appearance of a ring with a 2 nm wall thickness and a small hole in the middle. At the present stage in the development of imaging biological molecules by STM, it is not possible to draw definite conclusions concerning the dimensions of biomolecules.²⁶ How the needle tip interacts with biomolecules is still unknown. Therefore, these results must be interpreted with caution.

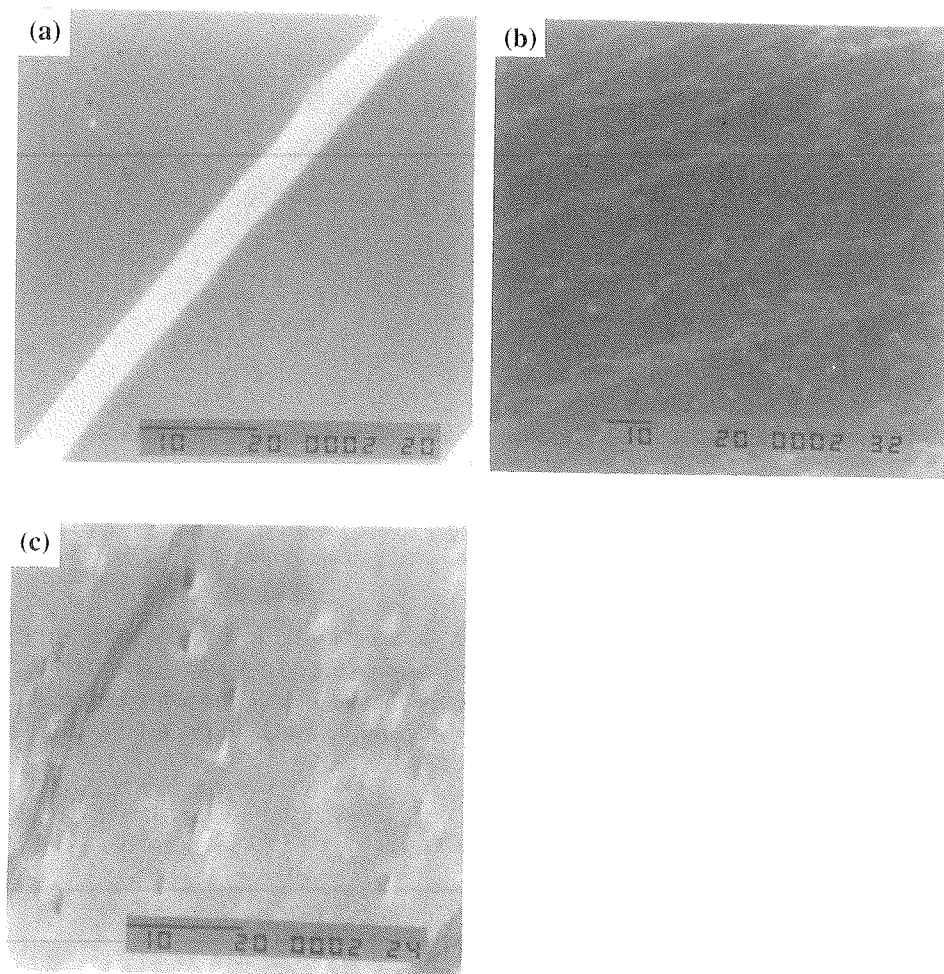


Figure 4. SEM images of glucose oxidase adsorbed on atomically flat gold facets. (a) SEM micrograph of the clean gold surface before deposition of glucose oxidase, (b) SEM micrograph of the protein layer deposited from a glucose oxidase solution of 0.1 mg/ml, (c) idem from a glucose oxidase solution of 5 mg/ml.

The lateral dimensions of the observed molecules are in agreement with the dimensions obtained from ellipsometry data on glucose oxidase adsorbed on a gold electrode.²⁷ The vertical dimensions of our imaged molecules, however, need some further comments. Ellipsometry suggests that the glucose oxidase molecule is an ellipsoid with a minor axis of 5 nm long. The vertical value we measured is smaller, but we expected this to be so for two reasons. First, it is known from other

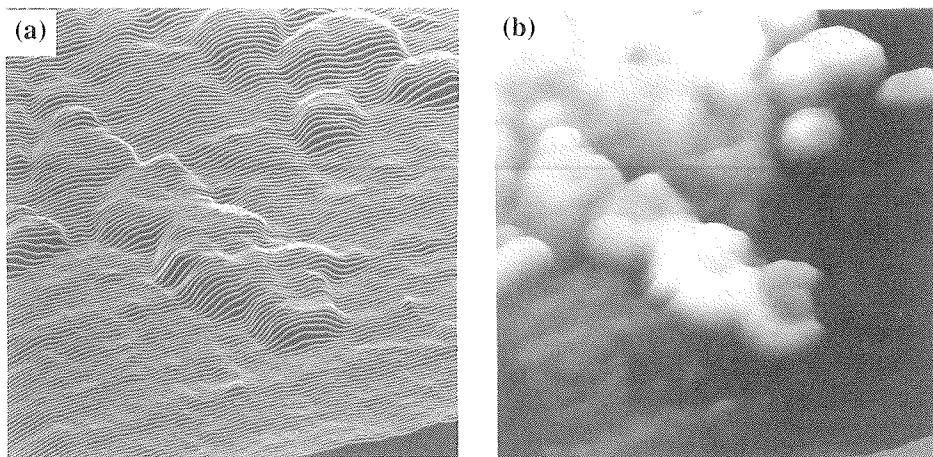


Figure 5. (a) Line and (b) intensity STM images of glucose oxidase molecules adsorbed on a Au facet; area $38 \times 38 \text{ nm}^2$ with vertical scale range ca. 3 nm, tunnel current = 50 pA, tip voltage = -150 mV. The images were taken under ambient-air and high humidity conditions (70%).

investigations²⁷ that the interaction between glucose oxidase and gold is very strong. This will lead to an irreversible adsorption of the enzyme on the gold surface. During this process, the enzyme molecules will slowly change their conformation, exposing more and more amino acid groups capable of forming bonds to the gold substrate.

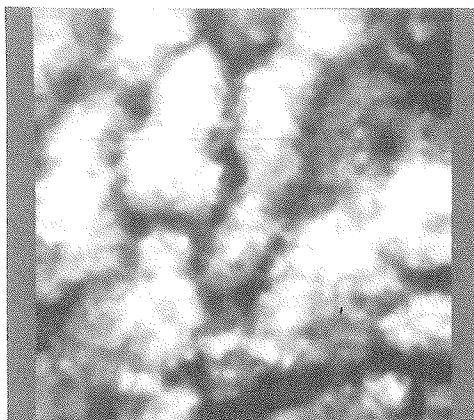


Figure 6. Top view STM image ($36 \times 36 \text{ nm}^2$) of glucose oxidase adsorbed on a Au facet (tunnel current = 100 pA, tip voltage = -50 mV). The image was taken under ambient-air and high humidity (70%).

This results in defolding of the tertiary structure and deactivation of the protein. Second, the tunneling current is not only dependent on the distance between the tip and the sample, but also on the local work function. Therefore, when the tip is scanning badly conducting material like proteins, the feedback loop of the instrument makes the tip go into the examined surface to keep the tunnel current constant (constant current mode). These two reasons lead to STM images that are not fully representative for the real tertiary structure of the active enzyme molecule.

Figure 6 shows an image of glucose oxidase molecules, obtained at a different bias voltage of the scanning tip. The lateral dimensions remain the same as before, but now there is no evidence of a ring structure. Our explanation is, that by changing the bias voltage (from -150 to -50 mV), different molecular orbitals are observed. Another important factor may be the ambient air humidity. This plays an important role when biological bulk specimens (generally non-conductive) are imaged. In concurrence with reports by Yuan *et al*,²⁸ we obtained the most reproducible results when the air humidity was high (70%). Imaging at such high humidity led to structures with significant vertical dimensions as was visible in the depth profiles (not shown).

Glucose oxidase on gold was also imaged while placing the tip in a droplet of water on the gold surface. In this way we obtained the same results as for imaging at high humidity (70%) on a dry gold surface. The samples changed significantly when we placed the STM inside a glass bulb, that was flushed with nitrogen. Imaging under these conditions led to "dragging effects" (*vide supra*). The same effects were observed when the STM sample was dried in the air after enzyme adsorption (see Experimental Section). In this case, the lack of water probably accelerated the denaturation process to a great extent.

5.2.3 Poly(pyrrole) microtubules

The poly(pyrrole) microtubules were imaged by SEM as was described in Chapter 4. The microtubules were isolated by washing away the template membrane with dichloromethane. The high electronic conductivity of the microtubules made it possible to image them directly without the necessity of coating them first with a gold layer. The absence of a gold layer offered the opportunity to characterize the samples also by X-ray analysis and to detect specific elements. Figures 7a and b show a SEM picture of the microtubules and the corresponding X-ray spectrum. The analyzed surface in Figure 7b was approximately $10 \times 100 \mu\text{m}^2$ and the analysis time was 2500 s. Under the measurement conditions only elements with atomic numbers larger than sodium could be detected and the detection limit for a specific element was ca. 0.1 wt%. The X-ray spectrum shows the presence of Cl as the major element. Iron might be present in concentrations less than 0.1 wt%. This means that the chloride anion acts as the counterion in the conducting polymer as is to be expected from the conditions used to synthesize the poly(pyrrole) microtubules. There is no local

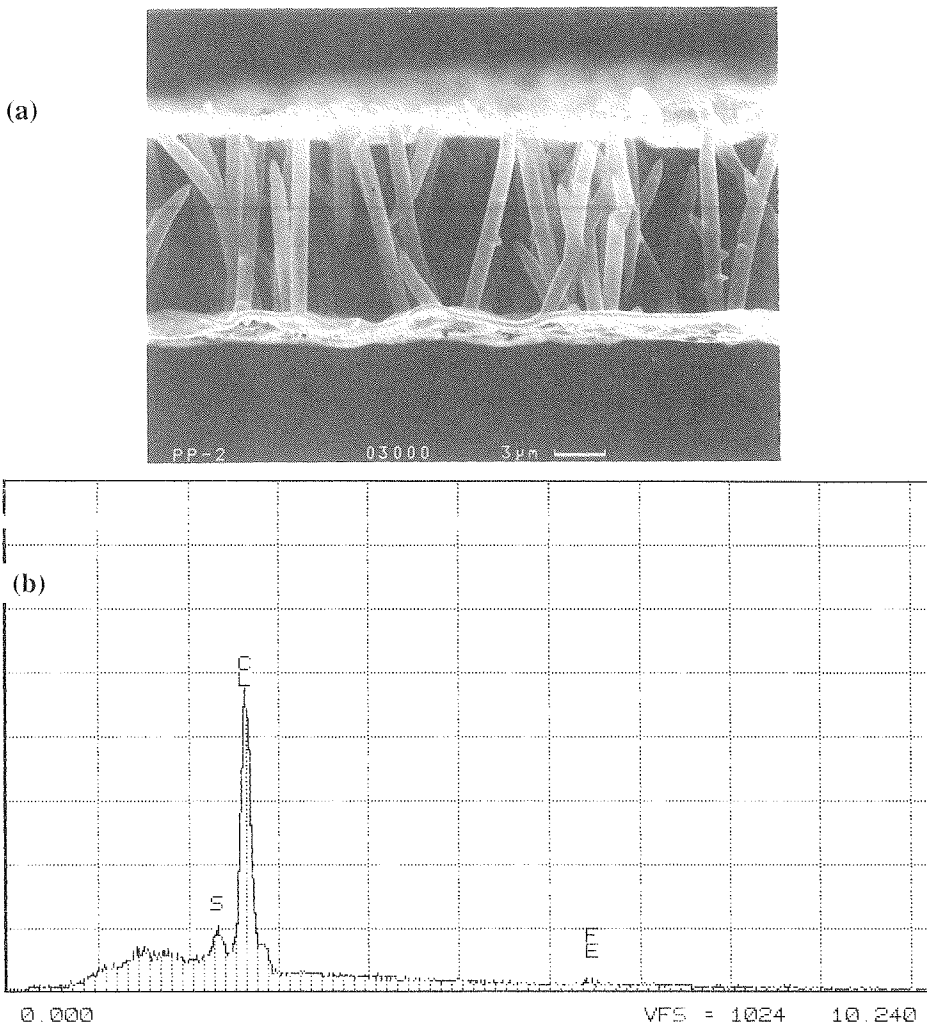


Figure 7. (a) Scanning electron micrograph of polypyrrole microtubules without a gold coating. The polycarbonate template material was washed away with dichloromethane. The pore size of the original membrane was 1000 nm and the membrane thickness was 11 μm . (b) X-ray spectrum of the sample of (a) obtained by scanning a surface of ca. $10 \times 100 \mu\text{m}^2$ over a period of 2500 s.

variation in the detected concentration of chlorine. This was confirmed by a spot analysis on different locations on the sample.

The internal surface of the poly(pyrrole) microtubules was studied by STM in a way as described in the Experimental Section. To this end a microtubule as used in

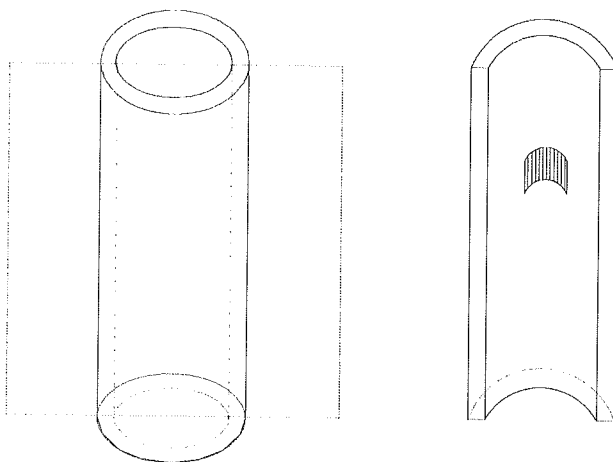


Figure 8. Schematic drawing showing which part of a polypyrrole microtubule was used for imaging by STM.

the biosensor described in Chapter 4 was cut in half along its cylindrical axis. The part of the surface that was imaged is shown schematically in Figure 8. A typical micrograph is presented in Figure 9a. The observed area is $80 \times 80 \text{ nm}^2$ and the vertical range is about 30 nm. The surface is strongly corrugated with ditches up to several

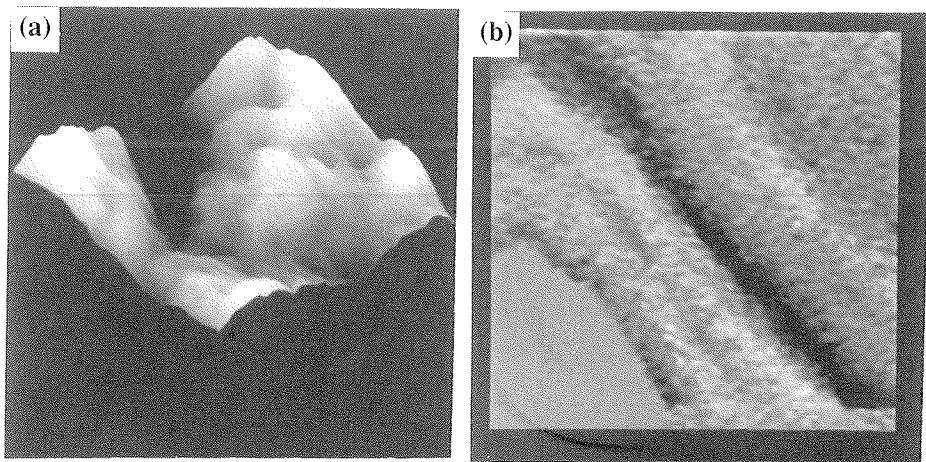


Figure 9. STM images of a cross-section of a poly(pyrrole) microtubule (tunnel current = 100 pA, tip voltage = -500 mV). (a) Detail of $80 \times 80 \text{ nm}^2$; the vertical scale range is ca. 40 nm, (b) $40 \times 40 \text{ nm}^2$ filtered image (gradient in x-direction).

nanometers deep and with corrugated walls as also observed for poly(pyrrole) on HOPG (*vide supra*). Figure 9b shows a filtered image (gradient in x-direction) of another location inside the poly(pyrrole) microtubule. Also in this picture the long ditches and steps on the surface are clearly visible. These images suggest that the inner surface of the poly(pyrrole) tubules is corrugated enough to adsorb glucose oxidase molecules. The most interesting feature is that the dimensions of the

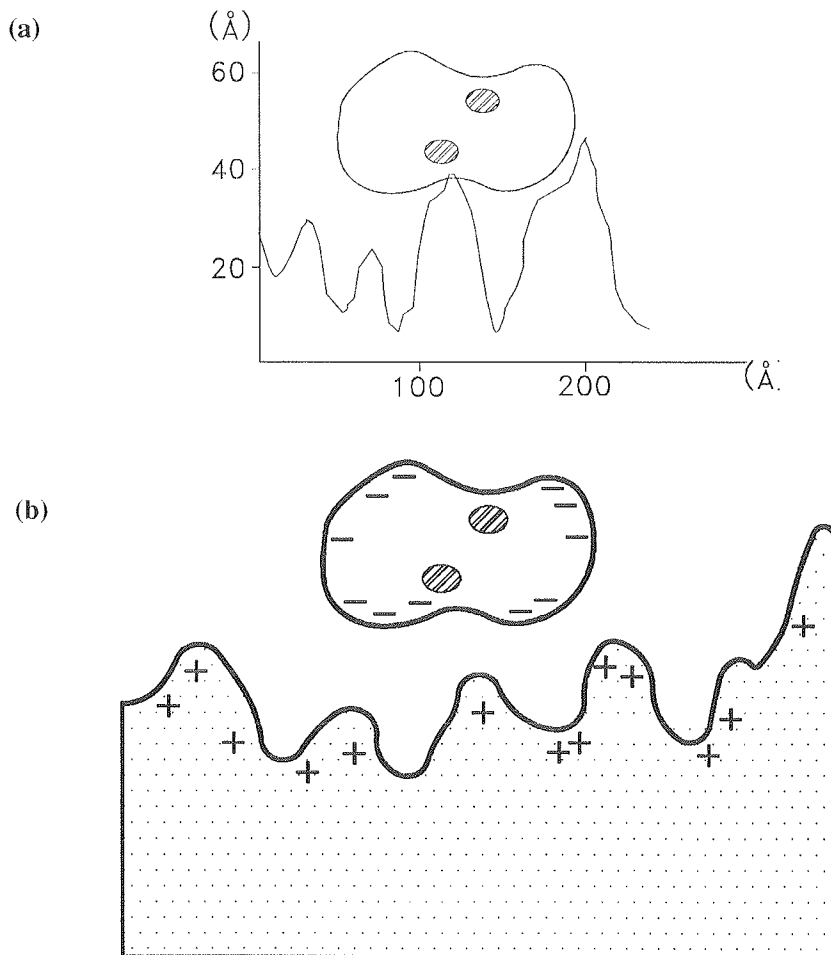


Figure 10. Model for the interaction of glucose oxidase with poly(pyrrole) microtubules: (a) cross-section of the internal surface of a poly(pyrrole) microtubule as measured by STM and a drawing of a glucose oxidase molecule having the dimensions as found by STM (Figure 5), (b) schematic representation of the electrostatic complex without salt present.

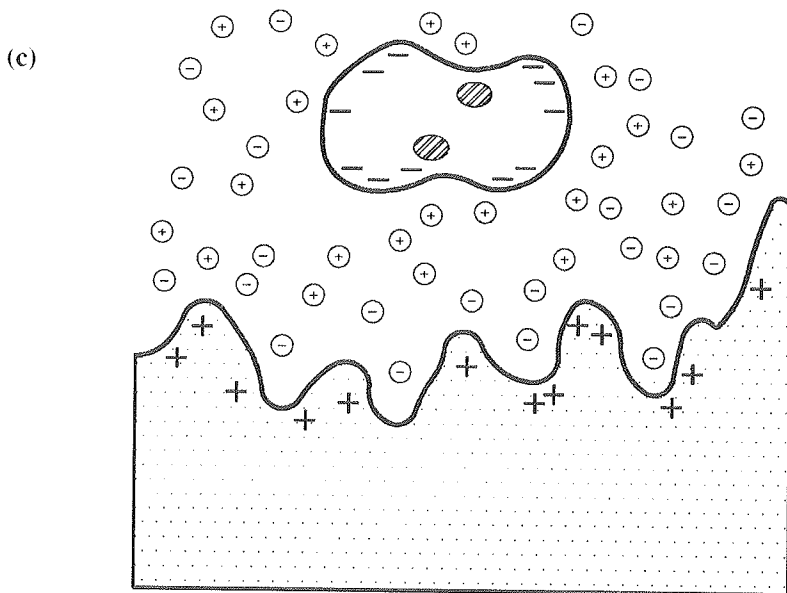


Figure 10. (Continued) (c) schematical representation of the electrostatic complex in the presence of salt.

poly(pyrrole) corrugations match the molecular dimensions of glucose oxidase. If we assume that the enzyme molecule is shaped like an "8", with the active centers in the groove of the "8", the poly(pyrrole) matrix can be imagined to interact very well with the active centers of the enzyme.

The surface interaction between glucose oxidase and poly(pyrrole) most likely is electrostatic in nature as poly(pyrrole) in its conducting state is a polycation²⁹ and glucose oxidase is negatively charged at neutral pH.²⁷ Experimental evidence for this electrostatic interaction was presented in Chapter 4. Apparently, the concave structure of the tubules is very important. It probably allows the poly(pyrrole) matrix to interact with glucose oxidase from different directions. This multi-site interaction may keep the enzyme biologically active and at the same time may increase the chance that direct electron transfer occurs.^{1,30,31} A model for the interaction between glucose oxidase and poly(pyrrole) is presented in Figure 10. Figure 10a shows a depth profile of a representative STM image of a poly(pyrrole) microtubule. In this figure on the same scale also a glucose oxidase molecule is shown. Its dimensions were taken from Figure 6. As can be seen, the dimensions of the enzyme molecule and the poly(pyrrole) surface corrugation match sufficiently to make a strong interaction feasible. The electrostatic charges that are involved are shown schematically in Figure 10b. From this model the behaviour of the biosensor under increased salt concentration (Chapter

4) can be explained. Increasing the concentration of ions leads to screening of the electrostatic charges and results in the suppression of the electron transfer. This screening is visualized in Figure 10c. Our model also explains why direct electron transfer to poly(pyrrole) is more efficient than electron transfer to oxygen. Oxygen molecules must diffuse from the bulk solution to the enzyme molecules in the microtubules. This is a relatively slow process which cannot compete favourably with the probably rapid process of electron tunneling.³²

5.3 Conclusions

We have obtained STM images of poly(pyrrole) films synthesized electrochemically under various polymerization conditions on a HOPG electrode. The STM images show that electrochemical deposition occurs at numerous and isolated sites all over the HOPG electrode surface. Initially, only a few polymerization sites are present, which slowly grow into dome structures that impinge on each other. The images reveal that electrochemical polymerization of pyrrole proceeds via a nucleation and growth mechanism. This is in line with the results obtained from cyclic voltammetry experiments (Chapter 3). The poly(pyrrole) films that are eventually obtained, exhibit disordered non-crystalline structures with many ditches up to some nm depth and width, and with 1 to 2 nm corrugations on the walls.

The adsorption of glucose oxidase on atomically flat gold facets has been followed by SEM and STM. We have been able to obtain the first clear STM images of individual glucose oxidase molecules adsorbed on a gold surface. These molecules are oval shaped with a longer axis of 14 - 18 and a shorter axis of 5 - 8 nm. These dimensions are in accordance with data obtained in the literature by ellipsometry.²⁷ The thickness of the molecules is somewhat smaller than expected. This can be attributed to strong adsorption of the enzyme molecules to the gold surface and also to the STM technique itself.²⁶

The STM images of the poly(pyrrole) microtubules suggest that the conducting polymer inside the tubules has a corrugated structure allowing for strong multi-site interaction with the glucose oxidase molecules.

Based on the STM studies a model has been proposed which explains the observed direct electronic communication between poly(pyrrole) and the redox enzyme in the biosensor. This model also explains why no denaturation of the enzyme occurs. It further accounts for the observed behaviour of the track-etch membrane sensor under increased salt concentrations and its stability under anaerobic as well as aerobic conditions.

5.4 Experimental section

SEM images were obtained on a JEOL T 300 scanning electron microscope or on a CAMSCAN 4DV scanning electron microscope. The X-ray spectrum was recorded with a Tracor 5500 X-ray micro-analysis system. The STM microscope was constructed at the Research Institute for Materials at the University of Nijmegen. It was an ambient-air operating machine with a temperature-compensated two-piezo tube construction and a differential screw tip approach system. The tip material was Pt-Ir and the microscope was used in the constant current mode. The set-up has been described in detail elsewhere.^{33,34}

Poly(pyrrole) was electrochemically deposited on HOPG as described in Chapter 3. To this end a freshly cleaved graphite surface was introduced into an aqueous solution, containing 0.3 M of pyrrole (Merck) and 0.15 M of potassium chloride. Cleaving of HOPG was achieved by placing a piece of adhesive tape on the surface and by subsequently removing the tape very carefully. In this way a few layers of HOPG were removed, leaving a clean and atomically flat graphite surface. The electrochemical treatment was a potential sweep from 0 to 1 V versus an Ag/AgCl reference electrode. The scan rate was 100 mV/s and the current was limited to 100 μ A (model CV-1B potentiostat, Bioanalytical Systems).

Poly(pyrrole) microtubules were synthesized within the pores of Cyclopore[®] or Nuclepore[®] track-etch filtration membranes, according to the procedure described in Chapter 4.^{10,11} Membranes with originally 800 and 1000 nm pores were used. The polymerization time was 1 min.

Isolated poly(pyrrole) microtubules were obtained as follows. A Nuclepore[®] polycarbonate membrane with 1000 nm pores was used as a template for the microtubules polymerization. The template material was subsequently washed away by placing the membrane in a Soxhlet apparatus and extracting for 17 h. using dichloromethane as a solvent. SEM samples of the isolated poly(pyrrole) microtubules were prepared by positioning the extracted sample between two graphite tablets. Because of the high electrical conductivity of the material, it was not necessary to apply a conductive coating to the sample.

STM samples of the track-etch membranes, containing the poly(pyrrole) microtubules, were prepared as follows. A small rectangular piece of the membrane material was placed on its side on the sample holder and glued down. After drying, the membrane was cut with a fresh razor blade as near to the holder surface as possible. In this way some of the poly(pyrrole) tubules within the membrane were cut along their cylindrical axis. The part of a microtubule that was imaged is shown schematically in Figure 8.

Glucose oxidase (E.C. 1.1.3.4) type II (25,000 U.g⁻¹) from *Aspergillus niger* (Sigma) was adsorbed on gold facets (atomically flat or only mono-atomic steps on

the surface) by introducing the latter into a phosphate buffered aqueous enzyme solution of pH 7.4 for 67 h. Enzyme concentrations of 5 mg/ml and of 0.5 mg/ml were used in the sample preparation. After adsorption, the gold facets were rinsed with distilled water. The samples were stored in the refrigerator in phosphate buffered saline solution (PBS, pH 7.4) with 10 mg/ml of glucose oxidase present. One sample, which was treated with an enzyme solution of 5 mg/ml, was dried in the air. The glucose oxidase samples were imaged as such.

References

1. Armstrong, F.A., Hill, H.A.O. and Walton, N.J., *Acc. Chem. Res.*, (1988) **21**: 407-413.
2. O'Hare, D., Parker, K.H. and Winlove, C.P., *Bioelectrochem. Bioenerg.*, (1990) **23**: 203-209.
3. Foulds, N.C. and Lowe, C.R., *Anal. Chem.*, (1988) **60**: 2473-2478.
4. Dicks, J.M., Hattori, S., Karube, I., Turner, A.P.F. and Yokozawa, T., *Ann. Biol. Clin.*, (1989) **47**: 607-619.
5. Schalkhammer, T., Mann-Buxbaum, E., Urban, G. and Pittner, F., *J. Chromatography*, (1990) **510**: 355-366.
6. Schuhmann, W., Lammert, R., Uhe, B. and Schmidt, H., *Sensors and Actuators*, (1990) **B1**: 537-541.
7. Kajiya, Y., Sugai, H., Iwakura, C. and Yoneyama, H., *Anal. Chem.*, (1991) **63**: 49-54.
8. Fortier, G., Brassard, E. and Bélanger, D., *Biosensors & Bioelectronics*, (1990) **5**: 473-490.
9. Rishpon, J. and Gottesfeld, S., *Biosensors & Bioelectronics*, (1991) **6**: 143-149.
10. Cai, Z. and Martin, C.R., *J. Am. Chem. Soc.*, (1989) **111**: 4138-4139.
11. Martin, C.R., Van Dyke, L.S., Cai, Z. and Liang, W., *J. Am. Chem. Soc.*, (1990) **112**: 8976-8977.
12. Degani, Y. and Heller, A., *J. Am. Chem. Soc.*, (1989) **111**: 2357-2358.
13. Pishko, M.V., Katakis, I., Lindquist, S., Ye, L., Gregg, B.A. and Heller, A., *Angew. Chem.*, (1990) **102**: 109.
14. Gregg, B.A. and Heller, A., *Anal. Chem.*, (1990) **62**: 258.
15. Mann-Buxbaum, E., Pittner, F., Schalkhammer, T., Jachimowicz, A., Jobst, G., Olcaytug, F. and Urban, G., *Sensors and Actuators*, (1990) **B1**: 518-522.
16. Roncali, J., Yassar, A. and Garnier, F., *J. Chem. Soc., Chem. Commun.*, (1988) 581.
17. Hyodo, K. and Omae, M., *Electrochim. Act.*, (1990) **35**: 1245-1250.
18. Witkowski, A., Freund, M.S. and Brajter-Toth, A., *Anal. Chem.*, (1991) **63**: 622-626.
19. Schuhmann, W., *Synth. Met.*, (1991) **41-430**: 429-432.
20. Yang, R., Dalsin, K.M., Evans, D.F., Christensen, L. and Hendrickson, W.A., *J. Phys. Chem.*, (1989) **93**: 511-512.
21. Mitchell, G.R. and Geri, A., *J. Phys. D: Appl. Phys.*, (1987) **20**: 1346-1353.
22. Asavapiryanont, S., Chandler, G.K., Gunawardena, G.A. and Pletcher, D., *J. Electroanal. Chem.*, (1984) **177**: 229-244.
23. Hillman, A.R. and Mallen, E.F., *J. Electroanal. Chem.*, (1987) **220**: 351-367.
24. Miller, L.L., Zinger, B. and Zhou, Q.X., *J. Am. Chem. Soc.*, (1987) **109**: 2267-2272.
25. Albery, W.J., Li, F. and Mount, A.R., *J. Electroanal. Chem.*, (1991) **310**: 239-253.
26. Garcia, R., *Biophys. J.*, (1991) **60**: 738.
27. Szucs, A., Hitchens, G.D. and Bockris, J.O., *J. Electrochem. Soc.*, (1989) **136**: 3748-3755.
28. Yuan, J-Y., Shao, Z. and Gao, C., *Phys. Rev. Lett.*, (1991) **67**: 863-866.
29. Fortier, G. and Bélanger, D., *Biotechnol. Bioeng.*, (1991) **37**: 854-858.
30. Armstrong, F.A., Bond, A.M., Hill, H.A.O., Oliver, B.N. and Psaltis, I.S.M., *J. Am. Chem. Soc.*, (1989) **111**: 9185-9189.
31. Guo, L.H. and Hill, H.A.O., *Adv. Inorg. Chem.*, (1991) **36**: 341-375.
32. Mikkelsen, S.R. and Lennox, R.B., *Anal. Biochem.*, (1991) **195**: 358-363.
33. Wierenga, H.A. *Thesis, University of Nijmegen*, (1989).
34. Timmerman, B.H. *Thesis, University of Nijmegen*, (1990).

6 Third generation amperometric biosensor for glucose. Poly(pyrrole) deposited within a matrix of uniform latex particles as mediator

Abstract

Uniform latex particles and agarose gels are utilized to create porous membranes in which poly(pyrrole) is electrochemically deposited. Within the pores of these modified membranes glucose oxidase can be adsorbed irreversibly while its catalytic activity is retained. From the enzyme membrane a glucose sensor is constructed which has a considerable lifetime under continuous use. With this sensor glucose can be measured amperometrically in the concentration range 1-60 mM. The sensor response is independent of oxygen concentration. Evidence is presented that direct electron transfer occurs between glucose oxidase and the poly(pyrrole) inside the latex membrane.

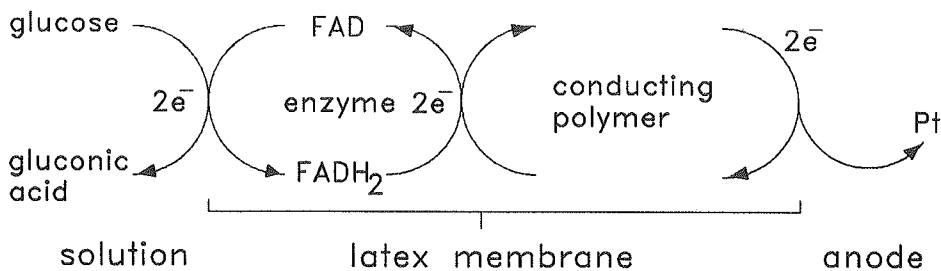
6.1 Introduction

Amperometric biosensors of the so-called third generation¹ are currently receiving great interest. These sensors are based on the principle of direct electron transfer from a biological receptor or enzyme to a modified or unmodified electrode (Chapter 1,2).²⁻⁵ Until now, only a few examples of large redox enzymes communicating directly with electrodes have been reported.⁶ The response current in these cases was very low.⁷ This poor electrochemistry has been ascribed to the fact that the active centers of the enzymes are usually surrounded by a thick, insulating protein shell.^{5,8} To realize direct electron transfer, it is required to develop an electrode material that can penetrate this shell and interact efficiently with the active center of the redox enzyme.² It has been suggested that poly(pyrrole) might be such

a material. Poly(pyrrole) has, therefore, been studied by many researchers for this purpose with varying success.^{7,9-13}

In Chapter 4 we described a glucose sensor which contains glucose oxidase immobilized in a special type of conducting poly(pyrrole), viz. in the form of microtubules. These microtubules had been synthesized using the pores of a track-etch membrane as templates.¹⁴⁻¹⁶ We presented evidence that this glucose sensor indeed worked according to the principle of direct electron transfer from the redox enzyme to the conducting polymer. It was shown that the track-etch sensor can be used to monitor glucose concentrations continuously for prolonged periods of time. This opens the possibility to construct an implantable device, which is of great medical interest.¹⁷⁻²¹ Another interesting application may be the use as a disposable sensor. However, from a technological point of view the track-etch membrane principle is not suitable for this application. Disposable sensors are generally prepared by a printing technique,²² which is not possible with our track-etch membrane. We had the idea that uniform latex particles (ULP's) might form an excellent porous matrix for poly(pyrrole) coating and successive enzyme immobilization. This in turn could be a way to develop disposable biosensors as the ULP matrix can be applied as an ink. Printing techniques can then be applied to construct multiple sensors in an automated fashion.

Poly(pyrrole) synthesized in aqueous media^{23,24} has a surface structure that is very rough and corrugated (see Chapter 5).^{11,25} Such an amorphous structure present inside the confined space of a ULP matrix could provide a very favourable environment for a redox enzyme. In this chapter we will show that our approach indeed can be used to construct a stable third generation biosensor, which is able to detect glucose in an amperometric way (Scheme 1, Figure 1).



Scheme 1. Electron shuttle showing the path of the electrons involved in the enzymatic oxidation of glucose.

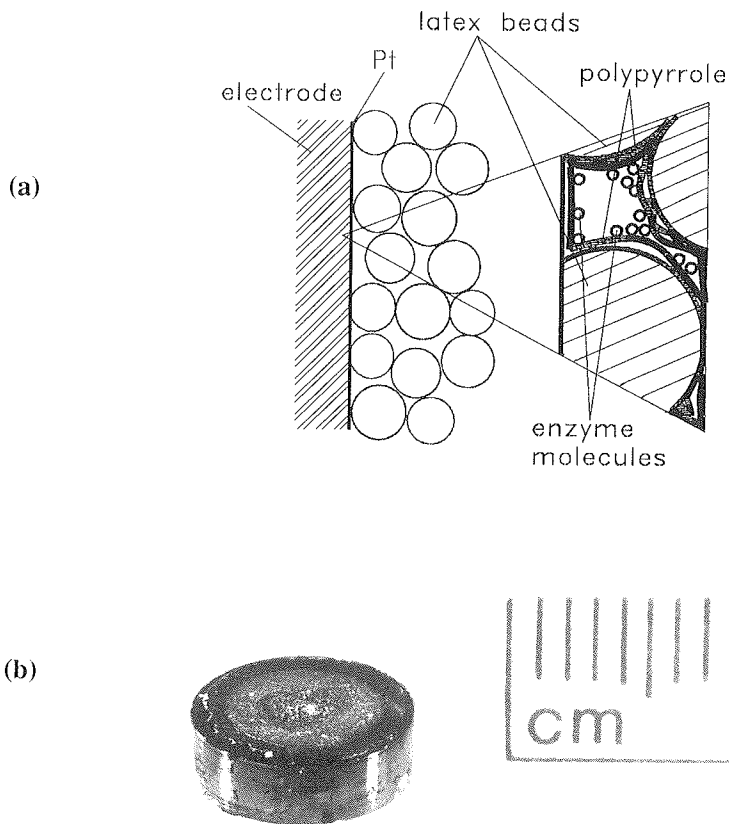


Figure 1. (a) Schematic drawing of the biosensor based on poly(pyrrole) incorporated in a latex membrane. (b) Photograph of the latex-poly(pyrrole) membrane biosensor.

6.2 Results and discussion

Latex membranes were cast on a freshly sputtered platinum surface from an aqueous solution, containing the suspended latex particles and agarose. The agarose was added to achieve a better fixation between the latex spheres and between these spheres and the electrode.²⁶ After casting, the latex was dried at low temperature to

get a uniform layer without cracks on the surface. Following drying, the modified electrode was given a heat-treatment, which resulted in a very strong layer.

6.2.1 Agarose content

The amount of agarose present in the latex suspension was varied to determine the minimum agarose content required to yield good membranes. Latex membranes were cast from solutions containing 0.125, 0.100, 0.075, and 0.050 weight% of agarose, respectively. An agarose content of 0.125 % led to latex membranes which were less accessible for poly(pyrrole) coating. Biosensors constructed from such membranes displayed lower activity and very long response times (*vide infra*). Amounts of agarose lower than 0.125 wt% resulted in strong latex membranes which could successfully be treated with poly(pyrrole). The lowest agarose content tested (0.050 wt%) still yielded membranes with strong adhesive properties. Therefore, in the further experiments, latex suspensions with 0.050 weight% of agarose were used.

6.2.2 Thickness

Thick membranes (ca. 5 μm)²⁶ as well as thin membranes (ca. 1 μm) were prepared by using two different latex concentrations (2.5 weight% and 0.5 weight%, respectively) in the droplet that was cast on the electrode. The droplet size was kept constant. In both cases strong and smooth layers were obtained. Latex particles of two different dimensions (112 and 220 nm diameter, respectively) were tested to prepare the membranes. Both particle sizes yielded membranes with interspherical pores in the order of 50-200 nm, as determined by scanning electron microscopy (*vide infra*, Figure 2).

6.2.3 Incorporation of poly(pyrrole) and characterization

The latex membranes were modified with poly(pyrrole) by means of an electrochemical polymerization. The polymerization medium consisted of phosphate buffered saline (PBS), containing 0.3 M of pyrrole. This medium was chosen because enzyme treatment of the poly(pyrrole) modified latex should preferably be performed in PBS buffer. By using the same medium during polymerization and enzyme treatment, exchange of dopant ions in the polymer with the solution was avoided. The latter might cause major changes in the conducting properties of the polymer as was already mentioned in Chapter 3.²⁷ The electrochemical polymerization was controlled galvanostatically. In this way we were able to vary the amount of poly(pyrrole) in the latex membranes by changing the polymerization time.

We found that galvanostatic polymerization gave more reproducible results than polymerization under potentiostatic control. The latter polymerization resulted in non-uniform coating of the latex membrane. Microscopic observation revealed that large areas on the electrode surface remained white (clean latex) while other areas showed colored spots containing very high concentrations of poly(pyrrole). Galvanostatic polymerization at moderate current densities (20 mA/cm^2) resulted in an evenly spreaded poly(pyrrole) coating of the latex.

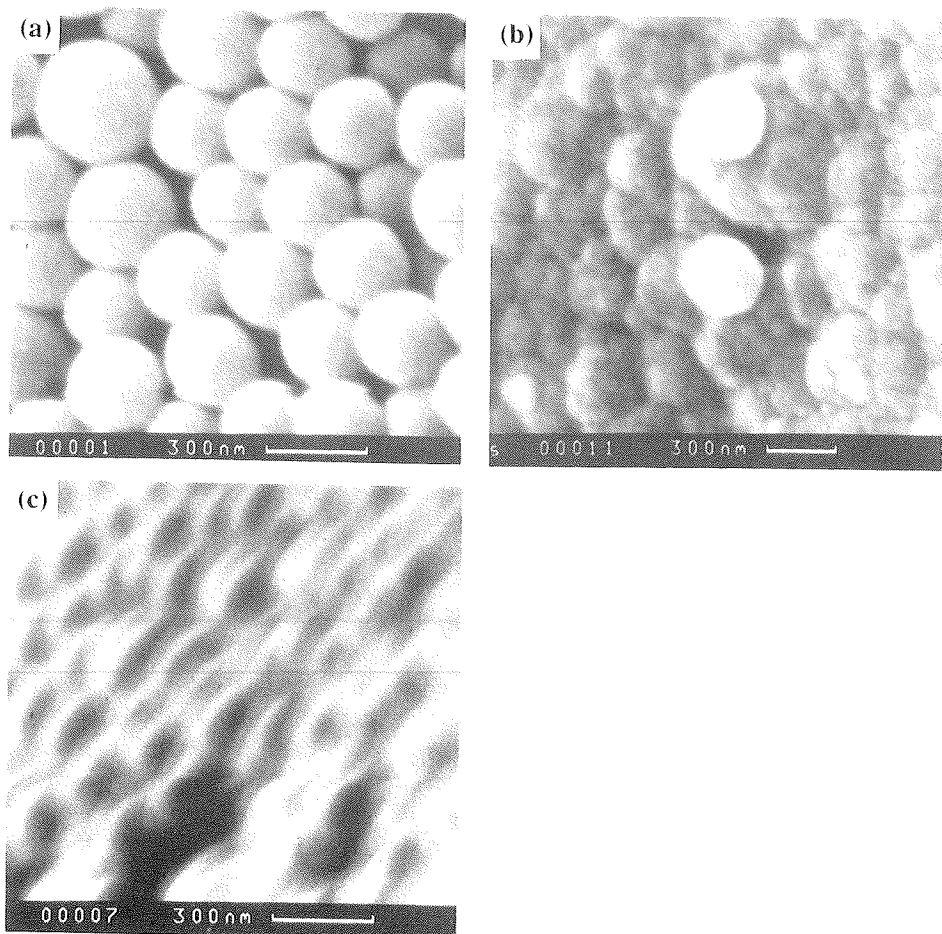


Figure 2. Scanning electron micrographs of $5 \mu\text{m}$ latex membranes containing 220 nm particles: (a) untreated membrane, (b) membrane treated with pyrrole for 15 s ; charge dose 300 mC/cm^2 , (c) membrane treated with pyrrole for 50 s ; charge dose 1000 mC/cm^2 .

The amount of charge (current \times time) in the polymerization reaction was varied from 100 to 1000 mC/cm². The blackening of the originally white latex layers was proportional to the amount of charge passed. Although only qualitative, this was a good indication of the proper polymerization of pyrrole in the matrix of the latex particles.

Scanning electron microscopy was used to image the coated latex membranes and to see how the membrane structure changed with polymerization time (Figure 2a-c). In Figure 2a a very open structure is visible between the spheres that make up the bare latex layer. In Figure 2b, the latex particles are coated with a thin layer of poly(pyrrole) (amount of charge passed is 300 mC/cm²). The internal surface now consists largely of poly(pyrrole) but the porous structure is still present. Two uncoated latex spheres, which can be used as a reference, are visible on the surface. When the latex membrane became coated with large amounts of poly(pyrrole), the porosity of the composite layer got lost. This is shown in Figure 2c for a thick latex layer, which was treated with poly(pyrrole) for 50 s. As will be shown below no enzyme electrodes can be made from these non-porous latex membranes.

6.2.4 Preparation of the enzyme electrodes and activity assay

An enzyme electrode was constructed from the poly(pyrrole) modified latex membranes by treating these membranes with glucose oxidase. This was achieved by agitating the membrane in an aqueous PBS solution, containing the enzyme, for 4 hours and successively drying overnight. The immobilization procedure was conducted at a temperature of 4 °C.

The enzyme electrodes were tested separately (i.e. independent of the biosensor activity) for enzymatic activity by the rotating disk electrode assay, described in detail in Chapter 4.^{28,29}

In Figure 3 the rotating disk electrode assay is shown for a glucose oxidase treated latex-poly(pyrrole) membrane with originally 112 nm spheres. This latex membrane was treated with an amount of poly(pyrrole) corresponding to a charge passing of 100 mC/cm². As can be seen, the current increases immediately after introduction of the membrane into the cell. Membranes with 220 nm spheres also showed this behaviour. The fact that after withdrawal of the membrane the activity returns to its initial value, is an indication that the enzyme is properly immobilized in the pores. Not properly immobilized material would have stayed in solution and the slope of the line after point 2 in the figure would have been higher. These experiments also showed that drying of the membrane after adsorption of the enzyme is essential. Enzyme was washed out completely when the membranes were tested for activity directly after enzyme treatment. For calibration a freshly prepared glucose oxidase solution, containing 0.125 U of the enzyme, was introduced into the electrochemical cell at point 5 in the figure. From the resulting rise in current it was concluded that

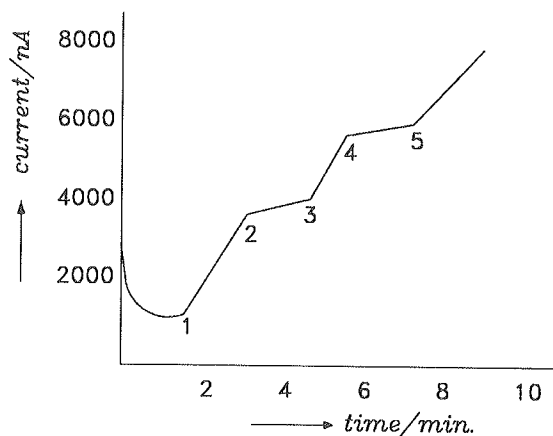


Figure 3. Rotating disk electrode assay of glucose oxidase immobilized on a $5\ \mu\text{m}$ membrane containing $112\ \text{nm}$ latex particles. (1) & (3): introduction of the latex membrane electrode into the cell, (2) & (4): withdrawal of the latex membrane electrode, (5): introduction of $0.125\ \text{U}$ of glucose oxidase.

approximately $0.2\ \text{U}$ of catalytically active glucose oxidase is present in the latex-poly(pyrrole) membrane of Figure 3.

A number of enzyme electrodes based on the latex-poly(pyrrole) composite membranes were tested for enzymatic activity with this assay. In Table 1 the results

Table 1. Enzymatic activity of different composite membranes, as determined by the RDE-assay (see text).^a

Charge (mC/cm^2)	$1\ \mu\text{m}^{\text{b}}$		$5\ \mu\text{m}^{\text{b}}$	
	$112\ \text{nm}^{\text{c}}$	$220\ \text{nm}^{\text{c}}$	$112\ \text{nm}^{\text{c}}$	$220\ \text{nm}^{\text{c}}$
100	+	+	x	x
150	+	+	x	x
200	+	+	+	+
300	+	+	+	+
400	-	+	+	+
500	-	-	+	+
1000	-	-	-	-

^aEnzymatically active membranes are marked (+), non-active membranes are marked (-), (x) = not tested.

^bThickness of the composite membrane.

^cSize of latex particles used in the composite membrane.

are listed for membranes composed of either 112 or 220 nm spheres, containing increasing amounts of poly(pyrrole). The poly(pyrrole) content is represented by the amount of charge passed in the electrochemical polymerization. It can be seen that up to a certain amount of charge enzymatically active membranes are obtained. Furthermore, the activity depends on the layer thickness of the membrane and not on the size of the particles. The thick layers were able to accommodate more poly(pyrrole) before they became unfit for enzyme immobilization. This is not surprising as thick layers contain more interspherical space than thin layers. The enzyme is immobilized by physical adsorption and probably forms a monolayer on the poly(pyrrole) surface. Thick latex membranes have a larger poly(pyrrole) surface. Consequently, a higher enzyme loading is to be expected. The observed independence of the enzyme activity on the particle size probably stems from the fact that the membranes with 112 and 220 nm spheres have interspherical pores of approximately the same dimensions as was concluded from electron microscopy (not shown).

6.2.5 Amperometric biosensor

In order to measure their biosensor activity the enzyme treated composite membranes were placed as the working electrode in an amperometric three electrode cell. This cell was part of a continuous flow system (Figure 4), which made it possible to switch between a buffer solution and a solution containing the substrate glucose (for a schematic representation of the flow cell see Chapter 4, Figure 7). Unless stated

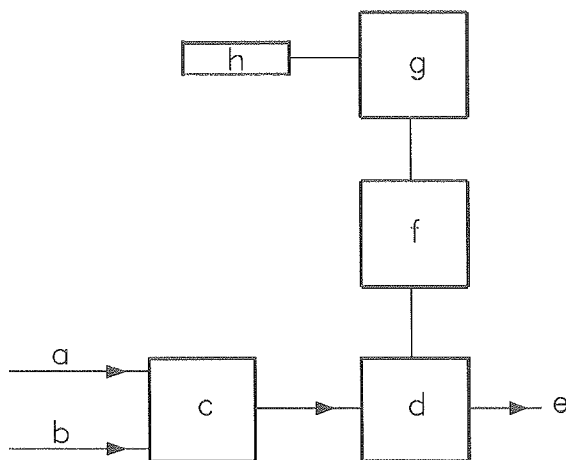


Figure 4. Set-up for the continuous flow measurements. (a) carrier solution containing phosphate buffered saline only, (b) sample solution containing glucose, (c) peristaltic pump, (d) flow cell, (e) waste, (f) potentiostat, (g) computer, (h) recorder.

otherwise, all experiments were conducted under an argon atmosphere and with 25 U/mL of catalase present in all solutions. The latter enzyme was added to eliminate any H₂O₂ accidentally produced by the enzyme due to the presence of oxygen.

In general, only the electrodes which showed clear enzymatic activity in the rotating disk electrode assay (Table 1) were tested as a biosensor. The amperometric

Table 2. Response times (in seconds) of different composite membranes.^a

Charge (mC/cm ²)	1 μm ^b		1 μm ^b	
	112 nm ^c	220 nm ^c	112 nm ^c	220 nm ^c
100	12	12	x	x
150	20	20	x	x
200	20	25	40	25
300	30	30	70	50
400	-	50	70	60
500	-	-	95	85

^aResponse to 5 mM glucose in PBS buffer; (-) = no enzyme activity, (x) = not tested.

^bThickness of the composite membrane.

^cSize of the latex particles used in the composite membrane

measurements were performed at a potential of 0.35 V versus Ag/AgCl. Non-specific electrochemical glucose oxidation at the platinum surface could in principle occur. Therefore, the electrodes were also tested for glucose sensitivity before they had been treated with glucose oxidase. No current response could be detected in these cases.

Enzyme electrodes based on latex membranes of 1 μm thickness showed a relatively low activity (approximately 10 ± 2 nA/mM glucose). However, the dynamic range was very good. The response time increased with the amount of charge passed during the pyrrole polymerization (Table 2). This response time is defined as the time needed to reach 95 % of the steady state current. It was only 12 s for the lowest poly(pyrrole) content (charge passed during polymerization 100 mC/cm²). When more than 400 mC/cm² of charge was passed no biosensor activity was found for the resulting enzyme treated electrodes. As already mentioned this is probably due to the fact that in these electrodes no interspherical surface is available for enzyme adsorption. For composite membranes prepared at 100-300 mC/cm², the biosensor activity was virtually equal. For one of these membranes (charge passing of 300 mC/cm²) the activity profile is shown in Figure 5. As can be seen the current response to glucose is virtually linear in the range of 0-20 mM. Also shown in Figure 5 is the activity profile for a biosensor containing an amount of poly(pyrrole) corresponding to 400 mC/cm². The dynamic range of this sensor is much lower. The use of 500

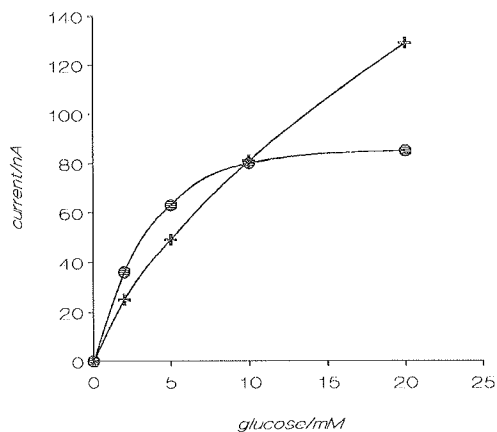


Figure 5. Current response of thin latex membranes (thickness ca. $1\ \mu\text{m}$, latex particle size $220\ \text{nm}$), measured at $0.35\ \text{V}$ vs. Ag/AgCl under an argon atmosphere in the presence of $25\ \text{U/ml}$ of catalase. Membranes containing poly(pyrrole) deposited at different charge passings: (+) $300\ \text{mC}/\text{cm}^2$; (●) $400\ \text{mC}/\text{cm}^2$.

mC/cm^2 or higher amounts of charge yielded membranes which were enzymatically inactive. The enzyme activity assay showed a similar trend (*vide supra*). No significant differences in activity were found when the thin latex membranes

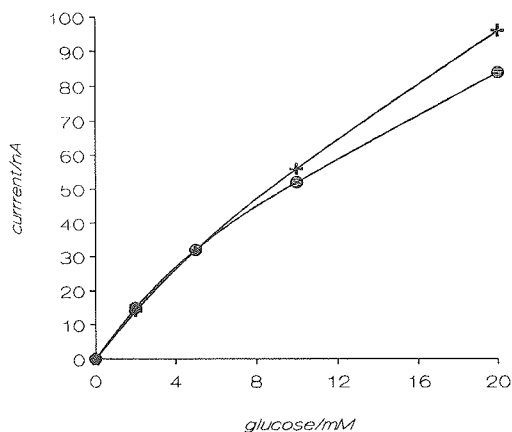


Figure 6. Current response curves of two glucose sensors, made under the same experimental conditions. Thickness of latex membrane ca. $1\ \mu\text{m}$, particle size ca. $220\ \text{nm}$. Poly(pyrrole) was deposited at a charge dose of $150\ \text{mC}/\text{cm}^2$. Measured at $0.35\ \text{V}$ vs. Ag/AgCl under an argon atmosphere with $25\ \text{U/ml}$ of catalase present.

contained 112 or 220 nm spheres. The accessibility of the membrane to glucose oxidase seems to be the critical factor. Once the pores become too small, the enzyme cannot penetrate the membrane structure anymore and immobilization does not occur.

Charge doses smaller than 100 mC/cm^2 were not investigated because the polymerization time became too short to get reproducible conditions. Even at low current densities (20 mA/cm^2), the polymerization time was less than 5 s, which is too short to reach a constant current under galvanostatic control.

The reproducibility of the results was tested on a number of separately prepared sensors. In Figure 6 data is shown for two sensors, containing an amount of poly(pyrrole) corresponding to a charge dose of 150 mC/cm^2 . The calibration lines are very similar, especially at low glucose concentrations.

Sensors constructed from thick composite membranes ($5 \mu\text{m}$), containing 112 or 220 nm latex particles showed good activities (Table 2) as expected in view of the results in Table 1. However, as can be seen in Figure 7 significant differences in the absolute current values were measured when the two types of latex membranes (viz. with 112 and 220 nm spheres, respectively) contained the same amounts of poly(pyrrole). In Figure 7a the current response curves are shown for enzyme electrodes composed of 112 nm diameter latex particles and amounts of poly(pyrrole) corresponding to 200 and 400 mC/cm^2 , respectively. Lower amounts of poly(pyrrole) were not tested (see also Table 1). Amounts corresponding to 500 mC/cm^2 yielded a sensor without activity, although the rotating disk assay had shown that these electrodes do contain enzyme (Table 1). Probably this enzyme is not in direct contact with the conducting polymer. Latex membranes with 220 nm particles and a poly(pyrrole) deposition corresponding to 500 mC/cm^2 still displayed biosensor activity in contrast to the membranes with 112 nm particles (Figure 7b). Higher poly(pyrrole) loadings yielded inactive membranes. The optimum in Figure 7b is for membranes with an amount of poly(pyrrole) corresponding to a charge dose of 400 mC/cm^2 . Lower amounts of poly(pyrrole) yielded less active and poorly performing membranes.

The maximum activity of the sensors derived from the $5 \mu\text{m}$ membranes is $60 \pm 10 \text{ nA/mM}$ glucose (calculated from the linear part of the curve for 400 mC/cm^2 in Figure 7b), which is higher than the activity of the $1 \mu\text{m}$ membranes (10 nA/mM glucose). This difference may be explained from the fact that the thick membranes have a larger surface of conducting polymer and can load more enzyme.

It should be noted that the response times in Table 2 are slightly dependent on the glucose concentration. However, the differences are small, e.g., the difference in response time for the measurement of 2 mM and 20 mM glucose is less than 5 s.

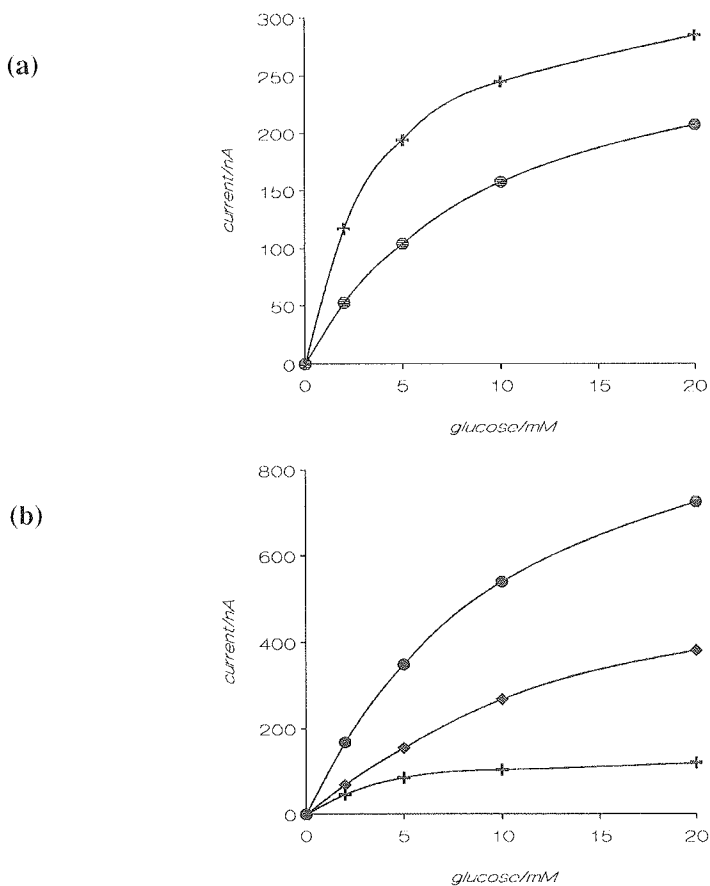


Figure 7. Current response of thick (ca. 5 μm) latex membranes, measured at 0.35 V vs. Ag/AgCl under an argon atmosphere with 25 U/ml of catalase present. Membranes containing 112 or 220 nm particles were treated with pyrrole at various charge doses. (a) 112 nm: (+) 200 mC/cm², (●) 400 mC/cm²; (b) 220 nm: (+) 200 mC/cm², (●) 400 mC/cm², (◆) 500 mC/cm².

6.2.6 Selectivity and lifetime

The sensitivity of the sensor to fructose, citrate, lactate, urea, uric acid and pyruvate was tested separately. No significant response was observed to any of these components when they were present at concentrations of 5 mM. Ascorbate (vitamin C) interfered strongly when present at 5 mM concentration. However, in real samples

the ascorbate concentration is usually much lower³⁰ (e.g. in milk 0.1 mM). Ascorbate interference was virtually unimportant at this concentration.

The current response of freshly prepared biosensors was tested for prolonged periods of time. To this end, the sensors were taken up in a flow system, which was kept at room temperature. The carrier stream contained 2 mM of glucose, which was continuously measured during this experiment. At fixed intervals (every 24 h) an additional amount of glucose leading to a total concentration of 5 mM was introduced

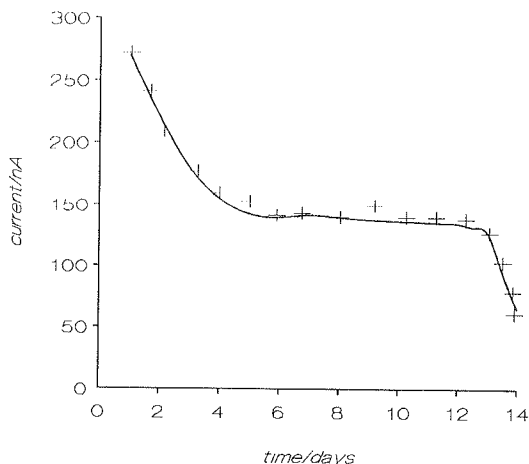


Figure 8. Stability of a biosensor under continuous operation. For explanation see text.

in the carrier stream and the increase in current was measured. In this way we were able to eliminate deviations due to baseline drift. In Figure 8 the activity of a biosensor ($5 \mu\text{m}$ membrane, 220 nm particles, charge dose 400 mC/cm^2) to 5 mM glucose is plotted as a function of time. The current response is not stable during the first days of the measurement. Probably in the beginning an amount of less firmly bound enzyme is slowly washed out. After 3 days, the sensor response remained the same for 10 days. This stability is sufficient for disposable applications.

6.2.7 Effect of oxygen

The effect of oxygen on the biosensor activity was studied at low potentials (from +0.10 to +0.35 V vs. Ag/AgCl) in a continuous flow system. No additional electron mediators were present. The accidental mediation of electron transfer by free flavin molecules can be excluded since any flavin co-factor, dissociated from the enzyme, is washed out immediately. The only low molecular weight mediator that can still be

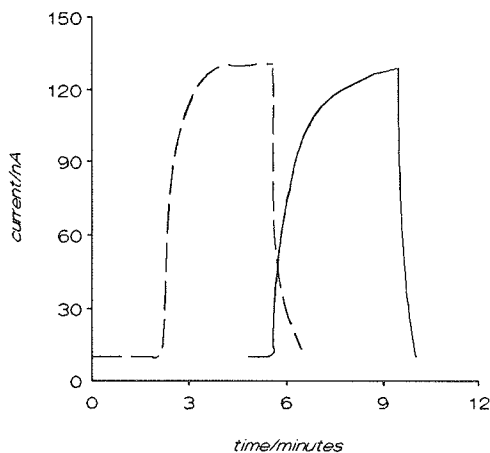


Figure 9. Current response of a biosensor upon the addition of 5 mM of glucose under different conditions. Measurement at 0.35 V vs. Ag/AgCl. Dashed line: air saturated solution open to the air; solid line: argon flushed solution under an argon atmosphere with 25 U/ml of catalase present.

operative in the system is oxygen. However, we found no significant difference in activity when measurements under ambient atmosphere were compared with measurements under argon. Figure 9 shows a typical plot of the response (at 0.35 V vs. Ag/AgCl) under an argon atmosphere using argon flushed solutions (solid line) and under ambient atmosphere using air saturated solutions (dashed line). The difference is less than 6 %, which is within the range of experimental error.

Oxygen mediation leads to hydrogen peroxide formation and at sufficiently low anodic potentials to a strongly negative response, because the latter molecule is catalytically reduced.^{31,32} In Figure 10 the response of our sensor membrane to 10 mM glucose is compared with the response of the same membrane to 0.0025 wt% of H₂O₂ at a potential of 0.10 V vs. Ag/AgCl. As can be seen the addition of H₂O₂ causes a large negative current. The addition of glucose leads to a positive current. The formation of even the smallest amount of hydrogen peroxide due to enzymatic glucose oxidation would have eliminated or probably inverted the current response to glucose. Therefore, we may conclude that no significant oxygen mediation takes place in our system and that the measured current is due to direct electron transport from glucose oxidase to the poly(pyrrole). Taking into account this direct electron transport, the working potential (maximum 0.35 V versus Ag/AgCl reference) of our composite membrane electrode is very low (see Chapter 7 for a detailed discussion). Poly(pyrrole) is electroactive in its oxidized state and the charge carried by the conducting polymer can be cycled repetitively (see Chapters 2 & 3).³³ The confined space in the interspherical pores of the latex membrane apparently brings the active

centers of the enzyme molecules in close contact with the conducting polymer. An analogous situation was observed for the track-etch membrane biosensor described in Chapter 4.

We found that drying after enzyme treatment of the latex-poly(pyrrole) membrane is essential for both the immobilization of the enzyme and the process of direct electron transfer. Water is likely to be a competing species for the enzyme with regard

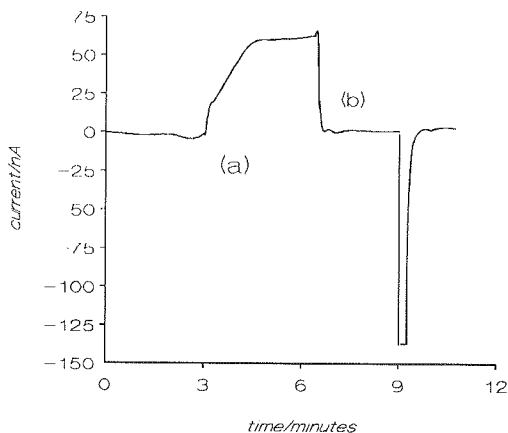


Figure 10. Current response of a membrane containing 220 nm latex particles and poly(pyrrole) deposited at a charge dose of 200 mC/cm². Measuring potential 0.10 V vs. Ag/AgCl. (a) 10 mM of glucose, sensor open to the air, (b) 0.0025 wt% of aqueous hydrogen peroxide.

to adsorption on the polymer surface. When water is removed by evaporation, enzyme adsorption is favoured.³⁴ Electrostatic interactions may play an important role in the immobilization process. Poly(pyrrole) in its conducting state is a polycation.³⁵ Glucose oxidase at neutral pH has at least 10 negative charges on its surface.³⁶ Because of these features the electroactive sites on the conducting polymer can be expected to interact strongly with the enzyme, thereby making direct electron transfer a favourable process.

6.3 Conclusions

We have shown that amperometric glucose sensors can be constructed from poly(pyrrole) modified latex membranes that are cast on a platinum electrode. Adsorption of glucose oxidase on the poly(pyrrole) surface within the pores of the membranes leads to immobilization without loss of enzymatic activity. Evidence is

presented which suggests that in the biosensor direct electron transfer occurs between glucose oxidase and the conducting polymer. The absence of H_2O_2 production and the stabilization of the enzyme in the pores of the composite membrane result in a device that has a considerable lifetime under continuous use.

In analogy with the track-etch sensor (Chapters 4 and 5) a completely different mechanism for the enzyme catalyzed glucose oxidation is expected when electron transfer via oxygen mediation is replaced by direct electron transfer. This will be further evaluated in the next chapter for both the track-etch membrane sensor and the latex membrane sensor.

6.4 Materials and methods

Glucose oxidase (E.C. 1.1.3.4) type II (25,000 U/g) from *Aspergillus niger* and catalase (E.C. 1.11.1.6, 2800 U/mg) from Bovine liver were obtained from Sigma. Benzoquinone was from Aldrich (FRG) and was sublimed prior to use. Pyrrole was from Merck and was distilled before use. Latex suspensions with particles of 112 and 220 nm were obtained from Perstorp analytical. Agarose type VIII was purchased from Sigma. All other reagents were of analytical grade.

The galvanostat was a home-built instrument (see Chapter 3). Its current output was monitored with a Fluke 45 digital multimeter. Electrochemical measurements were performed with an Antec CU-04-AZ control unit (Antec Leyden, The Netherlands) or with an Autolab potentiostat controlled by an Olivetti M24 Personal Computer and General Purpose Electrochemical System (GPES)-software (Eco Chemie, Utrecht, The Netherlands). Current output was recorded on a Yew 3056 pen recorder. Electron micrographs were made on a CAMSCAN scanning electron microscope (Cambridge Instruments).

Platinum coating

Glassy carbon disks of 8 mm diameter (Antec Leyden, The Netherlands) were used as the base electrode. The electrodes were polished with Alpha Micropolish Alumina No. 1C (1.0 micron, Buehler LTD., U.S.A.). Platinum was applied on the polished surface with an Edwards sputtercoater S150B. A platinum target of 8 cm diameter and 0.5 mm thickness was used as the platinum source. The layer thickness was monitored with an Edwards FTM5 unit. Sputtering was continued until the thickness of the platinum layers was 300 nm.

Preparation of the latex membranes

Agarose type VIII was dissolved by boiling the appropriate amount (0.1 or 0.25 wt%) for two min. in distilled water. Freshly made solutions, which were still hot, were used to make the latex membranes. A certain volume of the agarose solution was mixed thoroughly with an equal volume of the latex suspension. A 75 μl droplet was applied on a freshly platinum sputtered glassy carbon disk. After application, the electrode was placed overnight in the refrigerator. The dried latex electrode was subsequently heated in an oven at 60 °C for one h.

Incorporation of poly(pyrrole)

Latex electrodes were sealed with Teflon tape in such a way that only the latex surface made contact with the polymerization medium. A PBS buffer solution (pH 7.4) containing 0.3 M of pyrrole was used in the polymerization reaction. To allow the solution to penetrate the membrane sufficiently the latex membrane was placed in the solution for at least one min. before polymerization was started. Subsequently, a constant current (20 mA/cm²) was supplied to the cell for the appropriate amount of time. A platinum plate acted as the counter electrode. After polymerization the electrodes were rinsed with PBS buffer.

Immobilization of enzyme

Enzyme immobilization was achieved by agitating (Gyrotory Shaker model G2, New Brunswick Scientific, USA) the composite membranes in 3 ml of 5 mg/ml of glucose oxidase at a temperature of 4 °C for 4 h. The membranes were subsequently dried overnight over CaCl₂ in a desiccator.

Enzyme activity assay

Enzyme activity was assayed with a three electrode cell containing 5 mM of benzoquinone and 0.5 M of glucose in 20 ml of PBS buffer, pH 7.4. Prior to use, the glucose solution was allowed to mutarotate for at least 24 h. The assay was performed with a platinum rotating disk electrode (6 mm \varnothing) equipped with an Electrocraft corporation model E550 motor and an E552 speed control unit. The platinum working electrode was set at a potential of 0.350 V (Ag/AgCl reference) and was rotated at a speed of 2000 rpm. A platinum wire was used as the auxiliary electrode. The solution was flushed with argon before each experiment. During the assay argon was blanketed

over the solution. The actual assay was performed by monitoring the current output of the RDE while immersing a sample membrane into the solution.

Amperometric biosensor measurements

To perform amperometric measurements, the enzyme membrane was placed as the working electrode in a three electrode flow cell (Antec Leyden, The Netherlands). To insulate the active surface of the membrane from the auxiliary electrode, the former was covered with a Teflon spacer of 1 mm thickness. In the spacer a duct of approximately 0.15 cm^2 was left, allowing the membrane to make contact with the solution. An Ag/AgCl electrode was used as the reference electrode. The base of the flow cell acted as the auxiliary electrode (glassy carbon). Buffer solution was driven through the cell at a rate of 1.75 ml/min. (Watson Marlow 101U peristaltic pump). The potential of the membrane was set at 0.350 V. When the background current had been diminished sufficiently, the buffer solution was replaced by the glucose solution and the current response was monitored.

References

1. Turner, A.P.F., Karube, I. and Wilson, G.S. *Biosensors. Fundamentals and Applications*. Oxford University Press, New York: (1989).
2. Armstrong, F.A., Hill, H.A.O. and Walton, N.J., *Acc. Chem. Res.*, (1988) 21: 407-413.
3. Armstrong, F.A., Bond, A.M., Hill, H.A.O., Oliver, B.N. and Psalti, I.S.M., *J. Am. Chem. Soc.*, (1989) 111: 9185-9189.
4. Albery, W.J., Bartlett, P.N. and Cass, A.E.G., *Phil. Trans. R. Soc. Lond.*, (1987) B 316: 107-119.
5. Heller, A., *Acc. Chem. Res.*, (1990) 23: 128-134.
6. Yabuki, S., Shinohara, H. and Aizawa, M., *J. Chem. Soc., Chem. Commun.*, (1989): 945-946.
7. Kajiyama, Y., Sugai, H., Iwakura, C. and Yoneyama, H., *Anal. Chem.*, (1991) 63: 49-54.
8. Degani, Y. and Heller, A., *J. Am. Chem. Soc.*, (1989) 111: 2357-2358.
9. Fortier, G., Brassard, E. and Bélanger, D., *Biosensors & Bioelectronics*, (1990) 5: 473-490.
10. Bartlett, P.N. and Whitaker, R.G., *J. Electroanal. Chem.*, (1987) 224: 37-48.
11. Tamiya, E., Karube, I., Hattori, S., Suzuki, M. and Yokoyama, K., *Sensors and Actuators*, (1989) 18: 297-307.
12. Janda, P. and Weber, J., *J. Electroanal. Chem.*, (1991) 300: 119-127.
13. Yokoyama, K., Tamiya, E. and Karube, I., *Anal. Lett.*, (1989) 22: 2949-2959.
14. Koopal, C.G.J., De Ruiter, B. and Nolte, R.J.M., *J. Chem. Soc., Chem. Commun.*, (1991): 1691-1692.
15. Koopal, C.G.J., Feiters, M.C., De Ruiter, B., Schasfoort, R.B.M. and Nolte, R.J.M. *Glucose sensor utilizing poly(pyrrole) incorporated in track-etch membranes as the mediator. Biosensors & Bioelectronics*, (1992), in press.
16. Cai, Z. and Martin, C.R., *J. Am. Chem. Soc.*, (1989) 111: 4138-4139.
17. Koudelka, M., Rohner-Jeanrenaud, F., Terretaz, J., Bobbioni-Harsch, E., De Rooij, N.F. and Jeanrenaud, B., *Biosensors & Bioelectronics*, (1991) 6: 31-36.
18. Reach, G. and Wilson, G.S., *Anal. Chem.*, (1992) 64: 381-386.
19. Müller, A., Abel, P. and Fischer, U., *Biomed. Biochim. Act.*, (1986) 45: 769-777.
20. Xie, S.L. and Wilkins, E., *J. Biomed. Eng.*, (1991) 13: 375-378.
21. Von Woedtke, Th., Rebrin, K., Fischer, U., Abel, P., Wilke, W., Vogt, L. and Albrecht, G., *Biomed. Biochim. Act.*, (1989) 48: 943-952.
22. Kulyts, J. and D'Costa, E.J., *Biosensors & Bioelectronics*, (1991) 6: 109-115.
23. Zotti, G., Schiavon, G., Berlin, A. and Pagani, G., *Electrochim. Act.*, (1989) 34: 881-884.
24. Downard, A.J. and Pletcher, D., *J. Electroanal. Chem.*, (1986) 206: 139.
25. Czajka, R., Koopal, C.G.J., Feiters, M.C., Gerritsen, J.W., Nolte, R.J.M. and Van Kempen, H. *Scanning tunneling microscopy study of poly(pyrrole) films and of glucose oxidase as used in a third generation biosensor. J. Electroanal. Chem.*, (1992), in press.
26. Schasfoort, R.B.M., Kooyman, R.P.H., Bergveld, P. and Greve, J., *Biosensors & Bioelectronics*, (1990) 5: 103-124.
27. Krishna, V., Ho, Y.-H., Basak, S. and Rajeshwar, K., *J. Am. Chem. Soc.*, (1991) 113: 3325-3333.
28. Aubré-Lecat, A., Hervagault, C., Delacour, A., Beaudé, P., Bourdillon, C. and Remy, M., *Anal. Biochem.*, (1989) 178: 427-430.
29. Bourdillon, C. and Majda, M., *J. Am. Chem. Soc.*, (1990) 112: 1795-1799.
30. Clark Jr., L.C. *The Hydrogen Peroxide Sensing Platinum Anode as an Analytical Enzyme Electrode*. In: *Methods in Enzymology*, Vol. LVI. Academic Press, New York: (1979) pp. 448-479.
31. Hoare, J.P. *Oxygen*. In: *Standard Potentials in Aqueous Solution*. edited by Bard, A.J., Parsons, R. and Jordan, J. Marcel Dekker, Inc., New York: (1985) pp. 49-66.

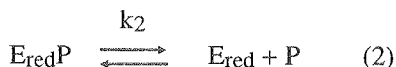
32. Delahay, P. *Voltammetry and Polarography at Constant Potential. Kinetic and Catalytic Processes*. In: *New Instrumental Methods in Electrochemistry*. Interscience Publishers, Inc., New York: (1965) 4th Ed., pp. 87-114.
33. Asavapiriyant, S., Chandler, G.K., Gunawardena, G.A. and Pletcher, D., *J. Electroanal. Chem.*, (1984) 177: 229-244.
34. Armstrong, F.A., Cox, P.A., Hill, H.A.O., Lowe, V.J. and Oliver, B.N., *J. Electroanal. Chem.*, (1987) 217: 331-366.
35. Fortier, G. and Bélanger, D., *Biotechnol. Bioeng.*, (1991) 37: 854-858.
36. Szucs, A., Hitchens, G.D. and Bockris, J.O., *J. Electrochem. Soc.*, (1989) 136: 3748-3755.

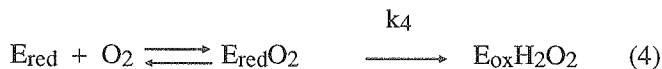
7 Kinetic study of the performance of the biosensors

7.1 Introduction

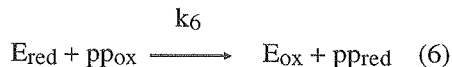
In the previous chapters two novel biosensor systems were described, viz. the track-etch membrane sensor and the latex-poly(pyrrole) membrane sensor. These membrane sensors contain a microporous matrix in which the conducting polymer poly(pyrrole) is deposited. It was shown that in the modified matrix glucose oxidase can be immobilized by physical adsorption while retaining its activity. The resulting systems displayed excellent sensor properties, which -amongst others- were ascribed to the fact that the redox enzyme transfers its electrons directly to the conducting matrix.

This chapter deals with a kinetic study of the performance of the two above-mentioned biosensor systems. The kinetics of the oxidation of glucose by glucose oxidase in homogeneous aqueous solution has been studied in detail in the literature.¹ Molecular oxygen is the electron acceptor in this case. The reaction involves seven steps (eqns. 1-5). Four steps are related to the oxidation of glucose and the dissociation of the product complex. Three other steps bear upon the binding of molecular oxygen, its conversion into hydrogen peroxide, and the dissociation of the latter molecule from the enzyme. This part of the sequence transfers the reduced enzyme back to the biologically active state.





In eqns. 1-5 E_{ox} and E_{red} are the oxidized and reduced forms of glucose oxidase, S is β -D-glucose and P is D-gluconolactone. In the track-etch and latex-poly(pyrrole) membrane sensors oxygen mediation does not occur. Reoxidation of reduced enzyme takes place by electron transfer to the conducting polymer. Equations 4 and 5 are no longer valid in our case. They are replaced by the single step:



where pp_{ox} and pp_{red} represent the oxidized and reduced states of poly(pyrrole), respectively. The constant k_6 is the heterogeneous electron transfer rate constant. Due to the presence of an oxidizing potential, electroactive sites on the conducting polymer that are reduced by the enzyme, are immediately reoxidized.

7.2 Results

We determined the apparent kinetic parameters of glucose oxidase in our sensors under steady-state conditions. This means that the current response due to varying concentrations of glucose is measured under conditions where the bulk substrate concentration does not change in time. A Michaelis-Menten equation of the following form was used:²

$$i_{\text{ss}} = \frac{i_{\text{max}}[S]}{K_M + [S]} \quad (7)$$

where i_{ss} is the measured steady-state current and i_{max} is the maximum catalytic current of the sensor. The biosensors operate under conditions where internal diffusion limitation of substrate may be significant. Therefore, only apparent K_M values (denoted by K_M') are determined. The maximum current, i_{max} , may vary from sensor to sensor. Its value depends on the enzyme loading, the available surface, and the amount of biochemically active enzyme. Therefore, i_{max} is not an intrinsic parameter of the immobilized enzyme.

7.2.1 Effect of glucose

The biosensor was placed as the indicator electrode in a three electrode flow cell. The applied potential was 0.35 V versus Ag/AgCl. The measurements were conducted under an argon atmosphere using argon flushed solutions. All solutions contained at least 20 U/ml catalase to destroy any accidentally produced hydrogen peroxide. Any response current observed upon the addition of glucose was presumed to result from direct electron transfer between the enzyme and the conducting polymer.^{3,4} The concentration of glucose was varied between 0 and 100 mM. We observed that the biosensors did not respond reliably to concentrations higher than 60 mM. Figure 1 shows the steady-state current as a function of the glucose concentration for a representative track-etch membrane electrode and a latex-poly(pyrrole) membrane electrode. Lineweaver-Burk plots of the data are given in Figure 2a and 2b. The kinetic parameters were calculated using three different procedures, viz. the Lineweaver-Burk,⁵ Hanes-Woolf,⁶ and Wilkinson⁷ procedure. All three gave the same results. The parameters are summarized in Table 1. For comparison, in Table 1 also literature values for free and for immobilized glucose oxidase are given. These literature values show a great discrepancy. Despite this, we may conclude that our values for K_M' are significantly lower than those reported in the literature.*

7.2.2 Effect of applied potential

The biosensor response in the glucose concentration range of 0-20 mM was determined at various potentials versus Ag/AgCl. The measurement conditions were the same as described above. A representative result for the track-etch membrane sensor is presented in Figure 3. The latex-poly(pyrrole) membrane sensor gave similar

*We encountered one publication in which a K_M' for glucose of 11.5 mM is mentioned.⁸ The authors claim that their K_M' -value is an order of magnitude larger than the K_M for the solubilized enzyme ($K_M = 33 \text{ mM}^9$). As this claim is not consistent with the K_M' -value given, we believe that the reported value of 11.5 mM is incorrect.

Table 1. Kinetic parameters of the membrane sensors and of some literature systems.

#	System	K_M' or K_M / mM glucose	i_{max} / μA	Ref.
1	Glucose oxidase in track-etch membrane sensor	14.7 ± 0.8^a 15.7 ± 2.2^a	3.05 ± 0.07^a 4.1 ± 0.3^a	This work
2	Glucose oxidase in latex membrane sensor	11.2 ± 0.4^a 10.9 ± 0.2^a	1.13 ± 0.02^a 1.12 ± 0.3^a	This work
3	Glucose oxidase entrapped in poly(pyrrole)	33.4 ± 0.7	7.2 ± 0.06	10
4	Idem	31	4.3	2
5	Glucose oxidase covalently bound to glassy carbon	66		11
6	Free glucose oxidase	60		1
7	Idem	33		9
8	Idem ^b	120	$V = 235 \text{ s}^{-1 \text{ c}}$	12

^aValues for independently prepared electrodes. Standard errors as calculated by the Wilkinson method.⁷

^b Measured at 0 °C.

^cMaximum velocity.

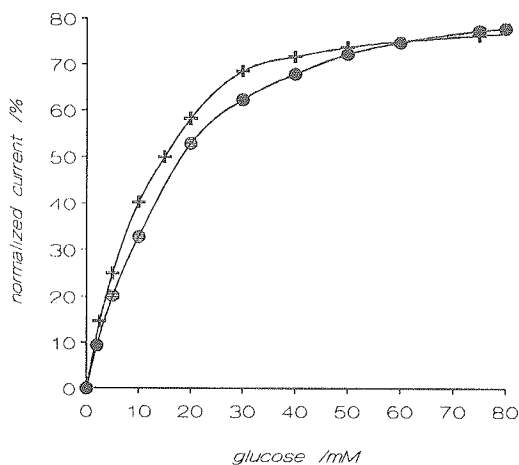


Figure 1. Plot of the steady-state current measured at 0.350 V (vs. Ag/AgCl) as a function of glucose concentration. (+) Track-etch membrane with 800 nm pores, treated with pyrrole/ FeCl_3 for 1 min.; (●) Latex membrane of approx. 5 μm thickness (220 nm beads), electropolymerized with pyrrole using an amount of charge corresponding to 400 mC/cm^2 . The membranes were incubated with 5 mg/ml of glucose oxidase. Measurements were conducted under an argon

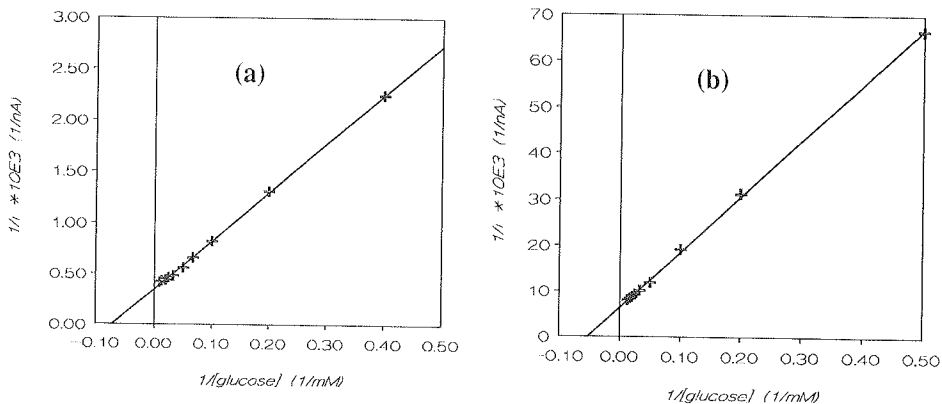


Figure 2. Lineweaver-Burk plots of the curves shown in Figure 1. (a) track-etch membrane, (b) latex poly(pyrrole) membrane. The solid lines are least squares fits of the data points.

response curves. In order to establish whether the biosensor response is predominantly limited by substrate transport or by interfacial dynamics at the electrode, Tafel-plots^{13,14} of the data points were made. The results for the track-etch membrane

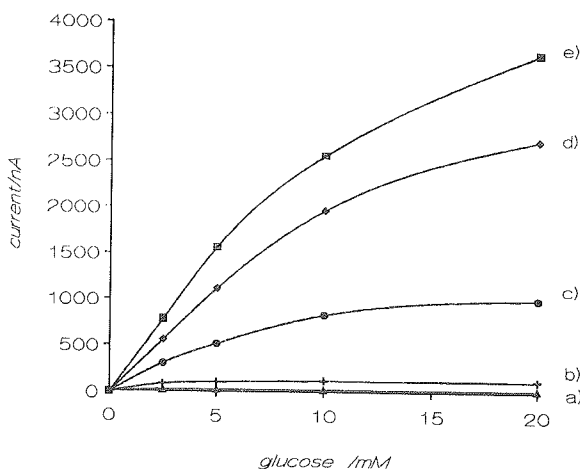


Figure 3. Steady-state currents for the track-etch membrane biosensor of Figure 1, measured at various potentials vs. Ag/AgCl and at various glucose concentrations. (a) 0.10 V; (b) 0.15 V; (c) 0.20 V; (d) 0.30 V; (e) 0.35 V. Measurements were performed under an argon atmosphere and under continuous flow conditions with 20 U/ml of catalase present.

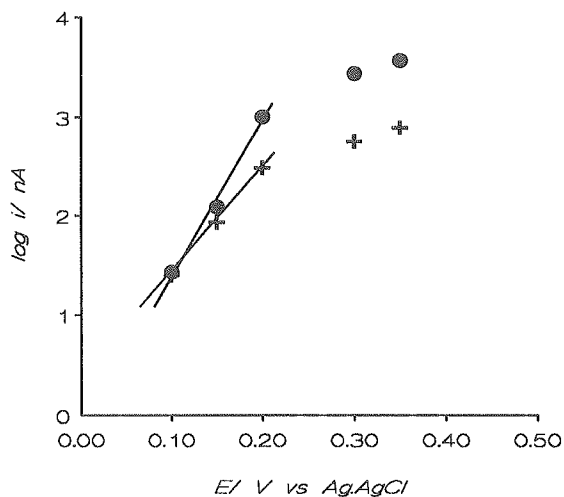


Figure 4. Tafel plots of the data points in Figure 3; (+) 2.5 mM glucose; (●) 20 mM glucose.

sensor at glucose concentrations of 2.5 and 20 mM are shown in Figure 4. As can be seen in this figure Tafel-like behaviour is evident at low potentials (straight lines drawn through the data points), but not at high potentials (see also Discussion).

7.2.3 Effect of pH and temperature

The pH dependence of our biosensors was determined at a glucose concentration of 2 mM. This relatively low concentration was chosen to avoid local variations in acidity due to the enzymatic production of gluconic acid. The result for a latex-poly(pyrrole) membrane sensor (220 nm beads, 5 μm thick, poly(pyrrole) deposition using a total charge dose of 400 mC/cm^2) is given in Figure 5. The other latex-poly(pyrrole) membrane or track-etch membrane sensors gave similar profiles. For comparison, in Figure 5 also a pH curve from the literature is given. It represents glucose oxidase entrapped in a poly(pyrrole) matrix during electrochemical immobilization.^{2,10}

The temperature dependence of the biosensors was determined by measuring the steady-state current due to the addition of a fixed amount of glucose (1 mM) in the temperature range 4–45 $^{\circ}\text{C}$. In Figure 6a the resulting temperature profile is shown for a track-etch membrane sensor. As can be seen the response of the sensor increases monotonically from 4 to 37 $^{\circ}\text{C}$ and then decreases. This behaviour was found to be reversible. An Arrhenius-like plot of the data from Figure 6a is shown in Figure 6b. The following relation was used to calculate the activation energy (E_a) from the data:

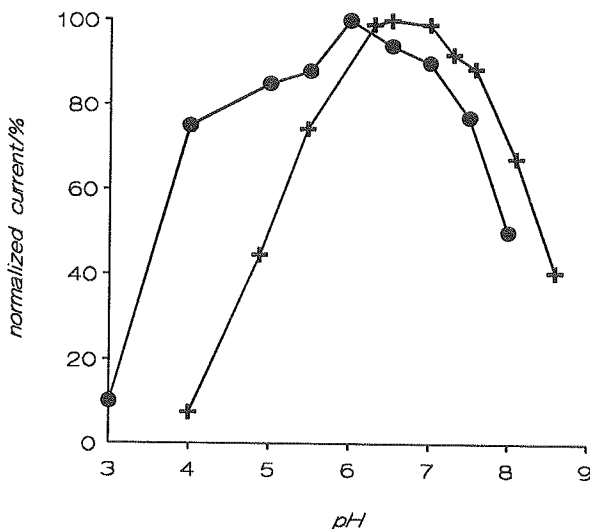


Figure 5. (+) The current response of a latex-poly(pyrrole) membrane biosensor at various pH's. The latex membrane was approx. 5 μm thick and prepared from 220 nm beads. Electropolymerization with pyrrole was performed using a total charge dose of 400 mC/cm^2 . After polymerization the membrane was treated with 5 mg/ml glucose oxidase for 4 h. The response to 2 mM glucose was measured at a potential of 0.35 V (vs. Ag/AgCl) either in citrate/phosphate or in borate buffer, depending on the pH. (●) pH curve of glucose oxidase entrapped in poly(pyrrole) from reference 2.

$$\ln(i) = \frac{-E_a}{RT} + \text{constant} \quad (8)$$

For the track-etch membrane sensor E_a amounted to 41 kJ/mole; for the latex-poly(pyrrole) membrane sensor a value of $E_a = 44$ kJ/mole was obtained. These activation energies are similar to those reported by others for glucose oxidase entrapped in poly(pyrrole) (see Discussion).¹⁰

7.2.4 Lifetime

The lifetime of the two biosensors was evaluated under conditions of continuous operation at room temperature as described in Chapters 4 and 6. A concentration of 2 mM glucose was continuously measured during the experiments. At fixed times a glucose concentration of 5 mM (latex sensor) or 10 mM (track-etch sensor) was introduced into the carrier stream and the increase in current was measured. In this

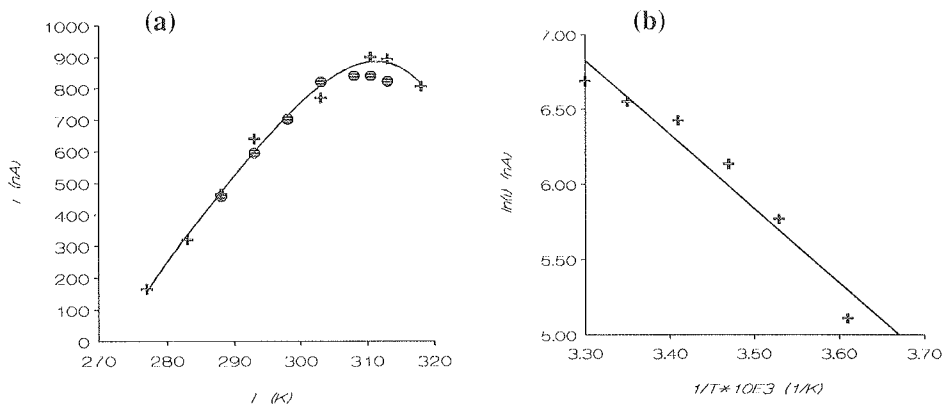


Figure 6. Steady-state current response of a track-etch membrane biosensor as a function of temperature. (a) Track-etch membrane with originally 800 nm pores, treated with pyrrole/ FeCl_3 for 1 min. The membrane was incubated with 5 mg/ml glucose oxidase for 0.5 h; (+) first temperature experiment; (●) second experiment after cooling the system to 15 °C. (b) Arrhenius plot of the data points.

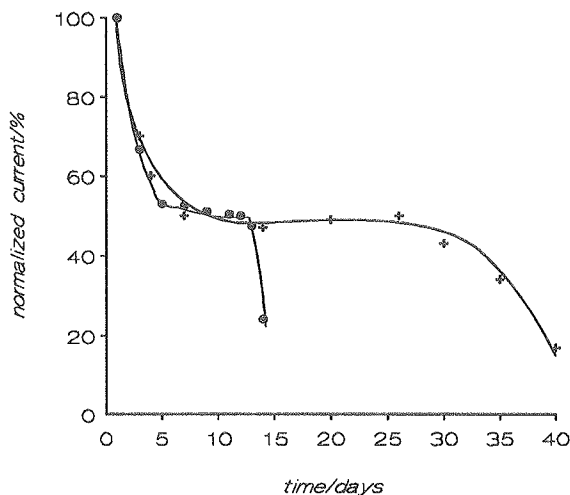


Figure 7. Stability plots of the biosensors at continuous operation (2 mM glucose) under ambient atmosphere. The activity of the sensors was measured by introducing an additional amount of glucose to the carrier stream (see text); (+) 800 nm track-etch membrane sensor treated for one min. with pyrrole/ FeCl_3 and subsequently incubated with 5 mg/ml glucose oxidase for 0.5 h; (●) 220 nm beads latex-poly(pyrrole) membrane of approx. 5 μm thickness electropolymerized with pyrrole using a total charge dose of 400 mC/cm^2 ; the membrane was treated with 5 mg/ml glucose oxidase for 4 h.

way we were able to account for the baseline drift that could occur during the experiments. A representative lifetime curve for both sensors is given in Figure 7.

7.3 Discussion

The immobilized glucose oxidase in our biosensors obeys Michaelis-Menten kinetics. Table 1 shows that the apparent Michaelis-Menten constant K_M' (entrance 1 and 2) is lower than $K_{M(\text{glucose})}$ for glucose oxidase in a homogeneous, air-saturated solution (entrance 6-8).¹ As a first tentative conclusion we may say that this low K_M' -value suggests that the matrix of our sensor electrodes is not covered with a multilayer of enzyme. Such a multilayer of immobilized enzyme would have imposed major diffusional restrictions on substrate transport and this would have been manifested as a significantly increased apparent Michaelis-Menten constant as compared to the free enzyme.¹¹ The decrease in Michaelis-Menten constant suggests that the reaction rate is partly limited by interfacial dynamics: electron transfer from the enzyme to the conducting polymer is probably rate determining in the total reaction sequence (see Chapter 2, eq. 14c).¹⁵⁻¹⁷ This conclusion is supported by the results from the experiments carried out at different electrode potentials (Figures 3 and 4). At low potentials (100-200 mV versus Ag/AgCl) a Tafel-like behaviour (Chapter 2) is observed both at low and high glucose concentrations. This is characteristic for a reaction sequence in which a heterogeneous electron transfer step at the electrode (see equation 6) is rate controlling. At higher potentials (250-350 mV vs. Ag/AgCl) a deviation from this Tafel-behaviour occurs (Figure 4), indicating that electron transfer is facilitated due to the higher overpotential.¹³ When the potential is sufficiently high, e.g., 0.35 V vs. Ag/AgCl, the reaction is controlled by a combination of substrate transport limitation (*vide infra*) and Michaelis-Menten type enzyme kinetics. This leads to the desired situation for a properly functioning biosensor membrane as was discussed in Chapter 2 (see also Figure 12 of Chapter 2).

The Lineweaver-Burk⁵ (Figure 2) and Hanes-Woolf⁶ (not shown) plots of the data revealed that at high glucose concentrations a deviation from linearity occurs. This indicates that internal mass transport of glucose is limited at these high concentrations (see also Chapter 2, eq. 14b).¹⁸ The result is that the concentration of glucose near the surface of the biosensor is lower than in solution, leading to a smaller current response.

Thus, two rate limiting processes probably take place at the same time in our biosensors. First, substrate transport limitation is imposed by the membrane structure, leading to a moderate increase of K_M' .¹¹ Under normal operating conditions ($E = 0.35$ V) this limitation becomes detectable at high substrate concentrations. Overruling

this effect, however, is a second process, viz. the interfacial dynamics governing the transport of electrons to the electrode. This causes a substantial decrease in K_M' .¹¹ Such a lowering of K_M' has also been observed in first-generation biosensors, i.e., sensors in which molecular oxygen is the electron acceptor. Glucose oxidase reacts very fast with this second substrate, the second-order rate constant is $1.26 \times 10^8 \text{ M}^{-1} \cdot \text{min}^{-1}$ at 15°C .¹ Because of this, oxygen is easily depleted at the surface of the matrix in which glucose oxidase is immobilized, leading to a decrease in apparent $K_{M(\text{glucose})}$.^{11,19}

At this moment the question arises how the interfacial electron transport can still be so effective that it competes successfully with electron transport to molecular oxygen. We believe that the active centers of the immobilized glucose oxidase molecules can be thought to be electrically wired to the oxidizing electrode by the poly(pyrrole) matrix.²⁰ The mediating moieties, viz. the redox active sites on the conducting polymer, transport the electrons over a very short distance ($\leq 5 \text{ nm}$, see Chapter 5). In addition, the conducting polymer can cycle the redox state of its electroactive sites with high electrochemical efficiency.²¹ This creates a fairly constant surface concentration of sites able to communicate with the active centers of glucose oxidase. Molecular oxygen, on the other hand, has to diffuse from the bulk solution into the biosensor membrane over a fairly long distance (normally in the order of $5 - 10 \mu\text{m}$) before it can bind to the enzyme and accept electrons. Oxygen, therefore, cannot compete effectively with the poly(pyrrole) molecules for regenerating the reduced enzyme molecules.¹⁹

Table 2. Optimum pH values for free glucose oxidase and glucose oxidase immobilized in various matrices.^a

Matrix	pH	Ref.
Track-etch sensor	6.2 - 7.1	This work
Latex sensor	5.9 - 6.9	This work
Poly(pyrrole) ^b	6.0	10
Activated carbon	6.3	22
Graphite	7.3	8
TTF/TCNQ ^c	7.4	23
Carbon fibre	7.8	24
Free enzyme	5.5 - 6.0	2, 9, 25

^aGlucose oxidase from *A. niger*

^bElectrochemical entrapment

^cTTF = tetrathiofulvalene, TCNQ = tetracyanoquinodimethane

The optimum pH-value for glucose oxidase in the two biosensors is higher than the value for the free enzyme in solution (Table 2).^{9,25} We tentatively attribute this shift in optimum pH to the different process of reduced enzyme regeneration in our systems, which is expected to lead to the production of excess protons. Also contributing to the shift in optimum pH could be the effect of the immobilization matrix itself. Such an effect has actually been found for glucose oxidase immobilized on various materials, e.g., carbon fibre,²⁴ graphite,⁸ and activated carbon²² (see Table 2). The most interesting result is that the optimum activity of our sensor systems ranges over approximately 1 pH unit,²⁶ in contrast to what is found for other sensors (Figure 5).^{2,8,22,24} This means that the enzyme has become relatively insensitive to (small) changes in bulk pH. Apparently, the poly(pyrrole) matrix creates a microscopic environment that stabilizes the response with respect to variations of pH in the bulk solution.²⁷

The temperature dependence of the biosensor response, as shown in Figure 6a, shows a maximum around 37-40 °C and then decreases. This behaviour has been reported before in the literature for glucose oxidase immobilized in poly(pyrrole).¹⁰ However, in our case this effect is reversible, suggesting that it is not caused by enzyme denaturation. The decrease in response can probably be attributed to a change in the protein structure, making the enzyme less catalytically active with respect to its substrate glucose.²⁸ The activation energies that have been calculated from the temperature dependent data (41 and 44 kJ/mole for the track-etch membrane sensor and the latex-poly(pyrrole) membrane sensor, respectively, see Results) agree nicely with the value reported by Fortier *et al.* for glucose oxidase entrapped in a poly(pyrrole) film (41 kJ/mole).¹⁰ At this stage it is not justified to draw conclusions from the temperature experiments with regard to the reaction mechanism. It can be said, however, that the catalytic action of glucose oxidase in our systems has not altered significantly compared to other systems in which poly(pyrrole) is used as the immobilizing matrix. In addition to this, we find that our matrices stabilize the enzyme molecules at higher temperatures.

7.4 Concluding remarks

Our kinetic analysis of the track-etch membrane and latex-poly(pyrrole) membrane biosensors has shown that the measurement potential is an important parameter. In Chapter 2, it was explained that for a proper biosensor performance it is required that mass transport, electron transport, and enzymatic conversion of substrate are in balance. The electrical potential of the sensor electrode strongly affects this balance. When this potential is low (less than approx. 0.2 V vs. Ag/AgCl) the rate of the enzymatic reaction becomes too low as compared to the rate of substrate

transport. It is reasonable to conclude that reoxidation of the reduced enzyme is the rate limiting process at these low potentials (eq. 6, page 118). The curves in Figure 3 and 4 support this conclusion. When the potential is sufficiently high, substrate transport and the steps involved in enzymatic conversion of substrate become rate determining. As a consequence, biosensors operating at an appropriate potential can be described by equation 14b of Chapter 2 and they will display a more or less linear behaviour of the current on the substrate concentration over a considerable range. The curve found for our biosensors is rather similar to the predicted response curve a in Figure 12 of Chapter 2.^{16,29} When the sensor is operating at the right potential small variations in the amount of enzyme will not affect the current response. As long as the amount of catalytically active enzyme is high enough to create a condition where substrate transport is rate controlling, a constant sensor response will be obtained. When enzyme denaturation occurs, this will not immediately be reflected in the current response. Only when denaturation has proceeded to such an extent that the amount of active enzyme inside the sensor becomes rate determining, the response suddenly drops.^{8,30,31} This is what is actually found for our biosensor systems (Figure 7). It is in accordance with the remarks in Chapter 2 about biosensor lifetime.

The lifetime of the latex-poly(pyrrole) membrane sensor is significantly lower than the lifetime of track-etch membrane sensor. This is a result of the lower mechanical stability of the latex membrane. The continuous flow of solution which is passed over the sensor during the lifetime measurements slowly degenerates this membrane.

7.5 Materials and methods

The construction of the biosensors was described in detail in Chapters 4 and 6. When not in use, the sensor membranes were stored in Oxseypt[®] 2 (Allergan Benelux, The Netherlands) to preserve them and to avoid bacterial or fungal contamination.

Glucose oxidase (E.C. 1.1.3.4) type II (25,000 U/g) from *Aspergillus niger* and catalase (E.C. 1.11.1.6, 2800 U/mg) from Bovine liver were obtained from Sigma. Phosphate buffered saline (PBS, pH 7.4, 10 mM phosphate) was made in distilled water which was filtered over a microfiltration membrane (Millipore). The PBS buffer solution was sterilized after preparation. Before use, 4 Omnicare[®] tablets (Allergan Benelux, The Netherlands) were added to every liter of buffer solution. In this way, at least 20 U/ml catalase were present beforehand in all preparations made with PBS. All other reagents were of analytical grade.

Electrochemical measurements were performed with an CU-04-AZ electrochemical controller (Antec Leyden, The Netherlands). This apparatus allowed for current off-sets up to 1000 nA. After filtering (RC time 2 s), the current output

was recorded on a Yew 3056 pen recorder. For the activity measurements, the enzyme membrane was placed as the working electrode in a three electrode flow cell (AMOR flow cell, Antec Leyden, The Netherlands). Specific details were described in Chapters 4 and 6. An Ag/AgCl electrode was used as the reference electrode. The base of the flow cell (glassy carbon) acted as the auxiliary electrode. PBS buffer solution was driven through the cell at a rate of 1.75 ml/min. using a Watson Marlow 503S 4 channel peristaltic pump. The potential of the membrane was set at the desired value by means of the electrochemical controller. During the measurements, the buffer solution was replaced by a glucose solution and the current response was monitored.

The current response to glucose (concentration 2 mM) as a function of pH was determined by using the appropriate buffer salts and adjusting them with hydrochloric acid (2N) or sodium hydroxide (1N) to the desired pH value. Buffer solutions of 10 mM sodiumphosphate/citric acid, 10 mM sodiumtetraborate/HCl, and 10 mM sodiumtetraborate/NaOH were used to cover the pH range 2.6-9.6. All buffers contained 0.15 M NaCl. The pH of the buffers and of the resulting glucose solutions was measured with a Metrohm 691 pH Meter.

The temperature measurements were performed in a thermostatically controlled water bath (Julabo U3, Julabo Labortechnik GMBH, West Germany). The flow cell was isolated from the water by the application of a layer of grease (Glisseal[®]) (Borer Chemie AG, Switzerland). For the measurements at temperatures below room temperature crushed ice was added. The cell was incubated at the various temperatures for at least 15 min. before the steady-state current response to a 1 mM glucose solution was measured.

References

1. Duke, F.R., Weibel, M., Page, D.J., Bulgrin, V.G. and Luthy, J., *J. Am. Chem. Soc.*, (1969) **91**: 3904-3909.
2. Fortier, G. and Bélanger, D., *Biotechnol. Bioeng.*, (1991) **37**: 854-858.
3. Koopal, C.G.J., De Ruiter, B. and Nolte, R.J.M., *J. Chem. Soc., Chem. Commun.*, (1991): 1691-1692.
4. Koopal, C.G.J., Feiters, M.C., De Ruiter, B., Schasfoort, R.B.M. and Nolte, R.J.M. *Glucose sensor utilizing poly(pyrrole) incorporated in track-etch membranes as the mediator. Biosensors & Bioelectronics*, (1992) (in press).
5. Lineweaver, H. and Burk, D., *J. Am. Chem. Soc.*, (1934) **56**: 658-666.
6. Hanes, C.S., *Biochem. J.*, (1932) **26**: 1406-1421.
7. Wilkinson, G.N., *Biochem. J.*, (1961) **80**: 324-332.
8. Ianniello, R.M. and Yacynych, A.M., *Anal. Chem.*, (1981) **53**: 2090-2095.
9. Swoboda, B.E.P. and Massey, V., *J. Biol. Chem.*, (1965) **240**: 2209-2215.
10. Fortier, G., Brassard, E. and Bélanger, D., *Biosensors & Bioelectronics*, (1990) **5**: 473-490.
11. Mikkelsen, S.R. and Lennox, R.B., *Anal. Biochem.*, (1991) **195**: 358-363.
12. Frederick, K.R., Tung, J.T., Emerick, R.S., Masiarz, F.R., Chamberlain, S.H., Vasavada, A., Rosenberg, S., Chakraborty, S., Schopfer, L.M. and Massey, V., *J. Biol. Chem.*, (1990) **265**: 3793-3802.
13. Bard, A.J. and Faulkner, L.R. *Electrochemical Methods. Fundamentals and Applications*. John Wiley & Sons, New York: (1980).
14. O'Hare, D., Parker, K.H. and Winlove, C.P., *Bioelectrochem. Bioenerg.*, (1990) **23**: 203-209.
15. Albery, W.J. and Bartlett, P.N., *J. Electroanal. Chem.*, (1985) **194**: 211-222.
16. Albery, W.J., Bartlett, P.N. and Craston, D.H., *J. Electroanal. Chem.*, (1985) **194**: 223-235.
17. Albery, W.J. and Knowles, J.R., *Biochem.*, (1976) **15**: 5588-5600.
18. Horvath, C. and Engasser, J., *Biotechnol. Bioeng.*, (1974) **16**: 909-923.
19. Cass, A.E.G., Davis, G., Francis, G.D., Hill, H.A.O., Aston, W.J., Higgins, I.J., Plotkin, E.V., Scott, L.D.L. and Turner, A.P.F., *Anal. Chem.*, (1984) **56**: 667-671.
20. Heller, A., *Acc. Chem. Res.*, (1990) **23**: 128-134.
21. Asavapiriyanont, S., Chandler, G.K., Gunawardena, G.A. and Pletcher, D., *J. Electroanal. Chem.*, (1984) **177**: 229-244.
22. Cho, Y.K. and Bailey, J.E., *Biotechnol. Bioeng.*, (1978) **20**: 1651-1665.
23. Gunasingham, H. and Tan, C., *Anal. Chim. Act.*, (1990) **229**: 83.
24. Ang, K.P., Gunasingham, H., Tay, B.T., Herath, V.S., Teo, P.Y.T., Thiak, P.C. and Kuah, B., *Analyst.*, (1987) **112**: 1433-1435.
25. Bourdillon, C., Thomas, V. and Thomas, D., *Enzyme Microb. Technol.*, (1982) **4**: 175-180.
26. Knowles, J.R., *CRC Crit. Rev. Biochem.*, (1976) **4**: 165-173.
27. Goldstein, L. *Kinetic Behaviour of Immobilized Enzyme Systems*. In: *Methods in Enzymology*. edited by Colowick, S.P. and Kaplan, N.O. New York: (1955) pp. 397-443.
28. Cornish-Bowden, A. *Fundamentals of Enzyme Kinetics*. Butterworths, London: (1979).
29. Green, M.J. and Hill, H.A.O., *J. Chem. Soc., Faraday Trans. 1.*, (1986) **82**: 1237-1243.
30. Foulds, N.C. and Lowe, C.R., *J. Chem. Soc., Faraday Trans. 1.*, (1986) **82**: 1259-1264.
31. Pandey, P.C., *J. Chem. Soc., Faraday Trans. 1.*, (1988) **84**: 2259-2265.

8 Highly stable first generation glucose sensor utilizing latex particles as the enzyme immobilizing matrix

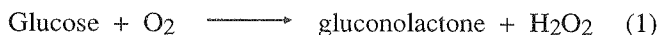
8.1 Introduction

In Chapter 6 we described how uniform latex particles (ULP's) can be used to construct a so-called third-generation biosensor. These particles were deposited on an electrode and coated with a thin layer of the conducting polymer poly(pyrrole). The poly(pyrrole) matrix was found to adsorb glucose oxidase and the resulting enzyme electrode could detect glucose without the need of an additional mediator. In this chapter we will show that latex particles themselves can also act as medium for immobilizing enzymes.¹⁻³ Furthermore, we will show that they can be applied to construct a first-generation biosensor that competes favourably with other first-generation biosensors reported in the literature.⁴⁻⁸

Latex polystyrene particles with sub-micron diameter are normally produced by emulsion polymerization in water.¹ They are mildly hydrophobic and carry a negative surface charge, because of the presence of sulphonate groups. Enzymes can be adsorbed physically on these particles.⁹ However, this adsorption is reversible and leakage of enzyme is encountered very frequently.¹⁰ Special ULP's with functional groups on the surface have been developed to overcome this problem. These functional groups allow for covalent attachment of the biomolecule to the surface of the latex beads. These functionalized beads, however, are very expensive.

Immobilization of glucose oxidase onto latex beads has been reported before in the literature and it has been suggested that the enzyme-loaded latex might be used as a biosensor.⁹ Until now, however, the construction of a mechanically stable first-generation biosensor from these beads has been impossible. We have found that stable membranes of uniform latex particles can be obtained if mixtures of latex and agarose are used to deposit the membrane (see Chapter 6).¹¹ This finding opens the possibility to develop a stable sensor device, as will be described in this chapter. The

device relies on the reaction of glucose oxidase with its natural co-substrate molecular oxygen:



The enzyme-catalyzed conversion of glucose produces hydrogen peroxide which can be detected by oxidation at the electrode on which the latex layer is deposited.*

8.2 Results and discussion

8.2.1 Construction of the latex electrodes

Glassy carbon (GC) electrodes were used as the basic electrode material. On these GC electrodes a thin layer of platinum was deposited. The latex layers were prepared from 112 and 220 nm latex particles. A droplet of a 75 μl aqueous latex suspension (0.125 wt% latex and 0.050 wt% agarose) was applied on the electrode surface and dried at 4 $^\circ\text{C}$. The dried membranes were either used as such or first heat treated at 60 $^\circ\text{C}$ for 1 hour. This yielded latex layers of approximately 5 μm thickness.

In Figure 1 scanning electron micrographs of the resulting latex membranes are presented. The images show a regular pattern of closely-packed polystyrene spheres.

8.2.2 Immobilization of glucose oxidase

Different methods were evaluated to prepare latex membranes showing glucose oxidase activity. In general, membranes that were not thermally treated were unsuitable to immobilize glucose oxidase. The stability of these membranes was not high enough to withstand the enzyme treatment. First, we tried to cast membranes from suspensions of latex beads, that also contained dissolved glucose oxidase. This procedure yielded very irregular and unstable membranes which could not be used. Secondly, we treated the latex membranes with a small droplet (50 μl) of the enzyme solution. The droplet was allowed to dry in the refrigerator. An enzyme concentration of 1 mg/ml gave a stable enzyme-latex membrane. Higher concentrations of enzyme

* It should be noted here that bare platinum electrodes are not suitable for this detection. They may display unpredictable behaviour as is discussed by Albery. He states that the measured current is more dependent on the number of windows open in the laboratory, the traffic passing by, and the movements of the experimenter, than on scientifically controllable parameters.¹² This unpredictable behaviour can be avoided by the use of membrane-covered electrodes.¹³

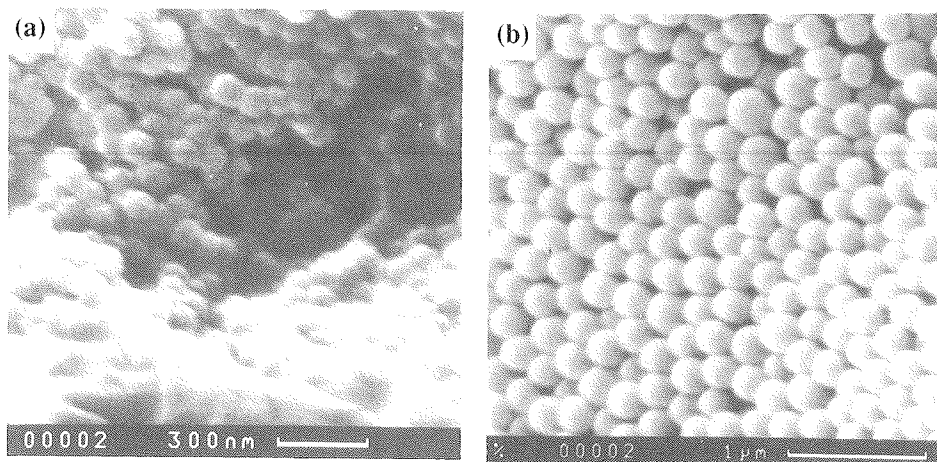


Figure 1. Scanning electron micrographs of polystyrene latex beads on a glassy carbon disk; (a) 112 nm particles, (b) 220 nm particles.

yielded damaged membranes which no longer adhered to the electrode surface. The high amount of enzyme was found to disrupt the latex structure during the drying process. A third procedure, viz. adsorption of glucose oxidase from solution proved to be the best method for loading the latex. The solution was kept at 4 °C and was agitated to promote penetration of the enzyme molecules into the microporous latex structure. The enzyme treatment was carried out for 4 hours, after which the membranes were dried. The resulting enzyme-latex membranes remained fully intact. Extreme drying over CaCl_2 after enzyme adsorption had no significant effect on their stability.

Some of the membranes were shortly treated with glutaraldehyde (GA) after enzyme adsorption. This bifunctional reagent causes cross-linking of the enzyme molecules and prevents them from leaking out of the latex membrane. The enzyme activity and stability of these GA-treated membranes were compared with those of the untreated membranes, as will be described in the following paragraph.

8.2.3 Enzyme activity

The enzyme-latex electrodes were tested for enzymatic activity following the procedure described in Chapters 4 and 6.^{14,15} In this procedure the natural co-substrate for glucose oxidase is replaced by the artificial electron acceptor benzoquinone. The latter molecule is reduced to hydroquinone, which can be detected

electrochemically at a rotating disk electrode. The measured current is an indication of the enzymatic activity of the latex membrane electrode.

The various membranes that were investigated are shown in Table 1. The measured enzyme activity and the degree of immobilization are given in a qualitative way. It can be concluded that treatment of the enzyme-loaded latex with glutaraldehyde yields active membranes with a relatively high enzyme loading. Drying the membranes after GA-treatment had no additional effect on the degree of immobilization, but the activity of the enzyme was lower.

Table 1. Immobilization and activity of glucose oxidase on latex membranes composed of 112 and 220 nm beads which are prepared under different conditions.^a

Conditions ^a	112 nm ^b		220 nm ^b	
	Activity	Immobilization	Activity	Immobilization
Rinsing, drying	Low	-	Low	-
Drying, rinsing	Moderate	-	Low	-
GA ^c , rinsing	High	+	High	+
GA ^c , drying	Moderate	+	High	+

^aSee text.

^bSize of the latex particles used in the membrane.

^cGlutaraldehyde.

Membranes that were not treated with GA after enzyme adsorption were active, but the enzyme molecules leaked out of the membrane during the activity assay. Untreated membranes that were rinsed directly after enzyme adsorption and then dried, displayed very low activities. These activities further decreased during the assay. First drying and subsequently rinsing slightly increased the activity of the membranes, but their immobilizing ability remained poor. The fact that drying has no substantial effect on the degree of enzyme loading is in contrast with the results found for the conducting polymer modified latex membranes (Chapter 6). These membranes immobilized the enzyme molecules very effectively after drying. As can be seen in Table 1 no large difference in enzyme activity or enzyme loading is observed between latex beads of 112 and 220 nm size.

In Figure 2 the enzyme activity is shown of a latex membrane composed of 112 nm beads, that was treated with glucose oxidase according to the optimized immobilization method, viz. adsorption to a thermally treated membrane, followed by glutaraldehyde cross-linking and rinsing in buffer solution. As can be seen the

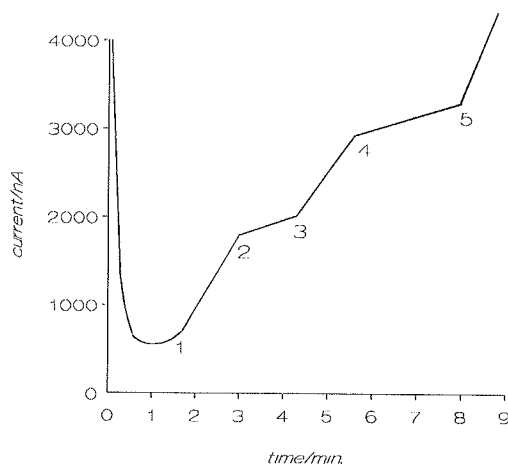


Figure 2. Measurement of enzyme activity of a latex membrane by the rotating disk electrode technique. (1) & (3): introduction of the latex electrode into the electrochemical cell; (2) & (4): withdrawal of the latex electrode; (5): introduction of 0.125 U of glucose oxidase to the cell.

current increases immediately upon introduction of the enzyme-latex membrane into the electrochemical cell (Figure 2, point 1). Withdrawal of the membrane causes the slope of the current to go back to the value before introduction. This means that the enzyme molecules are properly immobilized and do not leak out of the membrane. Improperly immobilized glucose oxidase would have stayed in solution after withdrawal of the membrane and would have caused a higher slope of the line after point 2. Membranes that were not treated with glutaraldehyde actually showed this behaviour. Figure 2 shows that repeated introduction and withdrawal of the membrane does not lead to a change in the amount of active, immobilized enzyme present (points 1-4). Calibration of the measured enzyme activity was achieved with a known quantity (5 μg , 0.125 U) of glucose oxidase, which was introduced at point 5 in Figure 2. From a comparison of the slopes of the curves for immobilized and added enzyme, it was concluded that approximately 0.1 U of active glucose oxidase is present in the membrane of Figure 2. Similar values were found for the membranes composed of 220 nm latex beads.

8.2.4 Biosensor activity

The biosensor activity of the latex membrane electrodes was measured in a continuous flow system as described in Chapter 4. In separate experiments it was first tested whether the bare glassy carbon and platinum electrodes showed an electrochemical response to glucose. A glucose solution of 100 mM was offered to

these electrodes which were poised at a potential of 0.75 V versus Ag/AgCl. No increase in current could be detected in these cases, indicating that non-specific electrochemical oxidation of glucose did not occur. The possibility of enzyme adsorption to the bare electrodes was also tested. Glassy carbon and platinum electrodes were treated with glucose oxidase for 24 hours, dried and rinsed in exactly the same way as the latex modified electrodes. No biosensor activity could be measured for these electrodes. Finally, latex membranes cast on GC and on Pt were tested for glucose sensitivity, without previous enzyme pretreatment. As expected, these electrodes did not respond to glucose.

Hydrogen peroxide in aqueous solution can be oxidized if the anodic potential is sufficiently high.¹⁶ The potential depends on the electrode used. Oxidation of hydrogen peroxide at bare platinum or carbon can be detected at potentials ranging from 0.6 to 1.6 V versus Ag/AgCl.^{8,12,17-20} For the biosensor activity measurements potentials were chosen that are in accordance with the literature values for other biosensors based on H₂O₂ detection.^{12,17,18}

The complete latex-membrane enzyme electrode system responded to glucose in a way as is shown in Figure 3. Shown is the current response to 5 mM glucose of a latex membrane sensor composed of 112 nm beads on a platinum electrode which was poised at a potential of 0.75 V vs. Ag/AgCl. All measurements were carried out in air-saturated phosphate buffered (10 mM, pH 7.4) saline solution. Latex membrane

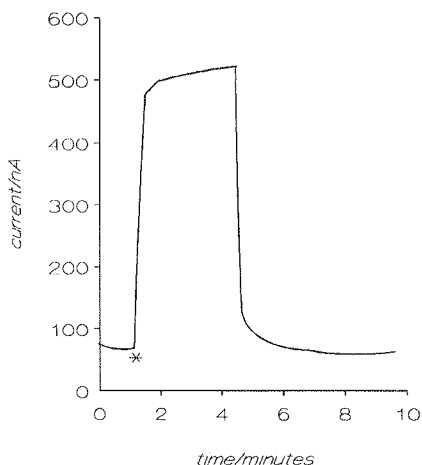


Figure 3. Current response of a latex membrane biosensor under continuous flow conditions. Latex membrane composed of 112 nm beads deposited on a platinum electrode, heat treated for 1 h. and incubated with a solution (3 ml) of 5 mg/ml of glucose oxidase for 4 h. Membrane treated after enzyme adsorption with 2.5 % glutaraldehyde for 10 min. The measuring potential is 0.75 V vs. Ag/AgCl. The measurement was performed in an air saturated phosphate buffered saline solution (pH 7.4). *Introduction of 5 mM glucose in the buffer stream.

sensors based on glassy carbon also showed this electrochemical response upon the addition of glucose. However, for these sensors a stable response current could only be obtained when the electrode potential was equal or higher than 0.75 V (vs. Ag/AgCl). Platinized glassy carbon latex-membrane electrodes were found to respond to glucose at a potential as low as 0.15 V (vs. Ag/AgCl). As a low measuring potential is a very important condition for an amperometric biosensor, we decided to

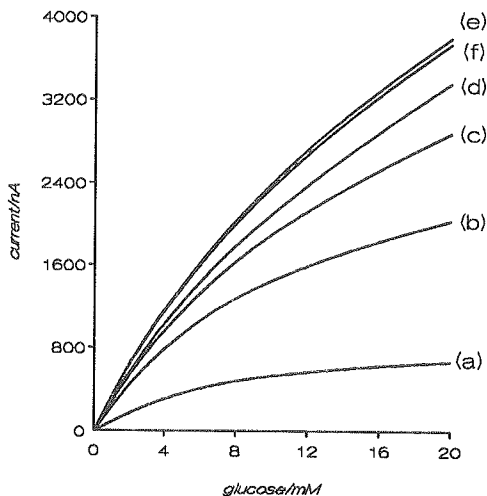


Figure 4. Plot of the steady-state current of a latex membrane measured at various potentials (vs. Ag/AgCl) as a function of the glucose concentration. Latex membrane composed of 220 nm beads deposited on a platinum covered glassy carbon electrode, heat treated for 1 h. and incubated with a solution (3 ml) of 5 mg/ml of glucose oxidase for 4 h. Membrane treated after enzyme adsorption with 2.5 % glutaraldehyde for 10 min. The measurements were conducted in an air saturated phosphate buffered saline solution (pH 7.4). (a): 0.15 V; (b): 0.20 V; (c): 0.25 V; (d): 0.35 V; (e): 0.50 V; (f): 0.75 V.

test in further experiments only these platinum covered glassy carbon electrodes.

The measuring potential of the electrode was varied from 0.15 to 0.75 V versus Ag/AgCl and the response to various glucose concentrations (0-20 mM) was evaluated. The results for a sensor based on 220 nm latex beads are shown in Figure 4. It can be seen that the most linear response is obtained at a potential of 0.50 V. Increasing this potential further had no effect on the current response. Potentials lower than 0.50 V led to a decrease in sensitivity of the biosensor, especially at higher glucose concentrations.

8.2.5 Kinetic evaluation of the biosensor response

It can be deduced from the curves in Figure 4 that the response current of the biosensor becomes limited at 0.50 V or higher. This limitation is probably imposed by the enzyme kinetics and the internal mass transport. At potentials lower than 0.25 V the kinetics of the electrochemical oxidation of hydrogen peroxide clearly is rate limiting. Further analysis of the data at intermediate potentials (0.25–0.35 V) revealed that under these conditions glucose oxidase immobilized on latex beads obeyed Michaelis-Menten kinetics. This is shown in Figure 5, where the data obtained at 0.35 V vs. Ag/AgCl are fitted to the Michaelis-Menten rate equation.²¹ It should be noted here that the model derived in Chapter 2 (direct electron transfer) can no longer be applied. For the present first-generation biosensor the classical two-substrate enzyme

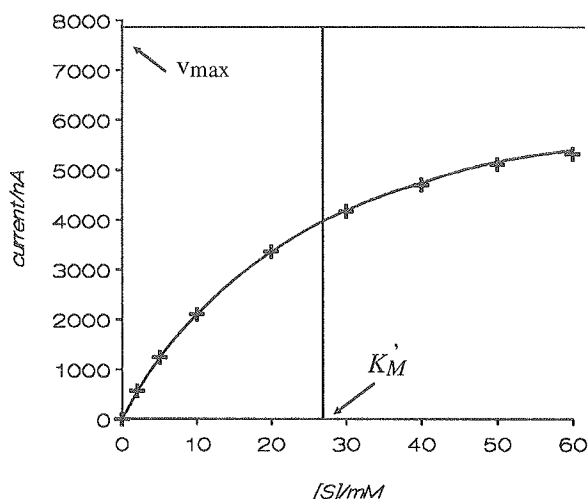


Figure 5. Fitting of the data of Figure 4 (curve d) to Michaelis-Menten type reaction kinetics (solid line).

kinetics should be used, which has been studied extensively both for glucose oxidase in homogeneous solution^{22,23} and for the enzyme immobilized in different heterogeneous systems.^{24,25} When the data in Figure 4 are plotted in linear form according to the Hanes-Woolf method²⁶ (Figure 6) it becomes evident that at higher potentials the system suffers from internal transport of substrate as suggested above.^{24,27,28} For instance, the data at 0.35 V fit very well to a straight line ($R = 0.9997$), whereas the data obtained at 0.50 V show a relatively poor fit ($R = 0.9962$). Most likely, oxygen is the rate limiting substrate in this case. This molecule has a high affinity for glucose oxidase and its depletion by enzymatic consumption could readily occur in the relatively thick (5 μm) latex membrane. The apparent K_M

$(K_M'(\text{glucose}))$ for glucose oxidase immobilized in our latex membrane measured at 0.35 V vs. Ag/AgCl amounted to approximately 27 ± 2 mM. This $K_M'(\text{glucose})$ value is in line with the fact that oxygen is the rate limiting substrate.²⁵ The $K_M'(\text{glucose})$ would have been higher than the true K_M for glucose (33 mM^{24}) if glucose transport had been limiting for the reaction.

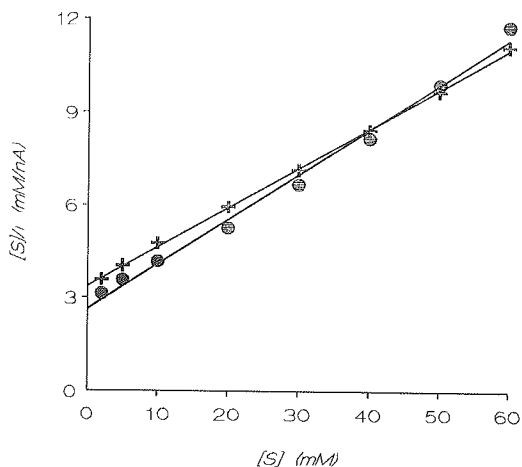


Figure 6. Hanes-Woolf plots of the current data obtained at a potential of 0.35 V (+) and at 0.50 V (●) vs. Ag/AgCl.

8.2.6 Dependence of the biosensor response on pH

The effect of the pH was investigated by measuring the current response due to 0.5 mM glucose in various buffered and air saturated solutions. The pH values of these solutions were varied between 3 and 10. The resulting pH profile is presented in Figure 7. For comparison, in this figure a pH profile for the enzyme in solution is also shown.^{24,29} The free enzyme has an optimum activity at pH 5.5. The enzyme immobilized in our latex-membrane electrode has an optimum at pH 7.5. The anionic character of the latex beads (see Introduction) could explain this shift to higher pH.²⁸⁻³¹ The observed optimum activity at pH 7.5 is very advantageous for clinical applications since this pH is the physiological pH value. Figure 7 furthermore reveals that glucose oxidase immobilized on our latex membrane remains active over a broad pH range. From pH 6 to 9, more than 75 % of the activity is retained. This is in contrast with the enzyme in solution, which has a quite sharp pH maximum (Figure 7).

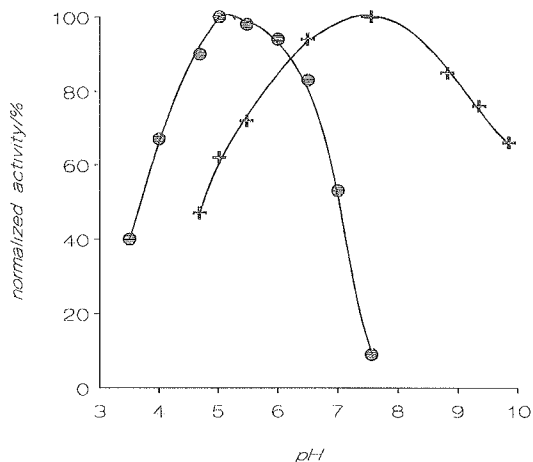


Figure 7. (+) Normalized steady-state current response of a latex membrane electrode to 0.5 mM glucose, measured at different pH values in citrate/phosphate or in borate buffer. The electrode potential was 0.35 V vs. Ag/AgCl. The latex membrane contained 220 nm beads and was deposited on platinum-coated glassy carbon. (●) pH profile of glucose oxidase in an air-saturated solution.²⁴

Application of the membrane sensor under various pH conditions, therefore, is very well possible.

8.2.7 Stability of the biosensor

The stability of the sensor was tested in phosphate buffered (pH 7.4) solutions containing glucose concentrations varying between 5 and 20 mM. The electrode potential was kept at 0.5 V vs. Ag/AgCl. More than 1000 glucose activity assays were performed automatically over a period of approximately 3 days. Each assay took 4 minutes. No decrease in activity was observed during this period. After 1250 assays the activity rapidly decreased probably as a result of enzyme deactivation by hydrogen peroxide.³² This reaction product is probably retained in the microporous latex membrane for a short period of time before it is oxidized at the electrode. This will have a deleterious effect on the enzyme activity.

The stability of the latex-membrane biosensor was also tested under conditions of intermittent use. In these experiments the sensor was held stand-by in the continuous-flow system when not in use. The resulting stability curve is shown in Figure 8. Under these conditions the response current is fairly stable for a period of 15 days. After this period the response rapidly decreased, probably for the same reason as mentioned above.

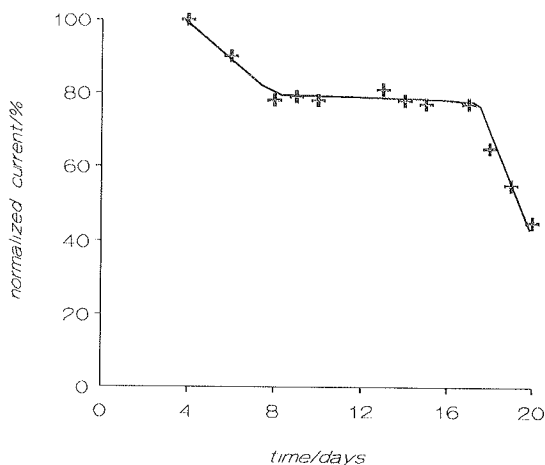


Figure 8. Normalized steady-state current response of a latex membrane electrode under discontinuous use as a function of time. The latex membrane contained 220 nm beads and was deposited on platinum-coated glassy carbon. The electrode potential was 0.75 V vs. Ag/AgCl.

8.3 Conclusion

The experiments described in this chapter show that a stable first-generation biosensor based on glucose oxidase immobilized on latex membranes can be constructed. The sensor activity is high over a broad pH range. The optimum pH value of 7.5 is favourable for a number of possible applications. The present biosensor can compete very well with other first-generation biosensors for glucose described in the literature.

8.4 Experimental

Materials and equipment

Glucose oxidase (E.C. 1.1.3.4) type II (25,000 U/g) from *Aspergillus niger* was obtained from Sigma. Benzoquinone was obtained from Aldrich (FRG) and was sublimed prior to use. The latex suspensions were purchased from Perstorp Analytical and contained beads of 112 or 220 nm. Agarose type VIII was obtained from Sigma.

Glucose was purchased from Merck. Solutions of this compound were allowed to mutarotate for at least 24 h. before use. All other reagents were of analytical grade.

The electrochemical measurements were performed with a CU-04-AZ electrochemical control unit (Antec Leyden, The Netherlands) or an Autolab potentiostat controlled by an Olivetti M24 Personal Computer and General Purpose Electrochemical System (GPES)-software (Eco Chemie, Utrecht, The Netherlands). The current output was recorded on a Yew 3056 pen recorder. Electron micrographs were made on a CAMSCAN scanning electron microscope (Cambridge Instruments).

Preparation of the latex electrodes

Glassy carbon disks of 8 mm diameter (Antec Leyden, The Netherlands) were used as the electrode material. The electrodes were polished with Alpha Micropolish Alumina No. 1C (1.0 micron, Buehler LTD., U.S.A.). Platinum was applied on the polished surface with an Edwards sputtercoater S150B. A platinum target of 8 cm diameter and 0.5 mm thickness was used as the platinum source. The layer thickness was monitored with an Edwards FTM5 unit. Sputtering was continued until the thickness of the platinum layers was 300 nm.

Agarose type VIII was dissolved (0.1 wt%) in boiling distilled water. Freshly made agarose solutions, which were still hot, were used to mix with the latex suspensions. A certain volume of a freshly prepared agarose solution was added to an equal volume of the latex suspension. A 75 μ l droplet of the resulting mixture was applied on a polished GC disk or on a freshly sputtered platinum disk. After application, the electrode was put in the refrigerator overnight. The dried latex electrodes were either used as such or put in the oven at 60 °C for one h.

Immobilization of glucose oxidase

All glucose oxidase solutions were prepared in phosphate buffered saline (PBS, pH 7.4). Enzyme adsorption was accomplished by agitating the latex coated electrodes in a solution (3 ml) of 5 mg/ml of glucose oxidase at a temperature of 4 °C for 4 h. (Gyrotory Shaker model G2, New Brunswick Scientific, USA). Adsorption experiments were also carried out by applying a droplet (50 μ l) of a 5 mg/ml solution of glucose oxidase onto the latex membrane. Subsequently, the membrane was dried in the refrigerator overnight. After the adsorption procedures the enzyme membranes were either rinsed and dried or treated further with glutaraldehyde (GA).

Cross-linking of the adsorbed enzyme was effected by placing the membranes in a solution containing 2.5 vol% of GA in PBS for 10 min. at room temperature. After this treatment the membranes were rinsed with PBS buffer.

When not used directly the sensor electrodes were stored in PBS solution in the refrigerator.

The enzymatic activity of the latex membranes was assayed according to the procedure described in Chapter 4. The complete biosensor electrode was placed in the electrochemical three electrode cell and the resulting current at a potential of 0.35 V vs. Ag/AgCl was monitored.

Amperometric biosensor activity measurements

To perform amperometric measurements, the enzyme membrane electrode was placed as the working electrode in the three electrode flow cell described in Chapter 4. Approximately 0.15 cm² of the membrane surface was in contact with the electrolyte solution. Buffer solution was driven through the cell at a speed of 1.75 ml/min. (Watson Marlow 101U peristaltic pump). The potential of the membrane was set at the required potential vs. the Ag/AgCl reference electrode. For the measurements the buffer solution was replaced by the glucose solutions in PBS and the current response was monitored.

Automatic assay of the biosensor response was achieved by using a solenoid valve (LFYA 1216032H; The Lee Co., CT, USA), that was controlled by a multi-function timer module (Stock nr. 341-395; Mulder-Hardenberg, Haarlem, The Netherlands). This set-up allowed for automatic switching between the buffer solution and a solution that contained glucose. The timer module was programmed in such a way that the flow-cell measured PBS buffer solution for 180 s and then switched to glucose for 90 s. This cycle was repeated until the measurement was stopped manually.

References

1. Kitano, H., Nakamura, K. and Ise, N., *J. Appl. Biochem.*, (1982) **4**: 34-40.
2. Clark, D.S., Bailey, J.E., Yen, R. and Rembaum, A., *Enzyme Microb. Technol.*, (1984) **6**: 317-320.
3. Suen, C.-H. and Morawetz, H., *Macromol. Chem.*, (1985) **186**: 255-260.
4. Schuhmann, W., Lammert, R., Uhe, B. and Schmidt, H., *Sensors and Actuators*, (1990) **B1**: 537-541.
5. Fortier, G., Brassard, E. and Bélanger, D., *Biosensors & Bioelectronics*, (1990) **5**: 473-490.
6. Turner, A.P.F., Karube, I. and Wilson, G.S. *Biosensors. Fundamentals and Applications*. Oxford University Press, New York: (1989).
7. Cammann, K., Lemke, U., Rohen, A., Sander, J., Wilken, H. and Winter, B., *Angew. Chem.*, (1991) **103**: 519-541.
8. Pandey, P.C., *J. Chem. Soc., Faraday Trans. 1.*, (1988) **84**: 2259-2265.
9. Kawaguchi, H., Koiwai, N. and Ohtsuka, Y., *J. Appl. Pol. Sci.*, (1988) **35**: 743-753.
10. Kawaguchi, H., Amagasa, H., Hagiya, T., Kimura, N. and Ohtsuka, Y., *Colloids and Surfaces*, (1985) **13**: 295-311.
11. Schasfoort, R.B.M., Kooyman, R.P.H., Bergveld, P. and Greve, J., *Biosensors & Bioelectronics*, (1990) **5**: 103-124.
12. Albery, W.J. *Electrode Kinetics*. Oxford University Press, London: (1975).
13. Clark Jr., L.C. *The Hydrogen Peroxide Sensing Platinum Anode as an Analytical Enzyme Electrode*. In: *Methods in Enzymology, Vol. LVI*. Academic Press, New York, (1979): pp. 448-479.
14. Aubré-Lecat, A., Hervagault, C., Delacour, A., Beaude, P., Bourdillon, C. and Remy, M., *Anal. Biochem.*, (1989) **178**: 427-430.
15. Bourdillon, C. and Majda, M., *J. Am. Chem. Soc.*, (1990) **112**: 1795-1799.
16. Hoare, J.P. *Oxygen*. In: *Standard Potentials in Aqueous Solution*. edited by Bard, A.J, Parsons, R. and Jordan, J., Marcel Dekker, Inc., New York, (1985): pp. 49-66.
17. Cass, A.E.G. *Biosensors. A Practical Approach*. Oxford University Press, New York: (1990).
18. Bindra, D.S., Zhang, Y., Wilson, G.S., Sternberg, R., Thévenot, D.R., Moatti, D. and Reach, G., *Anal. Chem.*, (1991) **63**: 1692-1696.
19. Foulds, N.C. and Lowe, C.R., *J. Chem. Soc., Faraday Trans. 1.*, (1986) **82**: 1259-1264.
20. Miyawaki, O. and Wingard Jr., L.B., *Biotechnol. Bioeng.*, (1984) **26**: 1364-1371.
21. Cornish-Bowden, A. *Fundamentals of Enzyme Kinetics*. Butterworths, London: (1979).
22. Swoboda, B.E.P. and Massey, V., *J. Biol. Chem.*, (1965) **240**: 2209-2215.
23. Duke, F.R., Weibel, M., Page, D.J., Bulgrin, V.G. and Luthy, J., *J. Am. Chem. Soc.*, (1969) **91**: 3904-3909.
24. Fortier, G. and Bélanger, D., *Biotechnol. Bioeng.*, (1991) **37**: 854-858.
25. Mikkelsen, S.R. and Lennox, R.B., *Anal. Biochem.*, (1991) **195**: 358-363.
26. Hanes, C.S., *Biochem. J.*, (1932) **26**: 1406-1421.
27. Horvath, C. and Engasser, J., *Biotechnol. Bioeng.*, (1974) **16**: 909-923.
28. Goldstein, L. *Kinetic Behaviour of Immobilized Enzyme Systems*. In: *Methods in Enzymology*. edited by Colowick, S.P. and Kaplan, N.O., New York, (1955): pp. 397-443.
29. Cho, Y.K. and Bailey, J.E., *Biotechnol. Bioeng.*, (1978) **20**: 1651-1665.
30. Ang, K.P., Gunasingham, H., Tay, B.T., Herath, V.S., Teo, P.Y.T., Thiak, P.C. and Kuah, B., *Analyst.*, (1987) **112**: 1433-1435.
31. Ianniello, R.M. and Yacynych, A.M., *Anal. Chem.*, (1981) **53**: 2090-2095.
32. Krishnaswamy, S. and Kitrell, J.R., *Biotechnol. Bioeng.*, (1978) **20**: 821-835.

Summary

In this thesis the development of third-generation amperometric glucose sensors, based on the redox enzyme glucose oxidase and conducting polymers, is described.

Amperometric biosensors of the third generation are characterized by the fact that direct electrochemical communication occurs between the electroactive center of a redox enzyme and an electrode. They differ in this respect from first- and second-generation biosensors, which make use of natural co-substrates and artificial mediators, respectively, to transport electrons between the enzyme and the electrode.

The first studies described in this thesis include the modification of planar electrode surfaces with conducting polymers. The aim is to get insight into the factors determining the direct electronic interaction between an electrode and glucose oxidase. The conducting polymers that were investigated are based on pyrrole, thiophene, and derivatives of these compounds. It was found that modification of planar electrode surfaces with conducting polymers does not create the proper conditions for enzyme immobilization and direct electron transfer.

In subsequent investigations microporous conducting polymer matrices are used to immobilize the enzyme. Two biosensor systems are developed based on these matrices. In the first system a track-etch filtration membrane is utilized as a template for pyrrole polymerization. Highly conducting hollow polypyrrole microtubules are formed in which glucose oxidase is adsorbed irreversibly. Evidence is presented that in the sensor constructed from these tubules glucose oxidase is in direct electronic contact with the electrode. The active parts of this biosensor, viz. the microtubules and the glucose oxidase molecules, are imaged on a nanometer scale by means of scanning tunneling microscopy. Based on the results from this study a model for the electronic interaction between the glucose oxidase molecules and the polypyrrole microtubules is proposed.

The second biosensor is based on a membrane of uniform latex particles. Polypyrrole is electrochemically synthesized within the interspherical pores of this latex membrane. Also this latex-polypyrrole composite membrane adsorbs glucose oxidase irreversibly and communicates with this enzyme in a direct manner.

Glucose concentrations in the range from 1-40 mM can be measured amperometrically under steady-state conditions with these biosensors. By applying flow injection conditions this range can be extended to 250 mM. The sensors operate at a low measuring potential (typically 0.350 V versus Ag/AgCl reference) resulting

in a highly selective response to glucose. The response is independent of the oxygen concentration and the biosensors display a considerable lifetime, even under continuous use.

The mechanism of the enzymatically catalyzed oxidation of glucose will be different if oxygen as the electron acceptor is replaced by a conducting polymer. A kinetic study of the performance of the two biosensors is presented which confirms this hypothesis. Different kinetic parameters are found for the immobilized glucose oxidase as compared to the enzyme in solution. Mediation by the conducting polymer is found to be very effective and no significant electron transfer to oxygen is observed. In addition to substrate transport limitation, which is to be expected for these microporous systems, the enzymatic reaction in the biosensors is limited by the applied potential.

In the last part of the thesis a first-generation biosensor based on latex membranes is described. This sensor measures glucose by detecting the hydrogen peroxide produced by the enzyme. Although somewhat outside the scope of this thesis, this sensor has been included as it competes very well with other first-generation glucose sensors described in the literature.

Samenvatting

Chemische sensoren zijn geminiaturiseerde meetinstrumenten die een chemische stof selectief kunnen detecteren. Indien het deel van de sensor dat verantwoordelijk is voor de selectiviteit bestaat uit moleculen van biologische oorsprong, wordt gesproken van een biosensor. Het biologische molecuul kan bijvoorbeeld een enzym zijn, een antilichaam of een DNA-molecuul.

Dit proefschrift heeft tot onderwerp de ontwikkeling van zogenaamde derde-generatie glucosesensoren, gebaseerd op het redoxenzym glucose oxidase en op elektrisch geleidende polymeren. Redoxenzymen katalyseren de oxydatie of reductie van specifieke substraten. De elektronen die hierbij zijn betrokken, worden in de derde-generatie biosensoren rechtstreeks aan de elektrode doorgegeven. Dit resulteert in een stroom die afhankelijk is van de aangeboden substraatconcentratie. Door bovengenoemde directe elektronoverdracht onderscheiden derde-generatie biosensoren zich van eerdere generaties biosensoren, die ofwel werken op basis van de detectie van enzymatisch gegenereerde producten, ofwel op basis van mobiele redox-koppels die het transport van lading verzorgen.

Het onderzoek beschreven in het eerste deel van dit proefschrift, behelst de modificatie van vlakke elektrode-oppervlakken met geleidende polymeren. Doel is te onderzoeken wat de juiste condities zijn voor directe elektronische communicatie tussen het redoxenzym glucose oxidase en een elektrode. De onderzochte polymeren zijn opgebouwd uit pyrrool- of thiofeeneenheden, danwel derivaten van deze verbindingen. In de loop van het onderzoek is gebleken dat de modificatie van vlakke elektroden met geleidende polymeren niet leidt tot enzymimmobilisatie en directe electronoverdracht.

Microporeuze matrices bestaande uit geleidend polymeer zijn vervolgens ontwikkeld om het gestelde doel te bereiken. Twee biosensoren worden beschreven die op basis van deze matrices zijn geconstrueerd. In beide sensoren bestaat de geleider uit polypyrrool en wordt glucose oxidase toegepast als het redoxenzym. In het eerste systeem is een zogenaamd track-etch filtratiemembraan gebruikt als een matrijs voor de polymerisatie van het pyrrool. Holle, microscopisch kleine buisjes van polypyrrool worden op deze wijze gevormd. De buisjes hebben een hoog elektrisch geleidend vermogen en blijken in staat te zijn om glucose oxidase irreversibel te binden en met dit enzym te communiceren. De twee belangrijke componenten van deze biosensor, te weten de holle polypyrrool buisjes en het

redoxenzym, zijn bestudeerd op een schaal in de orde van nanometers met behulp van scanning tunneling microscopie. Op grond van de resultaten van deze microscopische studie wordt een model voorgesteld, welke de waargenomen elektronische interactie tussen glucose oxidase moleculen en het polypyrrool kan verklaren.

De tweede biosensor is gebaseerd op een membraan van uniforme latexdeeltjes. Polypyrrool wordt elektrochemisch aangebracht in de ruimte die aanwezig is tussen de bolvormige latexdeeltjes. Het gemodificeerde latexmembraan kan irreversibel glucose oxidase binden en evenals het gemodificeerde "track-etch" membraan op directe wijze elektronisch communiceren met dit enzym.

De ontwikkelde biosensoren kunnen onder zogenaamde steady-state conditions glucose meten in een bereik van 1 tot 40 mM. Wanneer "flow injection conditions" worden toegepast kan dit bereik worden vergroot tot 250 mM. De sensoren werken bij een relatief lage meetpotentialiaal (typisch 350 mV t.o.v een zilver-zilverchloride referentie-elektrode) en vertonen een zeer selectieve respons op glucose. Deze respons is onafhankelijk van de zuurstofconcentratie. De sensoren hebben een lange levensduur, zelfs onder condities waarbij ze continu in gebruik zijn. Het kinetisch gedrag van de twee biosensoren is uitvoerig onderzocht. De enzymatisch gekatalyseerde oxydatie van glucose in de sensor verloopt volgens een afwijkend reactiemechanisme aangezien de rol van de zuurstof als elektronacceptor wordt overgenomen door het geleidend polymeer. Er worden dan ook kinetische parameters gevonden voor het geïmmobiliseerde enzym die anders zijn dan voor het enzym in oplossing. Uit de studie blijkt dat de elektronmediatie door het geleidend polymeer zeer effectief is en dat de enzymatische reactie gestuurd kan worden door de aangelegde potentialiaal.

Het laatste hoofdstuk van dit proefschrift beschrijft een eerste-generatie biosensor die is ontwikkeld op basis van de bovengenoemde latexmembranen. Deze sensor meet glucose door middel van enzymatisch geproduceerd waterstofperoxyde. Deze eerste-generatie biosensor valt enigszins buiten de scope van dit proefschrift maar is toch opgenomen omdat de sensor uitstekend kan concurreren met andere eerste-generatie glucosesensoren.

Curriculum vitae

De auteur van dit proefschrift werd op 15 december 1964 geboren te Amersfoort. In mei 1983 werd het diploma Atheneum-B behaald aan het Eemland College Zuid te Amersfoort. In hetzelfde jaar werd de scheikundestudie aangevangen aan de Rijksuniversiteit te Utrecht. Het propedeutisch examen werd afgelegd in april 1985. Het doctoraalexamen met als hoofdvak anorganische chemie (Prof. Ir. J.W. Geus) en als keuzevakken organometaalchemie (Prof. Dr. G. van Koten) en fysisch-organische chemie (Prof. Dr. W. Drenth) werd afgelegd in januari 1989. Op 1 mei 1989 werd de auteur aangesteld als wetenschappelijk assistent aan de vakgroep Organische Chemie van de Katholieke Universiteit Nijmegen. Het in dit proefschrift beschreven onderzoek werd uitgevoerd in de periode mei 1989 tot juli 1992. In de loop van deze periode werd de auteur gedetacheerd bij de afdeling Chemie van het Kunststoffen en Rubber Instituut (TNO-Industrie) te Delft en bij de afdeling Biotechnologie van het Instituut voor Biochemie en Chemie (TNO-Voeding) te Zeist. Tot 1 mei 1993 zal de auteur in dienst blijven van de Katholieke Universiteit Nijmegen waarna hij een functie hoopt te aanvaarden bij TNO-Voeding te Zeist.

